COST Action 710
Preprocessing of Meteorological Data for Dispersion Modelling

Report of Working Group 2

Mixing Height Determination for Dispersion Modelling

Petra Seibert

Frank Beyrich

Sven-Erik Gryning

Sylvain Joffre

Alix Rasmussen

Philippe Tercier

May 1997

TABLE OF CONTENTS

Executive summary

Substances emitted into the atmospheric boundary layer (ABL) are dispersed horizontally and vertically through the action of turbulence and eventually become mixed over this layer. Therefore, it has become customary to use the term "mixing layer" (ML). The ML coincides with the ABL if the latter is defined as the turbulent domain of the atmosphere adjacent to the ground. The ABL or ML height h is one of the fundamental parameters to characterize its structure and is required in dispersion models.

There are two basic possibilities for the practical determination of h. It can be obtained from profile measurements, either in-situ (radiosonde, tethersonde, tower) or by remote sounding (sodar, clear-air radar, lidar). The other possibility is to use parameterizations or simple models with only a few measured parameters as input. Most of the relevant methods suggested in the literature are reviewed in this report. In any case, it is possible to substitute output from numerical models (weather prediction or other, e.g. research) for observed parameters.

The most important methods have been tested on data sets from two operational sites (Cabauw/NL, Payerne/CH) and a major field campaign (SADE/D). Parcel and Richardson number methods to analyze radiosoundings and mixing heights derived from sodar and wind profiler data have been investigated. Modules to determine h through parameterizations and models implemented in currently used meteorological preprocessors have been tested, too. These preprocessors were OML, HPDM, FMI, Servizi Territorio, and RODOS. For the stable and mechanically-dominated unstable ABL, they use similarity formulae based on the friction velocity $u*$, the Monin-Obukhov-length, and the Coriolis parameter f while in the convective case simple slab models are integrated, based on an initial temperature profile and the surface heat and momentum fluxes.

A number of recommendations for operational mixing height determination have been formulated, including suggestions for the preprocessor development and for future research. The most important points are:

If suitable measured data are available, determination of h should be based on these data. In convective situations, the most reliable method is the parcel method applied to temperature profiles; bulk Richardson number methods can be used, too. MH determination in situations dominated by mechanical turbulence is much more difficult. If temperature and wind profiles are available, methods based on bulk Richardson numbers are considered to be the most appropriate. In many situations, data from remote sounding systems can give good results, but the available algorithms for their evaluation are not yet reliable enough to recommend them for operational purposes.

All the preprocessors had problems in specific situations. In the stable and neutral ABL, they rely on similarity formulae involving surface layer parameters and f, which is not satisfactory from a physical point of view. Richardson number methods appear to be better in this respect. However, the necessary input for these methods is often not available. Using one-dimensional numerical models with higher-order turbulence closure, adjusted to measurements, may become a solution in the future. If surface similarity methods are used, Nieuwstadt's (1981) equation appears to be superior to the $u*/f$ approach for stable conditions. Further recommendations concern the initialization of slab models, the ability of preprocessors to accept measured data, and the use of region-specific constants.

List of figures

List of tables

List of acronyms and symbols

Acronyms

ABL	Atmospheric Boundary Layer
CBL	Convective Boundary Layer
ETP	Evening Transition Period
EL	Entrainment Layer
ML	Mixing Layer
MH	Mixing Height
MOST	Monin-Obukhov Similarity Theory
LES	Large-Eddy Simulation
LLJ	Low-Level Jet
SBL	Stable Boundary Layer
SL	Surface Layer
TKE	Turbulent Kinetic Energy

Symbols

C_T^2, C_V^2, C_N^2	structure parameters for temperature, wind velocity and refractive index fluctuations
c_p	specific heat at constant pressure
D	structure function
f	Coriolis parameter
g	acceleration of gravity
H	sensible heat flux
h	mixing height
K_H, K_M	turbulent exchange co-efficients (eddy diffusivities) for heat and momentum
L	any length scale (specific length scales are defined where they appear)
L_*	Monin-Obukhov length ($L_* = -u_*^3 / [\beta\kappa \langle w'\Theta'\rangle_0]$)
n	index of refraction
N_{BV}	Brunt-Väisälä frequency ($N_{BV} = [\beta\gamma_\Theta]^{1/2}$)
Pr	Prandtl number ($Pr = K_M/K_H$)
p	air pressure
q	specific humidity
Ri	(gradient) Richardson number
Ri_b, Ri_f, Ri_c	bulk, flux, and critical Richardson number
r	mixing ratio
S	sodar backscatter intensity
T	temperature
T_d	dewpoint temperature

t	time
u, v	x, y-components of the horizontal wind vector
u_g, v_g	x, y-components of the geostrophic wind vector
u_*	friction velocity
V	(horizontal) wind speed
$\boldsymbol{V}$	(horizontal) wind vector
V_g	geostrophic wind speed
w	vertical wind component
w_s	large-scale vertical velocity
w_*	convective scaling velocity ($w_* = [\beta\, h\, \langle w'\Theta'\rangle_0]^{1/3}$)
z	height coordinate
z_0	roughness length
α	wind direction
β	buoyancy parameter ($\beta = g/T$)
γ, γ_Θ	vertical gradient of temperature / potential temperature
Δh_E	thickness of the entrainment layer
ε	TKE dissipation rate
$\Theta, \Theta_v, \Theta_e$	potential, virtual potential, equivalent potential temperature
κ	von-Kármán constant ($\kappa = 0.35..0.4$)
λ	wavelength
ζ, ζ_h	stability parameter ($\zeta = z/L_*$ or $\zeta_h = h/L_*$)
ρ	air density
σ_α	standard deviation of wind direction fluctuations
σ_v	standard deviation of lateral wind speed fluctuations
σ_w^2	vertical velocity variance
τ	shear stress
τ_{SBL}	time scale of the SBL height
φ	geographical latitude
ω	angular rotation velocity of the earth
$\langle w'\Theta'\rangle$	kinematic (potential) temperature flux

In addition, the following notation is applied:

Subscript 0 refers to values determined at the earth´s surface or within the surface layer.
Subscript h

Introduction

Environmental authorities need information and forecasts on the state, trends and impacts of pollutant concentrations at different scales. The complexity of the various processes affecting pollutant concentrations calls for the use of dispersion models. Air quality assessments using model results are required by different pieces of legislation on air quality. A key input to these models are the meteorological measurements, fields and parameters required to compute the transport, dispersion and removal of pollutants. Dispersion and removal (by dry deposition) of pollutants depend on atmospheric turbulence, but turbulence measurements per se are not routinely performed by the meteorological services. Thus, dispersion characteristics are either inferred from basic meteorological parameters such as wind, temperature and radiation using parameterization schemes or they are determined with specific models.

Assessments of air quality at the local or regional scale are required for a variety of purposes: emission control, air quality forecasts and implementation of legislation. For instance, within the framework directive on air quality assessment and management, models may be used to determine areas where air quality standards may be exceeded. Environmental impact assessments as part of licensing processes for industrial emitters usually require air pollution modelling. Since air pollutants cross borders and the European common market requires harmonized rules, it is important that the models used and developed by various organizations in different European countries provide comparable results. As a first step, this requires that the preprocessors or parameterization schemes embedded in the models are compared and the interpretation of their results are harmonized in a transparent way. It is also important to identify agreed data sets by which such preprocessors can be tested to compare their performance.

The COST Action 710 is a first and major initiative aiming at the intercomparison of some of the most important meteorological preprocessors for dispersion models used in Europe. Within this action, the work was divided between four different working groups:

(i) Surface energy balance
(ii) Mixing layer height
(iii) Vertical profiles of mean and turbulent quantities
(iv) Complex terrain

This document reports the findings of Working Group 2 on the mixing layer height. This COST action required an investigation on the mixing layer height because this height is a key parameter for air pollution models. It determines the volume available for the dispersion of pollutants and is involved in many predictive and diagnostical methods and/or models to assess pollutant concentrations close to the surface. The mixing layer height is not measured by standard meteorological practices, and moreover, it is often a rather unspecific parameter whose definition and estimation are not straightforward. Consequently, this report, although not exhaustive, reviews the various definitions of the mixing layer height, how it can be assessed, performs some intercomparisons between selected methods, and makes several recommendations concerning its definition, its theoretical and empirical determination as well as on the requirements for the validation of mixing height models. The analysis has been restricted to (at least locally) relatively flat and homogenous terrain.

1. Definition of the mixing height and its use in atmospheric dispersion models

1.1 The atmospheric boundary layer

The atmospheric boundary layer (ABL) is the layer where interactions take place between the earth's surface (which captures most of the incoming solar energy and redistributes it in different forms) and the large scale atmospheric flow (which is driven by this energy). This transfer of energy is partly accomplished by turbulent eddies. The ABL transfers not only sensible and latent heat but also momentum and atmospheric constituents between the surface and higher atmospheric levels.

This transfer of properties in the ABL is thus primordial for the dispersion of pollutants emitted mostly within the ABL. Moreover, the great importance of the exchange of many trace constituents (e.g., SO_2, NOx, O_3, CO_2, CH_4 and non-methane volatile organic compounds – NMVOCs) which are often emitted into or deposited from the atmosphere to terrestrial and aquatic ecosystems via the ABL has been recognized as one of the main links in global biogeochemical cycles. It is thus of primary importance to be able to understand, measure, parameterize, simulate and predict the structure and behaviour of the ABL.

Atmospheric turbulence is produced by two different mechanisms, namely wind shear and buoyancy. In the ABL, the main source of wind shear is surface friction, but there may be also wind shear due to baroclinity or certain mesoscale phenomena such as low-level jets, flow channelling or at the interface of different flow layers. Positive buoyancy is mainly produced by heating from the ground, sometimes also by radiative cooling of elevated (cloud) layers or by overturning of gravity waves. Negative buoyancy - as experienced by eddies under statically stable stratification – is an important sink for turbulent kinetic energy (TKE) in the atmosphere. The actual level of turbulence in the atmosphere is thus mainly the result of shear and / or buoyancy production, advection, buoyant destruction, and molecular dissipation.

The height h of the ABL is one of the fundamental parameters to characterize its structure. Measurements, parameterizations and predictions of the height of the ABL have many theoretical and practical applications such as the prediction of pollutant concentrations or of surface temperature, the scaling of turbulence measurements or the treatment of the ABL in numerical weather prediction and climate models.

It is beyond the scope of this report to give a very detailed description of the mean and turbulent structure of the ABL as well as on the variety of phenomena and processes to be observed within it. The interested reader may be referred to a number of textbooks on this subject which have been published in the last years (e.g. Arya, 1988, Stull, 1988, Sorbjan, 1989, Garratt, 1992, Kaimal and Finnigan, 1994). We will limit ourselves to briefly describing some basic characteristics of the ABL as far as it is necessary and helpful in order to understand the discussion in the following chapters as well as to introduce some basic concepts.

Two basic ABL-regimes can be distinguished according to the dominant production mechanism of the turbulence, namely the convective and the stable boundary layer.

Thermal heating induced by strong insolation causes positive buoyancy at the earth's surface and is the main source of turbulence in the convective boundary layer (CBL). In the CBL, organized convective structures (so-called thermal plumes) can be observed. They generate an intensive vertical exchange of energy and matter, and consequently all properties are rather well-mixed over most of the CBL. This mixing is often limited in its vertical extension by a stable layer (often an inversion) aloft, the height of which varies depending on the site and on the season. Typical values of this level over Europe range between a few hundred meters and 2-3 km above ground.

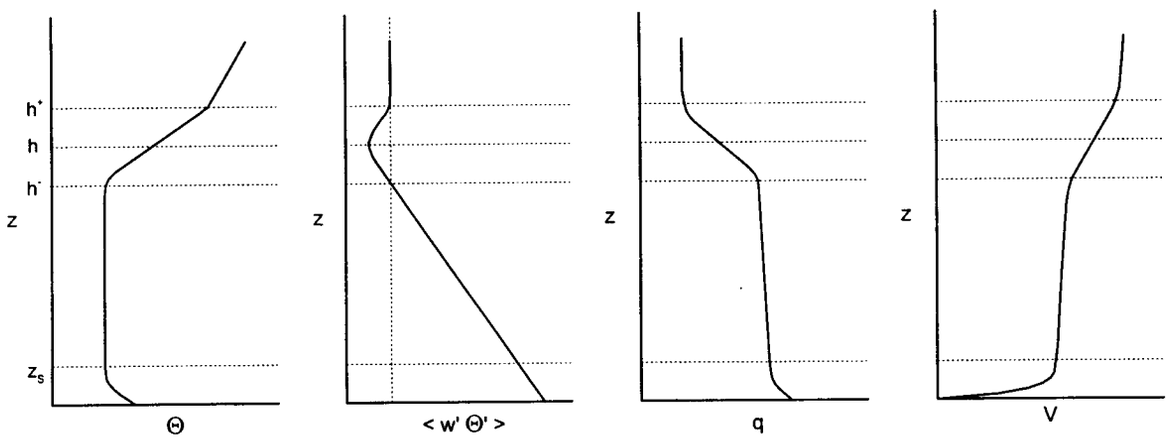

Figure 1: Idealized structure of the CBL.

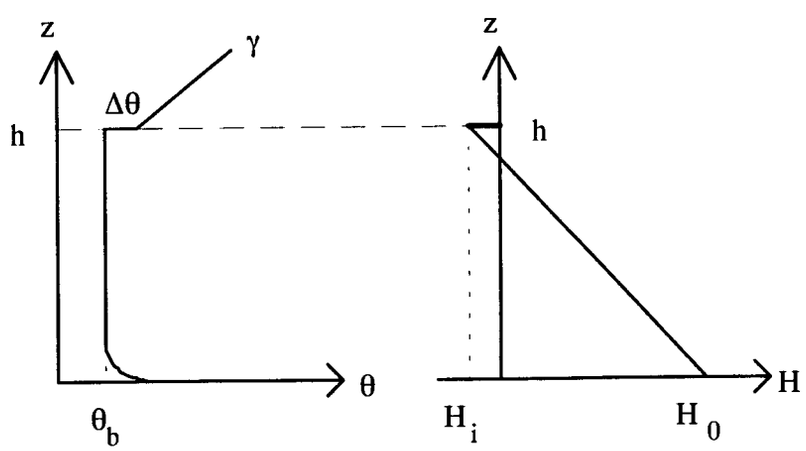

Figure 2: Idealized profiles of the potential temperature and the turbulent heat flux in a zero-order jump model of the CBL (Tennekes, 1973).

The typical structure of the CBL is sketched in Figure 1. Three different sublayers can be distinguished:

(i) The *surface layer* (SL) which covers about 5-10 % of the whole CBL. The SL is characterized by a super-adiabatic lapse rate, a decrease of specific humidity with height and a significant vertical wind shear. These features of the profiles of mean

meteorological variables can be, in most cases, well described by the Monin-Obukhov similarity theory (MOST). The turbulent fluxes of heat, moisture and momentum are assumed to be roughly constant with height in the SL.

(ii) The *well-mixed layer* (ML) embeds the major part of the CBL (50-80%). Within the ML, the vertical profiles of most mean meteorological variables are roughly constant with height due to the intensive vertical mixing. This especially holds for potential temperature but with minor restrictions also for specific humidity, concentrations of trace gases and aerosols, and for wind speed and wind direction.

(iii) The *entrainment layer* (EL), forms a transition zone between the ML and the stably stratified, quasi-nonturbulent free atmosphere above. It is characterized by two counteracting processes: the penetration of the most energetic thermals into the stable layer aloft, and the entrainment of warm and (in the absence of clouds) dry air from above into the ML. The EL is mostly defined in a horizontally or temporally averaged sense since the instantaneous transition zone between the ML and the free atmosphere can be quite thin. The EL comprises typically 10-30% of the total depth of the CBL, but can be even deeper than the ML, especially in the morning. Typical features of the EL are a strongly positive temperature lapse rate, a sharp decrease of specific humidity and sometimes significant vertical wind shear. Sharp gradients of aerosol and trace gas concentrations are also often observed across the EL. In so-called zero-order jump models, which are often used in practice, the depth of the EL is neglected (see Fig. 2).

The evolution of the CBL on clear, sunny days can be characterized by four basic stages (e.g., Carson, 1973; Stull, 1988; Garratt, 1992):

I Formation of a shallow CBL near the ground, starting with the morning insolation and growing gradually until the nocturnal surface inversion has been completely destroyed. The typical growth rate of the CBL-depth is 10...100 m/h.

II Rapid CBL-growth across the near-neutral residual layer of the previous day, up to the level of the capping inversion with a rate of 100...1000 m/h.

III Consolidation of the well-mixed CBL whereby its depth grows – if at all – only slowly, due to penetration of thermals into the stably stratified free atmosphere and influenced by large-scale vertical motions at the CBL-top.

IV Decay of the thermally driven turbulence and vertical mixing followed by the formation of a shallow stable layer close to the ground which converts the CBL into an elevated residual layer for the following day (see phase II).

Under stable conditions, in the absence of buoyant turbulence production, wind shear is the only mechanism creating turbulence, and stable background stratification associated with negative buoyancy will act as a sink for TKE. Therefore, in the stable boundary layer (SBL), a sensitive equilibrium exists between production and destruction of turbulence. Consequently, turbulence does not necessarily occur continuously but may have an intermittent or patchy character. Since the general level of turbulence is weak, other effects such as radiative cooling, gravity waves, advection or subsidence may also influence the structure of the SBL. Thus a great variety of SBL structure types can be observed.

The temperature profile in the SBL is strongly governed by longwave radiative cooling beginning at the surface and progressing upwards. Usually, this process results in the formation of a near-surface temperature inversion. Under conditions of weak pressure

gradients, weak surface winds and hence weak mechanical turbulence production, the strongest temperature gradients occur near the surface, and the vertical profile of (potential) temperature shows a curvature continuously decreasing with height (e.g. André and Mahrt, 1982; Stull, 1983a,b – see Fig. 3a). It can be described approximately by polynomial or exponential functions (Surridge and Swanepoel, 1987; Anfossi, 1989). Under such conditions it is very difficult to assess the height of the SBL.

If mechanical turbulence production is significant, at least two different regions can be distinguished within the SBL, as shown by observations and numerical modelling (Garratt and Brost, 1981; André and Mahrt, 1982; Wetzel, 1982; Estournel and Guedalia, 1985; see Fig. 3b). In the lower layer, the potential temperature profile is often characterized by a strong, nearly linear increase with height due to the interaction of radiative cooling of the earth surface and turbulent exchange. In the upper layer, radiative cooling of the atmosphere itself is the dominant mechanism resulting in a much weaker temperature gradient.

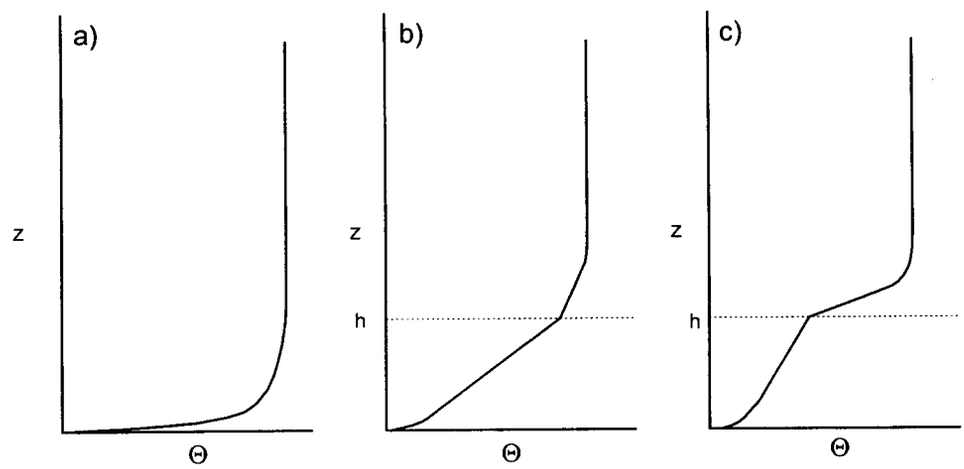

Figure 3: Typical vertical temperature profiles in the SBL; a) weak wind, strong stability; b) moderate wind; c) strong wind.

Under conditions of strong winds and weak radiative cooling, a layer with relatively effective mixing (though not really well-mixed) may be observed close to the ground. It is characterized by only a slight increase in potential temperature with height (Zeman, 1979; Roth et al., 1979; see Fig. 3c). This layer is capped by a quite shallow zone (10..30 m) with a very sharp, jump-like increase in temperature, followed by a zone of weaker stability aloft.

A common phenomenon connected to the SBL is the nocturnal low-level jet (LLJ). It is generated by an inertial oscillation of the ageostrophic wind vector in those layers that are decoupled from the influence of surface friction following the rapid decay of turbulence during the evening transition period (Blackadar, 1957). Its characteristic features are the appearence of a supergeostrophic wind speed maximum typically at heights between 100 m and 300 m and most distinctly apparent 4-7 hours after sunset (in midlatitudes), and a steady clockwise turning (in the Northern Hemisphere) of the wind vector (see Fig. 4). Wind shear below the LLJ axis may be as strong as $\approx 0.1\ s^{-1}$. The strength of the LLJ and the timing of its maximum intensity depend on the magnitude and phase of the ageostrophic wind component during the evening stabilization period. Due to small values of the ageostrophic wind component in the upper part of the daytime boundary layer and to the larger ageostrophic deviations near

the ground, the LLJ occurs first at higher altitudes, and subsequently descends with time thereby increasing in strength.

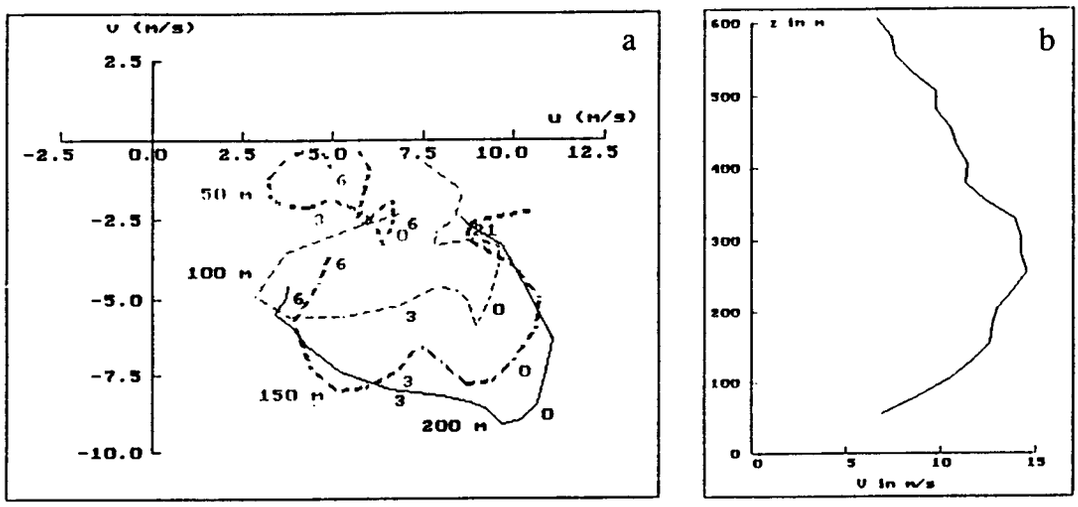

Figure 4: Example of a nocturnal low-level jet during the SANA field campaign at Melpitz in Eastern Germany, 31 Aug / 1 Sep 1991; a) hodographs at different levels; b) wind speed profile at 21 UTC (22 CET).

It should be remarked that this brief description of the ABL-structure only covers the idealized case of a non-disturbed ABL. The presence of clouds, mesoscale or synoptic scale perturbations (local wind systems, terrain heterogeneity or frontal activity) may result in considerable modifications of the ABL structure.

After having discussed these basic structural features of the ABL, we turn back to the problem of the ABL height. When dealing with pollutant dispersion problems, one needs to consider the layer over which pollutants are dispersed or mixed due to the prevailing atmospheric turbulence. This led to the concept of a mixing layer having a specific depth, whose definition and relation to the depth of the ABL will be discussed in the following section.

1.2 The concept of the mixing layer and definition of its height

Substances emitted into the ABL are gradually dispersed horizontally and vertically through the action of turbulence, and finally become completely mixed over this layer if sufficient time is given and if there are no significant sinks. Therefore, it has become customary in air pollution meteorology to use the term "mixed layer" or "mixing layer". On the other hand, since under stable conditions complete mixing is often not reached, e.g. for a plume from an elevated stack within the range covered by many dispersion models, the term "mixing layer" seems preferable, because it emphasizes more the process than the result. The term "mixed layer" shall be reserved for the well-mixed boundary layer typically encountered under sufficiently convective conditions. Obviously, the mixing layer coincides with the ABL if the latter is defined as the turbulent domain of the atmosphere adjacent to the ground.

However, other definitions of the ABL have also been used which may, e.g., include the domain influenced by nocturnal radiative exchange processes. The height (or depth –

depending on whether you look at it from below or from above) of the mixing layer is an important parameter in dispersion modelling and its determination is the subject of this report. It will be denoted by the short term *mixing height (MH)* and the letter h. Note that horizontal dispersion is not considered here, although, due to continuity, turbulent processes in the vertical always involve horizontal turbulent motion, too.

The practical determination of the MH, and sometimes even its definition, is not trivial, and there are many associated practical and theoretical problems. This is reflected in the following selection of definitions which have been given in the literature.

- The MH is defined as the height above the surface through which *relatively vigorous vertical mixing* occurs. (Holzworth, 1972)
- The MH refers to the *height* above ground *of the layer of the atmosphere adjacent to the surface* where vigorous mixing occurs as a *result of thermal and mechanical turbulence*. (Norton and Hoidale, 1976)
- In general h may be defined as the height up to which *significant turbulent transfer of heat, mass and momentum* between the local earth surface and the atmosphere occur when averaged over a *period of the order of one hour*. ... In air pollution meteorology, h is commonly known as the mixing depth. (Arya, 1981)
- The term MH is used ... to denote the level of a potential barrier to the dispersion of pollutants at the *interface between stable and less stable air* (Maughan et al., 1982).
- The mixing height, based on the temperature structure, can therefore be defined as the height at which a ground-based unstable to neutral vertical temperature profile becomes stable (Baxter, 1991).
- The MH (is) defined to describe the height to which the pollutants would mix over a *relatively short period of time, 1-2 hours* (Baxter, 1991).
- The MH defines the vertical extent of vigorous thermal turbulence *during daytime* heating and thus sets a limit to *upward mixing* of pollutants (Myrick et al., 1994).

It can be seen that these definitions represent quite different ideas on how to define the mixing height. It seems also that the MH definitions of different authors have to be seen in the context of the data available to them.

The definition we have adopted as a general guideline for our work is:

The mixing height is the height of the layer adjacent to the ground over which pollutants or any constituents emitted within this layer or entrained into it become vertically dispersed by convection or mechanical turbulence within a time scale of about an hour.

In order to proceed from this general definition to practical realizations, it is necessary to consider the structure of the stable and of the convective ABL.

Figure 1 depicted the structure of the CBL; the important feature with respect to the MH definition is the entrainment layer, a zone which is not well-mixed and where turbulence intensity declines from its bottom to its top. As shown in this figure, two extreme definitions h^- and h^+ for the mixing height are possible; the above definition corresponds to h^+. The most widespread definition, however, is the intermediate value h, often defined as the height where the gradient of the heat flux reverses its sign. It is usually applied for scaling purposes (e.g., to form the dimensionless vertical co-ordinate

z/h), and it is the definition closest to the thermodynamical CBL height definition in a zero-order jump model (i.e., a model where the thickness of the entrainment layer, $\Delta h_E = h^+ - h^-$, is neglected; see Fig. 2). Also the present report uses this definition in practical CBL applications, unless otherwise stated.. One should be aware, however, that turbulence extends beyond h.

The SBL can be divided into two layers: a layer of continuous turbulence and an outer layer of sporadic or intermittent turbulence. The corresponding MH values will be denoted h and h^+ (see Fig. 5). The layer of continuous turbulence with height h must not be confused with the surface layer which is the layer where MOST holds and which is a sublayer of the continuous turbulence layer. Since it is notoriously difficult to measure sporadic turbulence, and even more to develop a related scaling theory, h is the scaling height used in work with scaling the SBL. As in the convective case, however, this does not mean that turbulence is strictly confined to the region below h.

We encourage researchers to pay attention to which definitions of the MH or ABL height their work is based upon, and to specify it clearly. In this study, we have tried to do so with the notation introduced above.

Specific problem areas remain where the application of these definition has to be carefully discussed and possibly modified. We have not ventured to discuss and offer solutions for all of them. They include:

(i) The region of intermittent (sporadic) turbulence in the outer stable boundary layer (often related to (ii) and (iii)).

(ii) Regions of turbulence caused by the breaking of gravity waves under stable conditions.

(iii) Regions of turbulence generated by wind shear due to low level jets under stable conditions.

(iv) The entrainment layer at the top of the convective boundary layer.

(v) Situations with strong non-stationarity, e.g., the evening transition period between convective and stable conditions.

(vi) Situations with strong vertical transport into or within clouds, e.g., cloud venting of the CBL, or in frontal zones.

(vii) Situations where horizontal advection plays a major role, as in internal boundary layers.

(viii) Mountainous regions.

Further complication arises from the fact that slow fluctuations of the mean vertical and horizontal wind may occur in a laminar (nonturbulent) flow, often through gravity waves. They will not dilute a stack plume; but if mean concentrations averaged over periods at least comparable to the time scale of the fluctuations are considered, they will look as if diffusion had taken place. Since many air pollution models compute half-hourly or hourly mean concentrations, from a practical point of view, such pseudodispersion should be also included.

1.3 The role of the mixing height in dispersion models

The mixing height is a key parameter in models simulating the transport and turbulent diffusion of pollutants in the atmosphere. There are three major contexts in which the mixing height has to be known: the determination of the domain where turbulent dispersion takes place, the formulation of vertical profiles of turbulence characteristics (e.g., the standard deviations of the turbulent wind components), and the computation of concentration profiles with a reflective upper boundary condition.

1.3.1 Determination of the turbulent domain

Analytical dispersion models (e.g., Gaussian models) are based on the assumption that there is an atmospheric layer adjacent to the ground where turbulent dispersion takes place while there is no turbulence considered above this layer. The height of this layer is usually referred to as the "mixing height", irrespective whether pollutants emitted into this layer become well-mixed within short time or not. For receptors within the mixing layer, only pollutants whose effective source height is below the mixing height need to be considered.

On the other hand, fumigation (the entrainment of a reservoir layer of pollutants into a growing mixed layer) is usually not considered in these stationary models. Another situation where this approach becomes invalid is when a plume above the mixing height impinges on an obstacle, e.g. a hill or mountain slope.

A further complication is related to plume rise. Even if a stack is within the mixing layer, a sufficiently buoyant plume may rise above this layer, undergoing detrainment to a variable extent which determines the pollutant flux available for turbulent dispersion. While older models have often only crude algorithms to deal with this situation, more recent models try to treat the problem more accurately and especially aim at quantifying the portion of the pollutant flux that remains below the mixing height ("partial penetration"). These models require not only the mixing height as input, but also information on the vertical profile of stability.

Lagrangian puff (moving box) models are numerical models which follow an air parcel along its trajectory and simulate processes such as input from sources, vertical dispersion, dry and wet deposition, radioactive decay or chemical transformation. They often divide the simulation domain vertically into a (completely) mixed layer and one or more reservoir layers above, with a growth of the mixed layer into the reservoir layer(s) during the day and a sudden collapse of the mixed layer from a high convective value to a shallower mechanical value at the evening transition. It is essential for this type of models to specify the mixing height as a function of time and space.

1.3.2 Vertical profiles of turbulence characteristics

It is a typical property of advanced dispersion models to consider the vertical inhomogeneity of turbulence characteristics within the ABL (see, e.g., Gryning et al., 1987). Some models apply different formulae for the surface layer (SL) and for the rest of the ABL (outer layer), where the height of the SL is assumed to be 0.1 h. Analytical profiles are often used for quantities such as the standard deviation of turbulent velocity fluctuations or their Lagrangian time scales based on the similarity theory and thus related to the nondimensional vertical co-ordinate z/h. The formulation of vertical profiles is the task of Working Group 3 of COST-710, and details can be found in their report. Care has

to be taken that the definition of the mixing height used as model input, is consistent with what was assumed for the derivation of these profiles, though the difference between real situations and idealized situations to which these profiles refer has to be kept in mind.

The key scaling parameter for the convective boundary layer is the convective scaling velocity $w*$ which is proportional to $h^{1/3}$. Thus, in the CBL, not only the profile but also the intensity of turbulence depends on the mixing height.

In the case of models describing turbulent dispersion by means of the K-theory (flux equals K times the gradient, where K is the turbulent diffusivity), many K-profiles (such as the so-called O'Brien-profile, a polynomial depending on the value of K at the upper and lower boundary [O'Brien, 1970]) depend on its gradient at the lower boundary, and at the ABL height (or, in dispersion modelling language, the mixing height).

1.3.3 Computations of concentration profiles with a reflective upper boundary condition

It has been customary in many models to compute concentration profiles assuming complete reflection of the plume at the ground. This is justified for short-range dispersion models as deposition can often be neglected in this range; otherwise, suitable corrections can be applied. If a plume reaches the upper boundary of the turbulent domain, reflection is usually assumed there as well. In classical Gaussian models, this is achieved by adding "mirror sources" above the mixing height and below ground, in a number which depends on the strength of the vertical mixing, the source height, and the numerical accuracy desired. Other types of models can also realize this boundary condition by appropriate numerical techniques. Some simple models replace the reflective boundary condition by limiting the vertical standard deviation of the plume, σ_z, to $0.8\,h$. In all cases, the mixing height needs to be known.

2. Theories and methods to derive the mixing height from meteorological measurements

2.1 Theoretical background

The classical way of describing the structure of the ABL is through similarity theories (e.g. Kazanskii and Monin, 1960; Zilitinkevich and Deardorff, 1974) where the only influencing agents are rotation and buoyancy. It is generally assumed that the ABL structure depends on *external* parameters such as the Coriolis parameter and the surface roughness length z_0, and on *internal* turbulent parameters such as the surface momentum flux (proportional to the friction velocity $u*$) and the surface heat flux$<w'\Theta'>_0$. Classically, the ABL height is assumed to be a function of the length scales $L_E = u*/f$ and $L* = -u*^3/(\beta\kappa<w'\Theta'>_0)$. Zilitinkevich and Deardorff have also introduced the intrinsic ABL height h as a relevant scale since it embodies the effects of non-stationarity, especially under strong unstable conditions when the ABL grows quickly through powerful convective thermals. Then, according to this general similarity theory, the statistical properties of the ABL, nondimensionalized with the proper scales, depend on $h/L*$ and h/L_E.

However, depending on the distance from the surface at which one investigates the properties of the ABL, and on the stability conditions, certain scales may become irrelevant. Thus, the ABL can be subdivided into different domains each characterized by a set of scaling parameters (see Holtslag and Nieuwstadt, 1986). The neutral boundary layer is an asymptotic limit of the stable and the unstable regime. The different scaling regions are presented in Figures 5a and 5b for unstable and stable conditions, respectively, where the stability parameter $h/L*$ is the horizontal axis and the scaled height z/h is the vertical axis.

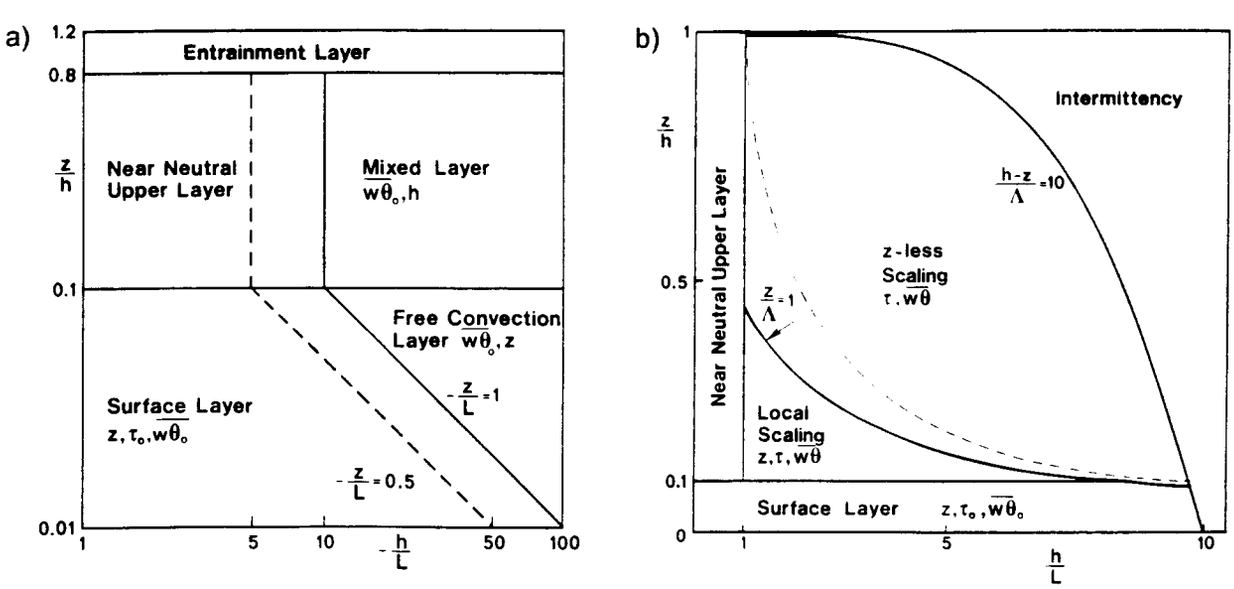

Figure 5: Scaling regimes in the ABL after Holtslag and Nieuwstadt (1986). a) CBL; b) SBL.

The unstable ABL is divided into five separate regions: the surface layer, the free convective layer, the near-neutral upper layer, the mixed layer and the entrainment layer. The basic scaling parameters are z, h and the surface momentum and heat fluxes, $\tau_0 = -\rho\langle w'u'\rangle = \rho u_*^2$ and $H_0 = \rho c_p\langle w'\Theta_o'\rangle = -\rho c_p\theta_* u_*$, where θ_* is the temperature scale. The stable domain differs from the unstable one with local scales expressed in terms of local fluxes prevailing in specific regions.

Kitaigorodskii (1988) and Kitaigorodskii and Joffre (1988) have extended these similarity theories to include the effect of the background stratification of the atmosphere and they demonstrated the relevance of a new length scale $L_N = u_*/N_{BV}$, with N_{BV} the Brunt-Väisälä frequency above the ML.

Solving the equations describing turbulent flows is constrained by the famous closure problem. In case of marginal turbulence, such as under stable conditions or close to the top of the boundary layer where turbulence has to perform work against the restoring force of gravity, it is practical to look at the turbulent kinetic energy (TKE) budget via the concept of the Richardson number. The so-called flux Richardson number Ri_f is the ratio of the buoyant production / destruction of TKE to generation by shear:

$$Ri_f = \frac{g}{T_0}\frac{\langle w'\Theta'\rangle}{\langle -u'w'\rangle\,\partial u/\partial z + \langle -v'w'\rangle\,\partial v/\partial z}.$$

Using the flux-gradient scheme for the parameterization of turbulent fluxes with the eddy diffusivity coefficients K_H and K_M for heat and momentum, respectively, and assuming K_H and K_M to be equal as a first approximation, Ri_f becomes the gradient Richardson number Ri:

$$Ri = \frac{g}{T_0}\frac{\partial\Theta/\partial z}{(\partial u/\partial z)^2 + (\partial v/\partial z)^2}$$

Theory and observation show that under homogeneous and quasi-stationary conditions, turbulence vanishes if the Ri number exceeds a critical value Ri_c which is around 0.25.

Substitution of the gradients by finite difference expressions leads to the bulk Ri_b number. The critical value of Ri_b can be different than that of the gradient Richardson number.

As described before, there are several obstacles for a detailed characterization and understanding of the ABL: it is not always well defined, turbulent fluxes are not routinely observed and by all means are seldom measured above the surface layer and turbulent characteristics are strongly non-homogeneous in time and space and even intermittent in certain domains and regimes.

Development of remote sensing techniques has enabled a certain breakthrough in the monitoring of turbulence intensity and of the ABL height. Active electromagnetic or acoustic wave probing responds to variable scattering properties of the turbulence through the inhomogeneities of the refractive index of the atmosphere. One important concept is the structure function D which can be simply parameterized in the spectral inertial subrange of turbulence:

$D(r) = \langle[S(z) - S(z+r)]^2\rangle = C_s^2\, r^{2/3}$

where C_s^2 is the structure parameter for the variable S and r is the separation between the two measurements. The index of refraction n is related to temperature T, moisture q and pressure p to varying degrees depending on the type of the remote sensor (basically the electromagnetic or acoustic frequency and signal). Thus, the magnitude of the returned signal gives C_n^2 from which estimates of C_T^2 , C_q^2 and C_p^2 can be derived (Lenschow, 1986; Wyngaard and LeMone, 1980). In the case of acoustic waves (sodar) and backscatter angles other than 180°, the structure parameter of the radial wind component is relevant, too.

2.2 Practical determination of the mixing height

Different ways exist to determine or to estimate the mixing height for practical applications. The most important ones will be described in the following sub-sections.

2.2.1 Determination of the mixing height from measurements

A detailed description of various methods and techniques for probing the ABL is given in Lenschow (1986). Special attention is given to remote sensing in Schwiesow (1986) and Clifford et al. (1994). A brief characterization of profiling techniques for MH determination can also be found in Weill (1982).

a) Mixing height estimations from radiosoundings

Radiosoundings are the most common source of data which can be used to determine the mixing height for operational purposes. Rawinsonde measurements extend well beyond the height of the whole ABL, they are widely distributed throughout Europe, and the data are continuously quality-controlled. On the other hand, it is a shortcoming of the sounding programme that, as a rule, at most of the stations, PTU-measurements are only taken twice daily at specified synoptic times. Consequently the soundings can only be used in order to have a reference level at launching time (00 UTC, 12 UTC) to be compared with model evaluations of the MH. Advanced meteorological preprocessors utilize information from both ground meteorological measurements and sounding profiles in order to better characterize the boundary layer structure and evaluate the MH, especially for convective conditions (e.g., Olesen et al., 1987, 1992). Other fundamental limitations of radiosoundings are the poor vertical resolution of standard aerological data with respect to boundary layer studies (see Appendix A3) and the loss of accuracy due to the sensor lag constant bounded with the ascent rate of the sonde. Due to the relatively high ascent rate, the radiosonde gives only a "snapshot"-like information on the ABL structure which might be of limited representativity. For research purposes, the use of special boundary layer sondes with shorter time constant of the meteorological sensors and a smaller balloon (i.e. a slower ascent rate) may partially compensate the shortcomings of sensor response.

Routine rawinsonde measurements can be analyzed to determine temperature inversion and temperature lapse conditions in the lower part of the atmosphere. Under convective conditions, the mixing height is often identified with the base of an elevated inversion or stable layer, or the height of a significant reduction in air moisture. Some authors recommend to take the inversion base altitude increased by half of the depth of the inversion layer as the characteristic CBL height (Stull, 1988).

Holzworth (1964, 1967, 1972) and others have developed objective methods (categories and summation techniques) to simplify and homogenize the analysis of the often

complex stratification of the ABL and to estimate the mixing height (under convective conditions). The basic idea of the "Holzworth method" is to follow the dry adiabate starting at the surface with the measured or expected (maximum) temperature up to its intersection with the temperature profile from the most recent radiosounding. Different refinements to this simple scheme have been suggested to account for temperature advection, subsidence and other effects (e.g., Miller, 1967; Garrett, 1981). It should be remarked, however, that this method strongly depends on the surface temperature, and a high uncertainty in the estimated MH value may result in situations without a pronounced inversion at the CBL top. Different authors pointed out that the MH determined by the "Holzworth method" is not strongly correlated with observed trace gas concentrations (e.g., Aron, 1983; Jones, 1985).

More recently, methods based on conserved variables were developed which permit analysis of air mass structures and vertical mixing (Betts and Albrecht, 1987). They involve the mixing ratio r (with liquid water r_T), the potential temperature Θ, the virtual potential temperature Θ_v, the equivalent potential temperature Θ_e, the saturation equivalent potential temperature Θ_{es} and the difference p^* between the actual pressure and the corresponding pressure of saturated air as calculated from observations of temperature, dewpoint and pressure.

Figure 6 shows an example of a typical 12 UTC (13 LST) sounding on a clear summer day with well-developed CBL. The top of the EL (~3000 m asl) is marked by a minimum of p^* and a maximum of Θ_{es} The base of the capping inversion (~2500 m asl) is characterized by a sudden decrease of p^* associated with a local minimum of Θ_{es}. The inversion itself shows a relatively constant, low value of p^* which is also found often in the presence of clouds.

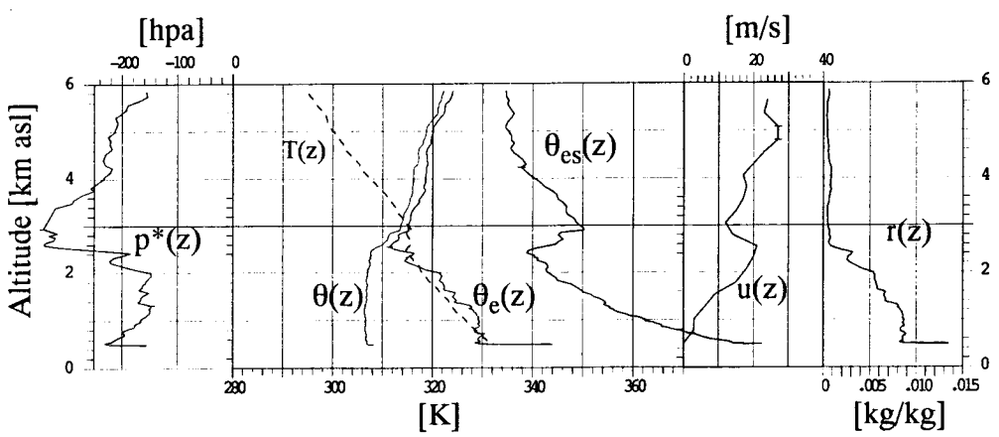

Figure 6: Typical summer daytime sounding (Payerne, Switzerland, 29 July 1993, 15 UTC) with profiles of the conservative variables suggested by Betts and Albrecht (1987). See text for explanations.

Betts and Albrecht (1987) have developed these criteria on the basis of averaged and smoothed profiles. They estimated that averaging the basic data at each 10 hPa pressure level best preserved the vertical thermodynamic profiles of the individual soundings. For the study of an individual profile, a refinement of the criteria is necessary to differentiate the main features from secondary stratification. Such a refinement has

been performed by Tercier et al. (1995) to determine the mixing height from radiosoundings in the POLLUMET field campaign.

Another popular approach is the use of bulk Richardson number methods (e.g., Troen and Mahrt, 1986; Holtslag and van Ulden, 1996). They differ mainly in the choice of the level for the near-surface temperature and wind, parameterization of shear production of turbulence in the surface layer, and the consideration of an excess temperature under convective conditions.

Parcel methods can be understood as a simplification of the Ri number methods where the shear contribution is neglected. Thus they are only suited for unstable conditions. Wotawa et al. (1996) applied a parcel model using vertical profiles of temperature and specific humidity and taking the MH as the height where the dry static energy of a lifted parcel equals the one at the starting (surface) level plus an eddy excess energy (see Section 3.7.2 of this report). This eddy excess energy is calculated from the surface fluxes of buoyancy and momentum using a mixed-layer scaling approach of Troen and Mahrt (1986), suggested also by Beljaars and Betts (1992).

Mixing height estimations based on (standard) radiosonde data may result in quite high uncertainties (e.g. Russell et al., 1974; Hanna et al., 1985; Martin et al., 1988). Special problems occur for the stable (nocturnal) boundary layer since no universal relationship seems to exist between the profiles of temperature, humidity or wind and turbulence parameters (heat or momentum fluxes, turbulent kinetic energy).

Mixing height estimation from tethered balloon or aircraft data is, in principle, not very different from the analysis of radiosonde data as long as the other measurement platforms also provide profiles of mean meteorological parameters. The possibility to carry out measurements of turbulent parameters or trace gas concentration profiles aboard an instrumented aircraft or by using special sondes under a tethered balloon offers additional possibilities for mixing height estimation from the shape or characteristic signatures of these profiles. The operation of both systems, however, is very expensive and therefore is not suited for routine applications.

A summary of the most popular methods and algorithms to derive the MH from direct vertical sounding data is given in Table 1. Simple numerical models are also included in order to illustrate the different criteria (definitions) proposed by various authors. The table is mainly descriptive. A critical assessment of the advantages and shortcomings of the most widespread techniques will be given in Section 2.3.

Table 1: MH determination from soundings or numerical model results. The type of MH as determined by each of the method is indicated by the symbols $\bar{h}$, h and $\bar{h}$ as defined in Section 1 (where possible).

Convective Boundary Layer (CBL)		
based on wind profile	based on temperature / humidity profiles	based on turbulence profiles
Height of a zone with significant wind shear in wind speed and / or wind direction	$\partial T/\partial z > 0$ (base of an elevated inversion) $\rightarrow \bar{h}$ (e.g. Deardorff, 1974; Baxter, 1991; Betts, 1992) $\partial\Theta/\partial z > 0$ (base of an elevated stable layer) $\rightarrow \bar{h}$ (e.g. Coulter, 1979; Hanna et al., 1985) $\gamma_\Theta < c_\gamma \gamma_{ad} \rightarrow \bar{h}$ (Garrett, 1981, c_γ =0.8) (Sasano et al., 1982, c_γ =0.6) Height at which a rising parcel becomes neutrally buoyant (e.g., Holzworth, 1967; Troen and Mahrt, 1986) Height at which moisture suddenly decreases (e.g., Melas, 1991; Lyra et al., 1992) Upper level of a layer with positive instability energy (Kuznetsova, 1989) h_{Ri}: $Ri \geq Ri_C$ with Ri_C =0.25 (Vogelezang & Holtslag, 1996)	$-\langle w'\Theta'\rangle$ = Max. $\rightarrow h$ (e.g. Deardorff, 1974; Weill et al., 1980) $\langle w'\Theta'\rangle = 0 \rightarrow \bar{h}$ (e.g. Gamo and Yokoyama, 1979; Sorbjan et al., 1991) Height at which ε suddenly decreases (Kukharets and Tsvang, 1979; Pekour, 1990) Local maximum of C_T^2 (e.g., Sorbjan et al., 1991) Significant decrease in vertical acceleration on an aircraft (Druilhet et al., 1983;, Hildebrand, 1988)

Table 1 (continuation)

Stable Boundary Layer (SBL)		
based on wind profiles	based on temperature / humidity profiles	based on turbulence parameters
$\partial V/\partial z$ = Min. or $\partial\alpha/\partial z$ = Min. $\rightarrow h^+$ (Wetzel, 1982; Coulter, 1990b)	$\partial T/\partial z$ =0 (top of the surface inversion) $\rightarrow h^+$ (e.g. Coulter, 1990)	h_τ: height at which some turbulence parameter has decayed to a few % of its surface layer value, e.g.:
$V = V_{max}$ (height of the LLJ axis) $\rightarrow h^+$ (e.g. Clarke, 1970)	$\partial\Theta/\partial z < 3.5$ K km^{-1} (André and Mahrt, 1982) or $\partial\Theta/\partial z = 0$ (top of a stable layer) $\rightarrow h^+$	$\tau = 0.10\,\tau_0$ (Nieuwstadt and Driedonks, 1979) $\tau = 0.05\,\tau_0$ (Caughey et al., 1979, Brost and Wyngaard, 1978, Zeman, 1979, Melkaya, 1987) $\tau=0.02\,\tau_0$ (Etling and Wippermann, 1975) $\tau=0.01\,\tau_0$ (Businger and Arya, 1974)
Height of the V minimum above the LLJ axis $\rightarrow h^+$ (Businger and Arya, 1974)	$\Delta\Theta=0.05(\Delta\Theta)_0$ (Delage, 1974) $\Delta\Theta=0.02(\Delta\Theta)_0$ (Stull, 1983a) $T(h)=(T_{max}-T_0)/e$ (Surridge &Swanepoel, 1987)	
Upper boundary of a layer of significant wind shear (Kitaigorodskii and Joffre, 1988)	Height up to which significant cooling can be recognized from a sequence of T profiles (Melgarejo and Deardorff, 1974)	h_{TKE}: $TKE = 0.05\,(TKE)_0$ (Tjemkes and Duynkerke, 1989)
	Height of the lowest discontinuity in the T profile $\rightarrow h$ (Hanna, 1969)	h_H: $\langle w'\Theta'\rangle = 0.10\,\langle w'\Theta'\rangle_0$ (Nieuwstadt and Driedonks, 1979)
	Height at which the Θ_v profile significantly starts to deviate from a linear curve $\rightarrow h$ (Wetzel, 1982)	$\langle w'\Theta'\rangle = 0.05\,\langle w'\Theta'\rangle_0$ (Brost and Wyngaard, 1978;, Caughey, 1982, Nieuwstadt, 1984a; Mel'kaya, 1987, Estournel and Guedalia, 1990, Derbyshire, 1990)
	h_{Ri}: $Ri \geq Ri_C$ with $Ri_C = 0.25$ (Garratt, 1982a) (Vogelezang & Holtslag, 1996) $Ri_C = 0.5$ (Mahrt et al., 1982)	$\langle w'\Theta'\rangle = 0.01\,\langle w'\Theta'\rangle_0$ (Yu, 1978)
		$\sigma_\alpha(i) = 1.5\,[\sigma_\alpha(i+1) + \sigma_\alpha(i+2)]/2$ (Kurzeja et al., 1991)

b) Mixing height estimation from remote sensing systems

In many countries remote sensing systems (lidars, sodars, wind profiling radars) are more and more introduced into operational application. They provide an interesting alternative for MH estimation. The basic advantages of remote sensing systems are the possibility of continuous operation and the fact that the systems do not cause any distortion or modification of the investigated flow.

Among the different remote sensing systems, the sodar is one of the simpler and less expensive systems, making it well suited for routine operation. The physical principle underlying the operation of sodars is the scattering of sound at small-scale inhomogeneities in the vertical profile of the acoustic refractive index. These are basically due to temperature inhomogeneities and can be the result of either turbulent fluctuations or of the local gradient of the mean temperature. The intensity of these inhomogeneities can be quantitatively characterized by the structure parameters of the refractive index C_n^2 and of temperature C_T^2, respectively, which hence determine the backscatter sound intensity measured with the acoustic sounder. Experimental studies as well as results of numerical models have shown certain typical features of the vertical profiles of C_T^2 under stable and convective conditions, which can be used to derive the MH from profiles of the backscatter intensity. In addition, sodar systems with Doppler capability allow determination of the mean wind and vertical velocity variance profiles which may also be employed for MH determination using idealized model assumptions. Methods and algorithms to derive the mixing height from sodar data are listed in Table 2 (where lidar and wind profiler are also included). A more comprehensive summary has recently been given by Beyrich (1994b, 1996). On the other hand, it must be remarked that the vertical range of most sodars is limited to a maximum of about 1 km; often it is much less. Nevertheless, MH estimates have been one of the "classical" applications of acoustic sounders for about 20 years.

Lidars allow the measurement of aerosol or trace gas concentration profiles and may therefore be considered to provide direct measurements of the MH. Since the top of a convectively mixed layer is often associated with strong gradients of the aerosol content, a simple aerosol backscatter lidar seems especially suited to determine the convective MH. The data analysis of differential absorption lidars, used to measure the concentration profiles of trace gases, requires an aerosol correction. This may result in quite high uncertainties of the derived gas concentrations in regions with strong changes of aerosol content and composition, i.e., just at the top of the ML. However, even the interpretation of data from aerosol lidars is not often straightforward, since it does not allow to decide whether the detected aerosol layers are really the result of ongoing vertical mixing or whether they originate from advective transport or past accumulation processes (e.g. Russell et al., 1974; Coulter, 1979; Baxter, 1991). Under stable conditions, problems in mixing height estimation from lidar data come from the fact that the vertical gradients in the aerosol content are much smaller than those at the top of the convective ML. Moreover, in the evening, it usually takes some time until a sufficiently clear discontinuity in the backscatter intensity profile develops at the top of the SBL, within the previously well-mixed layer (e.g., Russell et al., 1974).

Table 2: Criteria for MH estimation from remote sensing data

ABL Regime / Instrument	Stable Boundary Layer	Convective Boundary layer
Sodar	Upper boundary of the ground-based echo layer in the sodargram plot (e.g. Wyckoff et al., 1973; Arya, 1981; Pekour and Kallistratova, 1993) Decrease of echo intensity S below a certain threshold (Holets and Swanson, 1984; Tombach and Ettenheim, 1985) Maximum of $\partial S/\partial z$ (Piringer, 1988; Beljaars and Agterberg, 1988) Minimum of S above a zone of strong decrease (Klapisz and Weill, 1985; Dupont, 1991) Maximum of $\partial V/\partial z$ (Jones et al., 1984) Local maximum of σ_S / S (REMTECH, 1985)	Lower boundary of an elevated echo layer (Frisch and Clifford, 1974, Kaimal et al., 1982) Centre of an elevated echo layer, in case of strong height variability: upper envelope (Noonkester, 1976) Maximum of $\partial S/\partial z$ (Holets and Swanson, 1984; Beljaars and Agterberg, 1988) Secondary maximum of S (Weill et al., 1978; Sorbjan et al., 1991; Beyrich, 1995) Strong decrease of σ_w^2 (Best et al., 1986) Height of convective echo structures, multiplied by a certain factor (Singal et al., 1983; Walczewski, 1989) Extrapolation of w profile within convective plumes (Singal and Aggarwal, 1979) Similarity methods based on profiles of C_T^2, σ_w^2, λ_{max} (Weill et al., 1980; Kaimal et al., 1982; Melas, 1990, 1993; Seibert and Langer, 1996)
Windprofiler	Height at which C_n^2 has decreased to 5% of its maximum value (Connolly and Dagle, 1991)	Height of the elevated maximum of C_n^2 (Angevine et al., 1994; Dye et al., 1995)
Lidar	Height of first discontinuity in backscatter intensity profile(Dupont, 1991)	Height at which backscatter intensity rapidly decreases (Dupont, 1991; Jochum et al., 1991; van Pul et al., 1994)

A very promising device for direct and continuous measurement of the mixing height in a deep CBL seems to be the boundary layer wind profiler, especially the vertical profiles of backscattered signal intensity (Angevine et al., 1994; Gaynor et al., 1994; Dye et al., 1995). Similar to the acoustic sounder, the backscatter intensity of the electromagnetic signal is proportional to the structure parameter of the refractive index (in this case for electromagnetic waves) which depends on small-scale fluctuations and inhomogeneities of the temperature and moisture fields, whereby the influence of moisture is the dominant one. The vertical profile of C_n^2 usually shows a secondary maximum at the top of a well-developed CBL. However, the moisture profile is often not as well-mixed as that of temperature which may result in some ambiguity of the derived MH values. Additional problems occur in the presence of "fair-weather" cumulus clouds (even if only shallow) in the upper part of the ML.

The combination of different remote sensing systems (e.g. sodar + wind profiler or sodar + lidar) offers a promising way towards the direct and continuous monitoring of the evolution of the mixing height throughout the complete diurnal cycle (e.g., Beyrich and Görsdorf, 1995). However, it must be conceded that the interpretation of data measured with remote sensing systems is not always straightforward. On the other hand, this holds true also for the direct measuring systems and may (at least partially) be attributed to the general problem of MH definition as discussed in Section 2.2.1.

c) Other empirical methods

Another indirect estimation of the MH described in the literature is based on measurements of concentration changes of the non-reactive noble gas radon, which is basically emitted from natural sources by exhalation from the soil (Guedalia et al., 1980; Nicolas et al., 1985, 1988). However, as pointed out in Guedalia et al. (1980), such measurements do not allow a direct estimate of the MH but rather provide a value which might be called an "equivalent mixing height" characterizing the overall dispersion conditions.

Similarly, attempts have been reported to estimate the MH from simultaneous measurements of SO_2 ground concentration and the total column depth (e.g., Cappellani and Bielli, 1995). This method assumes the SO_2 mixing ratio to be either constant with height or to follow a specific profile inside the ML and the complete absence of SO_2 above the ML. It is obvious that such a method will be applicable only for certain regions and very specific atmospheric conditions and even then large uncertainties have to be expected.

2.2.2 Comparison of different empirical methods for the determination of the mixing height

Considering the great variety of methods for MH estimation from measurements, experimental results on the relationship between MH values derived from different sounding systems should be briefly discussed. Table 3 presents an overview of the characteristics of these systems with respect to operational MH determination.

Table 3: Measuring platforms and methods for MH determination

Method	Advantages	Shortcomings	Examples
direct measuring techniques / sensor platforms			
Radiosonde	- routine ascents for many years all over the world, therefore especially suited for climatological studies - measured data transmitted via international communication networks with very short time delay, therefore well suited for operational use - compatibility with measurements in the free atmosphere	- crossing the ABL along a slanted path within a few minutes, provides a "snapshot"-like profile - limited height resolution of routine ascents - operationally only 2-4 soundings per day at fixed times, even during field experiments higher sequence than 1.5-3 hours not possible - tracking problems at low levels (site-dependent)	Holzworth, 1964, 1967 Norton and Hoidale, 1976 Gutsche and Lefebvre, 1981 Bernhardt et al., 1982
Tethered balloon	- ascent velocity can be chosen according to the desired vertical resolution - turbulence and trace gas concentration measurements possible	- limited to field campaigns, no unmanned operation - synchronous profile measurement difficult - limited measurement range, casually below 500 m - not possible in cases of high wind speed or strong convection	van Gogh and Zib, 1978 Hayashi, 1980 Batchvarova and Gryning, 1994 Derbyshire, 1995
Mast	- installation of a large number of different sensor types possible including detailed turbulence measurements - continuous operation	- very high installation / operation costs - limited range: 200-300 m - high vertical resolution requires a high number of sensors (increasing costs)	Kottmeier, 1982 Kurzeja et al., 1991 Cabauw Tower (NL) Boulder Atmospheric Obs. (USA)

Table 3 (continuation)

Aircraft and Remote Sensing Techniques			
Aircraft	- possibility to operate many different sensors, including mean meteorology, chemistry, and turbulence sensors, as well as remote sensing systems - provides spatial information, admirably suited for mesoscale studies	- high costs, only for special field studies - operation mostly limited to daylight hours - lowest flight level subject to restrictions (security)	Druilhet et al., 1983 Hildebrand, 1988 Jochum et al., 1991
Radar / Windprofiler	- ground based and aircraft based operation possible (for radar only) - alternating RHI/PPI-Scan for 3D-studies (for radar only) - high sampling rate and continuous operation	- lowest range normally not below 200 m - limited vertical resolution (50-250 m) - expensive - frequency allocation problems within Europe - interpretation not always straightforward	Noonkester, 1976 Kaimal et al., 1982 Connolly and Dagle, 1991 Angevine et al., 1994
Lidar	- ground-based and aircraft-based operation possible - alternating RHI/PPI-Scan for 3D-studies - high sampling rate - return signals originate directly from aerosols ("pollution")	- expensive - unattended operation often not possible for safety reasons - limited range resolution and lowest range gate - tracer necessary (gas, aerosol) - interpretation sometimes ambiguous	Sasano et al., 1982 Boers et al., 1984 Hashmonay et al., 1991 Dupont, 1991 McElroy and Smith, 1991 van Pul et al., 1994
Sodar	- relatively simple, not very expensive: suited for unmanned long-term operation - high temporal and vertical resolution	- limited sounding range (500-1000 m) - sensitivity to environmental noise - noise contamination to the environment - interpretation requires experience, sometimes ambiguous	Russell and Uthe, 1978a,b Nieuwstadt, 1984b, Jones, 1985 Singal, 1988 Beyrich, 1993,1994b,1995

A complete agreement between MH values derived from different sounding systems cannot be expected *a priori* due to several reasons, the most important ones being:

- The description of the structure of the ABL can be based on mean meteorological variables (temperature, humidity, wind) or on turbulent parameters (fluxes, variances, TKE, structure parameters). Vertical profiles of the different parameters are influenced in a different way by the processes occurring at the earth's surface. In addition, a lot of turbulent and non-turbulent processes (heating and cooling, convection and subsidence, radiation processes, baroclinity, advection, gravity waves, phase changes of water) interact with each other within the ABL and influence the vertical profiles. It is often difficult, if not impossible, to separate the various contributions to the observed structure of the ABL. On the other hand, the different sounding systems measure different atmospheric parameters with varying height resolution and accuracy.

- Especially under stable conditions, when the intensity of turbulence is relatively weak, it might be very difficult to find a clear upper boundary of the ML or ABL. Vertical profiles (of turbulent parameters) are sometimes smooth without any clear signatures together with an asymptotic decrease towards values close to zero which are typical for the residual layer. In such cases, selecting different threshold values to define the upper boundary of the ML may result in considerably different MH values.

a) CBL mixing height measurements using different sounding systems

Comprehensive experiments to compare MH values derived from different measurement systems (radiosonde, sodar, radar, lidar, aircraft) under convective conditions have been described e.g. by Russell et al. (1974), Noonkester (1976), Coulter (1979), Kaimal et al. (1982), Baxter (1991) and Marsik et al. (1995). These studies show that the relative differences are mostly less than 10 %, provided that the elevated inversion capping the well-mixed CBL is not too weak and has a well-defined lower base. Conclusions on possible systematic deviations between different estimates of the MH are not consistent (except for the lidar – see below). This should be attributed to different criteria applied to analyze the profiles as well as to the often limited number of observations and in some cases also to spatial differences between the sites where the different systems had been operated. Comparing radiosonde or tethered balloon data with sodar observations, van Gogh and Zib (1978), Russell and Uthe (1978a,b), and Beyrich (1995) found no systematic differences, while Wyckoff et al. (1973), Tombach and Chan (1976), and Fanaki (1986) reported slightly higher MH values derived from temperature profiles, whereas Coulter (1979) found just the opposite.

In cases of a weak inversion or a not perfectly mixed CBL, measurements from different systems and even the analysis of the same potential temperature profile by several experienced meteorologists may easily result in relative differences of 25 % or even larger (e.g., Hanna et al., 1985; Martin et al., 1988).

MH values derived from lidar measurements have generally been found to be slightly but systematically higher than values derived from temperature profiles or sodar measurements (e.g. Coulter, 1979; Hanna et al., 1985; Gerasimov et al., 1988; Martin et al., 1988; Dupont, 1991). This is basically explained by the fact that the most energetic convective plumes penetrate into the stable or inversion layer thereby transporting aerosols up to levels higher than the mean height of the inversion or stable layer base. Under certain conditions, pollutants trapped within the stable capping inversion or free atmosphere can cause a systematic overestimation of MH values from lidar observations

(McElroy and Smith, 1991). On the other hand, Sasano et al. (1982) found no systematic differences between lidar observations and MH values derived from radiosoundings, which might be due to the criterion that they applied to deduce the MH from the potential temperature profile (cf. Table 1). Also van Pul et al. (1994) found a high correlation between MH values derived from lidar measurements and radiosoundings.

b) SBL mixing height measurements using wind and temperature profiles

The comparison of MH values derived from different observing systems under stable conditions is much more difficult. This is due to certain features of the structure and evolution of the SBL the most important ones are briefly mentioned here:

1) Static stability acts as a sink for turbulent kinetic energy. This results in a sensitive equilibrium between the mechanical production of TKE and its destruction by the stable stratification (leading to the sometimes intermittent character of turbulence in the SBL).

2) The generally weak intensity of turbulence under stable conditions renders it difficult to measure turbulent quantities (fluxes, variances) with sufficient accuracy.

3) Other processes determining the structure of the SBL (gravity waves, advection, radiative cooling, drainage flows over sloped terrain, inertial oscillations of the wind vector) are often of a magnitude comparable to that of turbulent processes.

4) The time scales of most of the relevant processes are much longer than in the CBL. Therefore, the SBL is often far from stationarity.

Due to these peculiarities, the structure of the SBL may be quite different depending on the dominant processes (see also Section 1.1) that are considered when deriving criteria for the MH determination or when comparing different estimates of the MH under stable conditions.

A comparison of different SBL height scales derived from temperature and wind profiles (and in some cases also considering modelling results) is described in e.g. Hanna (1969), Yu (1978), Mahrt and Heald (1979), Mahrt et al. (1979, 1982), Arya (1981), and Wetzel (1982). In most cases a good correlation between the depth of the ground-based inversion and the height of the stable layer top was found. On the contrary, no significant relationship exists between the height scales based on the temperature profile and the height of the low-level wind maximum. This is basically due to the different time evolution of the temperature and wind profiles during the night. Thus, the surface inversion under undisturbed meteorological conditions normally grows with time due to continuous radiative cooling (see e.g. besides the above Anfossi et al., 1976; Klöppel et al., 1978; Stull, 1983a; Godowitch et al., 1985).

On the contrary the axis of the nocturnal low-level jet, seems to exhibit more of a tendency to descend during the night, although the observations are sometimes contradictory (e.g. Beyrich and Klose, 1988; Mahrt et al., 1979; Godowitch et al., 1985; Smedman, 1988). From the analysis of wind profiles measured in the early stage of the nocturnal boundary layer evolution, Mahrt (1981a) concluded that *"the boundary layer depth ... (is) a continuous, although rapidly decreasing function of time"*. Numerical model simulations (e.g. Delage, 1974; Dörnbrack, 1989) also show – at least for stationary external conditions (with constant cooling rate and geostrophic wind) – a decrease of the height of the nocturnal wind maximum as it can be expected from the theory of the nocturnal inertial oscillation (Blackadar, 1957). However, non-stationary

forcing, advection or baroclinity may cause a different behaviour. Normally, a temperature-derived SBL height scale is smaller than the height of the wind maximum at the beginning of the night, whereas towards its end the opposite often holds true. Godowitch et al. (1985) observed the subsidence of the wind maximum below the top of the surface inversion around midnight at midlatitudes. Numerical simulations by Delage (1974) showed the same feature about 6-8 h after the initialization of the model from neutral conditions.

Thus, strictly speaking, the structure and the evolution stage of the SBL should be considered when deriving the stable MH from temperature or wind profiles, or when comparing MH values derived from different observing systems under stable conditions. This, however, has rarely been done in those studies reported in the literature.

c) SBL mixing height estimations based on turbulence data

The derivation of conclusions regarding the temporal evolution of MH estimates for the turbulent SBL and their relationship to MH values derived from mean profiles is even more complicated. The main reason is that detailed profile measurements of turbulent quantities under stable conditions are scarce in the literature. In addition, a great variety of definitions and criteria for the turbulent SBL height can be found in the literature (Stull, 1983a: "*There appear to be as many definitions of the SBL depth as there are investigators*").

Caughey (1982) pointed out, that *"there is no simple relationship between the SBL depth and the depth of the surface inversion layer. As this layer deepens and becomes more intense, (the depth of significant turbulent exchange) decreases, i.e. significant turbulence exchange becomes confined to a shallow layer close to the ground"*. Similar observations have been reported by Garratt (1982a) and Smedman (1991). Kurzeja et al. (1991) found a good correlation between the top height of the surface inversion and a turbulent SBL height derived from profile measurements of the wind direction standard deviation at the beginning of the night and in general between the latter height and the height of the wind maximum under strongly stable conditions. These results suggest that the relationship between different characteristic height values depends on the type of structure of the SBL as already concluded above.

Model calculations often show an increase of the SBL height defined by the turbulence profile or a different time behaviour during different phases of the SBL evolution (e.g., Nieuwstadt and Driedonks, 1979; Bes'chastnov, 1984). Nevertheless, even the generalization of model simulations with respect to different turbulent SBL height criteria is quite difficult. Model simulations using a one-dimensional ABL model with an algebraically approximated second-order closure (Dörnbrack, 1989) have shown that the turbulent MH scales (derived from the vertical profiles of heat flux, momentum flux, and turbulent kinetic energy) exhibit both a different behaviour in time and a different relationship between each other, depending on the external conditions (Beyrich, 1994b).

Another turbulent SBL height scale, which has been determined empirically from profile measurements by several authors is the level at which the gradient Richardson number *Ri* exceeds its critical value. However, there is still some controversy about the numerical value of the critical Richardson number. The proper choice depends to some extent on the height resolution of the profile data from which the *Ri*-number is derived. Comparisons with other SBL height scales suggest a closer relation between a *Ri*-number based SBL height and the height of the wind maximum than between the former one and the

depth of the surface inversion. In general, the *Ri*-number based SBL height is lower than the height of the wind maximum since a decrease of vertical wind shear resulting in supercritical *Ri*-number values normally occurs somewhere below the axis of the low-level jet.

Thus, it is clear, that the question which of the SBL height scales suggested in the literature is best suited to characterize the vertical mixing of pollutants under stable conditions has not received yet a final answer. The level at which the turbulent heat flux has decreased to 5 % of its surface layer value is often used as a definition of the MH under stable conditions. Mason and Derbyshire (1990) deduced from large-eddy simulations (LES) that *"if radiative heat transfer is negligible, the flux of heat is roughly analogous to that of contaminants emitted from low level sources, and so definitions of SBL depth based on the buoyancy flux profile are easy to relate to a 'mixing depth' appropriate for dispersion applications"*.

d) SBL mixing height values derived from remote sensing data

Among the remote sensing instruments, solely the acoustic sounder seems capable in providing MH data under stable conditions (Joffre, 1981). Radar profilers and lidars have mostly a range resolution which does not allow to resolve the SBL in detail. In addition, their first usable range gate is often at or above the SBL top, a fact which sometimes even limits the application of a conventional sodar (Garratt, 1982b; Smedman, 1988; Baxter, 1991). But even the interpretation of sodar data in terms of MH determination under stable conditions is controversial (Hanna, 1992: *"Have you ever carefully looked at time series of h observations by Doppler acoustic sounders – I believe that they are very unreliable"*).

Results from a comparison of sodar measurements with MH values derived from temperature and wind profiles are quite inconsistent. Correlation coefficients of the sodar-based MH and the height of the nocturnal wind maximum are typically in the range between 0.3 and 0.65 (Arya, 1981; Hanna et al., 1985). A lot of authors report on comparisons between sodar observations and the height of the nocturnal surface inversion. No systematic differences were found by Hicks et al. (1977), Singal and Aggarwal (1979), Hayashi (1980), or Fitzharris et al.(1983). Singal et al. (1985) reported reasonable agreement in only 30 % of all cases for long-time observations over five years. However, in their study there was a spatial separation of about 20 km between the sodar site and the radiosonde starting point. Some authors concluded that the sodar-based MH is generally lower than the surface inversion height (Nieuwstadt and Driedonks, 1979; Bacci et al., 1984; Klose and Schäke, 1991). Piringer (1988) found agreement with the top of the lowermost strongly stable layer of a layered surface inversion. Gland (1981) concluded that there is *"no evident connection between ... the form of the pattern of echo intensity and inversion features"*. A similar conclusion was drawn by Dohrn et al. (1982).

Comparisons of sodar observations with turbulent MH scales have been described in only very few case studies. Nieuwstadt and Driedonks (1979) as well as Tjemkes and Duynkerke (1989) reported a reasonable agreement between sodar data and the height at which sensible heat flux or turbulent kinetic energy have decreased to 5 % of their surface layer values, which was deduced from model simulations. However, Nieuwstadt and Driedonks (1979) remarked, *"that it is not clear, whether the height where the heat*

flux vanishes is completely equivalent to the boundary layer height found from the acoustic sounder registration".

Comparing MH values derived from simultaneous sodar and lidar operation, good agreement was found by Dupont (1991) and Devara et al. (1995) for a small number of case studies in a simply structured SBL. Van Pul et al. (1994) found a high correlation between the SBL height derived from lidar measurements (based on the first gradient in the backscatter profile) and radiosonde profiles (first significant level in the potential temperature profile).

Beyrich and Weill (1993) have demonstrated that the relationship between a sodar derived value for the stable MH and any other height scale strongly depends on the stage of the SBL evolution. They concluded that different criteria have to be applied to derive a MH value from sodar signal intensity profiles depending on the actual shape of these profiles. Beyrich (1994a) demonstrated that a well-developed nocturnal low-level jet governs the time evolution of the stable MH especially in the second half of the night.

Comparing ozone profiles measured with a tethered balloon and sodar data under conditions of a complex structured SBL, Beyrich et al. (1996) reported a generally good agreement of the MH values derived from both systems.

2.2.3 *Determination of the MH by modelling and parameterization*

Continuous profile measurements for the operational determination of the MH are not generally available. Therefore, both simple parameterizations based on standard surface observations and / or single profile data, as well as numerical models are widely used in the practice of meteorological and environmental services.

Model simulations or parameterizations certainly do provide numerical values of the MH with desired resolution in height and time. However, each model or parameterization scheme has to be considered as an (over-)simplification of the reality. Hanna et al. (1985) found that the root mean square errors of MH values derived from numerical models were often twice as large as the observed MH variability. The situation with respect to numerical models may have improved since, as nonhydrostatic models with a few kilometres horizontal resolution and turbulence closures based on a prognostic equation of the turbulent kinetic energy are widespread research tools nowadays and will be used as operational NWP models in the future (see, e.g., Schlünzen, 1994). However, we are not aware of a systematic comparison of MHs dervied from such models with those derived from observations. It is intrinsic to these models that they are prognostic, and unless for-dimensional variational data assimilation is applied, they will not be able to make full use of existing observations. Even these contemporary 3-dimensional numerical models are not able to simulate the structure of the ABL in all its complexity, and their application to a long time series still is hampered by the massive computational requirements. Their use is justified especially in situations with strong horizontal inhomogeneities.

One-dimensional models with (local) turbulence closure of the order of 1.5, 2 or in a few cases even higher have been used by different authors over the last 20 years in order to estimate the height of the stable turbulent boundary layer (e.g. Delage, 1974; Wyngaard; 1975, Brost and Wyngaard, 1978; André et al., 1978; Rao and Snodgrass, 1979; Nieuwstadt and Driedonks, 1979; Mel'kaya, 1987; Dörnbrack, 1989; Tjemkes and Duynkerke, 1989; Estournel and Guedalia, 1990). They were also employed to justify or determine the parameterization constants appearing in simple diagnostic formulae for

the SBL depth. However, the variety of methods and the rules which were applied to define the SBL height is quite large (see Table 1, Section 2.2.1). In addition, the model results have rarely been compared with comprehensive observational data sets. Nevertheless, they could be considered an alternative to oversimplified parameterizations, especially if coupled to observations.

Simple diagnostic or prognostic parameterization equations for the MH are still very attractive for operational purposes because of their simplicity and the limited number of required input data. They are also used within comprehensive parameterization schemes for the treatment of the ABL in some numerical weather prediction and climate models.

a) Modelling and parameterization of the MH in stable conditions

Parameterizations of the height of the turbulent stable boundary layer (SBL) have been the subject of numerous theoretical and experimental activities within the last 25 years, and a lot of equations have been suggested in the literature (e.g. Hanna, 1969; Zilitinkevich, 1972; Etling and Wippermann, 1975; Arya, 1981; Mahrt, 1981b; Nieuwstadt, 1984b; Koracin and Berkowicz, 1988; Singal, 1990).

Both diagnostic and prognostic relationships have been proposed and there has been a controversial debate on the use of either the one or the other type of equations (Nieuwstadt, 1981, 1984b; Garratt, 1982a,b). The evolution of the SBL is highly nonstationary, especially during the first hours after sunset, but even later during the night a quasi-stationary regime is approached very slowly, if at all. A prognostic equation which contains all relevant mechanisms governing the structure and evolution of the SBL should be superior to each diagnostic relationship in modelling the MH evolution under stable conditions. However, comparisons of different diagnostic and prognostic relationships with observations do not clearly favour the one or other type. For practical use it is also helpful that diagnostic equations do not require an initial value of the MH as input.

A second controversy has been whether it is possible to parameterize the SBL height solely based on surface layer measurements (mainly $u*$, $L*$), or whether bulk SBL parameters (Θ_h–Θ_0, V_h, Ri_b) should be considered additionally or even exclusively (e.g., Mahrt, 1981b; Garratt, 1982b; Smedman, 1991; Vogelezang and Holtslag, 1996).

A comprehensive survey of suggested parameterizations for the SBL height is given in Appendix A1. The most popular diagnostic equations are

$$h = c_1 \, u* \, / \, |f|$$

and

$$h = c_2 \, (u* \, L* \, / \, |f|)^{1/2}$$

which both have been derived from the equation for the Ekman layer depth and by using scaling arguments. There are several reasons to use these equations with caution, even if most of the verification studies done in the past do not seem to favour the application of more elaborated parameterizations.

The most important objections are:

- The Ekman layer concept has been originally derived for a stationary, neutral boundary layer.

- It seems physically questionable to consider $1/f$ as the only relevant time scale and as one of the most relevant independent parameters.

As an alternative to using $1/f$ as time scale, some authors (e.g., Kitaigorodskii and Joffre, 1988) have suggested to use $1/N_{BV}$ (cf. Eqs. A1.1.10 and A1.1.11 in Appendix A1.1), replacing the latitude dependent time scale by a stability-dependent one. This model has been corroborated by measurements in the Arctic (Overland and Davidson, 1992), by Lidar measurements in the Netherlands (van Pul et al., 1994), and by LES-computations (Vogelezang and Holtslag, 1996).

Another type of diagnostic equations considering the bulk structure of the SBL is based on the assumption that turbulence production must vanish at the top of the SBL and the Richardson number must therefore exceed its critical value. This results in an equation of the type

$h = Ri_c (\Delta V)^2 / (\beta \, \Delta\Theta)$

Equations of this type proposed in the literature differ basically in the choice of the levels over which ΔV and $\Delta\Theta$ are determined and in the value of Ri_c (cf. Eqs. A1.1.17 to A1.1.20 in Appendix A1). Joffre (1981) found that the value of Ri_c depends on the parameter $h\,f / u_*$ with the classical value of 0.25 being relevant for small values of $h\,f / u_*$ (≤ 0.1, i.e. small rotational effect), but large values of $Ri_c \sim 7$ can be reached when $h\,f / u_* \geq 0.3$ (see also Maryon and Best, 1992).

The prognostic equations which have been proposed to parameterize the SBL height often describe a relaxation process during which h approaches a certain equilibrium value h_e. The speed of this process is governed by a time scale T_h. Their general form is:

$$\frac{dh}{dt} = \frac{(he - h)}{\tau_{SBL}}$$

The equilibrium height h_e is often parameterized through one of the two diagnostic equations given above. The characteristic time scale has been proposed to be proportional, e.g., to the inverse of the Coriolis parameter $1/f$, to a combination of surface layer scaling variables such as L_*/u_*, or to the inverse of a normalized cooling rate $\Delta\Theta \, (\partial \, \Theta_0 / \partial \, t)^{-1}$, where $\Delta\Theta$ is $T_h - T_0$.

The verification of such diagnostic or prognostic relationships has long been performed with the aid of radiosonde data (e.g., Hanna, 1969; Yu, 1978; Mahrt and Heald, 1979; Wetzel, 1982). Since the early Eighties, sodar observations have increasingly been used for this purpose (e.g. Arya, 1981; Nieuwstadt, 1984b; Koracin and Berkowicz, 1988; Beyrich, 1993, 1994b). The prognostic equations have rarely been tested at all and only single case studies are reported in the literature. For the diagnostic equations, correlation coefficients typically range between 0.4 and 0.7, quite often with large scatter. Also, the numerical constants appearing in all the parameterizations vary considerably, and it seems difficult to recommend any universal and site-independent value. In addition, the problem of separating "within-night" and "between-night" variability of the SBL height (André, 1982) has not found proper consideration in most of the studies. Hence, there is still a need for verification studies of the different SBL height parameterizations using comprehensive data sets.

b) Modelling and parameterization of the MH in convective conditions

A few diagnostic relations based on similarity theory have also been suggested to parameterize the depth of the convective boundary layer (e.g., Tennekes, 1970; Zilitinkevich, 1972; San José and Casanova, 1988). However, these are valid only under certain conditions (e.g. free convection) and are not of much practical relevance.

Today, the integration of mixed-layer slab models is a well established way to simulate the evolution of the convective MH. It provides reliable results if thermal heating is really the main driving force of the CBL evolution. These models use values of the surface heat flux and friction velocity as well as an initial temperature profile as basic input parameters. The latter one represents a general problem for the application of such models, since normally the network of radiosounding stations is not dense enough for boundary layer studies (which is not the basic goal of performing radiosoundings !), and the representativity of a given station depends much on the surrounding terrain. This is a non-negligible limitation considering the orography and landscape patchiness typical of large parts of Europe.

Prognostic equations describing the growth of the CBL are normally derived from a parameterization of the TKE budget equation which is either averaged over the whole mixed layer or specified at the ML top. The equations proposed by various authors mainly differ in which terms in the TKE budget equation have been neglected and how the remaining terms are parameterized. The spectrum ranges from simply considering surface heating as the only relevant driving force (Betts, 1973; Carson, 1973; Tennekes, 1973) to additional consideration of

- mechanical turbulence production due to surface friction (Tennekes, 1973; Driedonks, 1981; 1982b)
- local changes of TKE at the level z=h (so-called "*spin-up*" effect, Zilitinkevich, 1975b),
- wind shear across the entrainment layer (Stull, 1976a; Driedonks, 1981; Manins, 1982; Rayner and Watson, 1991)
- explicit parameterization of TKE dissipation (Zeman and Tennekes, 1977),
- and finally rather complex equations taking also into account energy losses in connection with gravity waves (Stull, 1976c; Zilitinkevich, 1989a) or the influences of moisture and advection (Steyn, 1990).

A survey of relationships suggested in the literature to describe the ML growth during daytime is given in Appendix A2. Comparisons of different relationships from Appendix A2 with observational data are described by, e.g., Driedonks (1981, 1982b) or Arya and Byun (1987). These studies as well as sensitivity experiments carried out by Beyrich (1994b) have shown that the observed variability of the MH during daytime can be, as a rule, well described if surface heating and mechanical turbulence production due to surface friction are taken into account. Driedonks and Tennekes (1984) pointed out that *"encroachment handles 80 % of the problem, a crude parameterization of* $\langle w'\Theta' \rangle_h$ *adds about 10 %, further refinements tend to get lost in the unavoidable inaccuracies of most experiments ... (and upper) mechanical turbulence production terms (accounting for inversion layer wind shear) can be neglected, because they are more trouble than they are worth"*

The two effects of surface heating and friction are properly parameterized in the following two equations:

$$\frac{dh}{dt} = A\frac{<w'\Theta'>_0}{\Delta\Theta} + B\frac{{u_*}^3}{\beta h \Delta\Theta} = \frac{A w_*^3 + B u_*^3}{\beta h \Delta\Theta}$$ (Driedonks,1982a)

and

$$\frac{dh}{dt} = (1+2A)\frac{\langle w'\Theta'\rangle_0}{\gamma_\Theta h} + 2B\frac{u_*^3}{\gamma_\Theta \beta h^2} = \frac{(1+2A)w_*^3 + 2Bu_*^3}{\gamma_\Theta \beta h^2}.$$

(Gryning and Batchvarova , 1990a).

The values for the constants A and B which are given in the literature differ considerably, ranging between 0 and 1 (for A) and 0 and > 10 (for B) (see, e.g. Stull, 1976a; Heidt, 1977; Dubosclard, 1980; Young, 1988; Zilitinkevich, 1989a and Sorbjan et al., 1991).

Many authors use A=0.2 as a typical value (e.g. Tennekes, 1973; Yamada and Berman, 1979; Driedonks, 1982b; Zilitinkevich, 1989a). However, recent experimental results from different climatic regions suggest a higher typical value of $A \approx 0.4$ which better fits observations of mixed-layer growth (e.g. Tennekes and van Ulden, 1974; Clarke, 1990; Betts, 1992; Culf, 1992).

If mechanical turbulence production is neglected, the constant A represents the ratio between the entrainment layer and surface layer heat fluxes: $-\langle w'\Theta'\rangle_h$ / $\langle w'\Theta'\rangle_0$. Carson (1973) pointed out that this ratio is not constant throughout the day. He therefore suggested the use of different values for A corresponding to different stages of the CBL evolution (see also Bonino et al., 1989). Garrett (1981) proposed a seasonal variability of A for operational application.

For B Tennekes (1973) proposed B=2.5, a value used later also by Kolarova et al. (1989) or Gryning and Batchvarova (1990a). Driedonks (1981, 1982b) achieved the best agreement with observations using B=5, a value which was also applied by, e.g., Chong (1985) and Zilitinkevich et al. (1992).

The possible ranges for A and B reported in the literature significantly affect the simulated CBL growth. It has been demonstrated by Beyrich (1994b) that a variation of their values over the typical range reported in the literature results in differences of the simulated evolution of the MH much larger than those which would originate from an application of a more complex equation (see Fig. 7). Beyrich (1995) therefore suggested to adapt the model constants to actual observations (e.g., from sodar or wind profiler data) to improve the model output results.

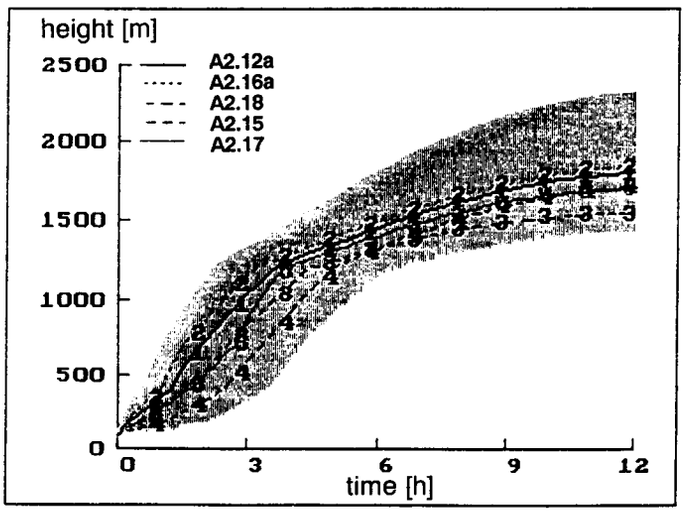

Figure 7: Growth of the CBL according to formulae of varying complexity (lines denoted with the number of the respective eqs. in the Appendix) and varying the constants A and B within their range given in the literature (shaded area). Adapted from Beyrich (1994b).

Another type of model for the simulation of the CBL development has been developed by Liechti and Neininger (1993). This model was originally aimed at supporting soaring flight forecasts and is designed to give also parameters such as the magnitude and vertical extension of updrafts in thermals and the development of capping cumuli. Its speciality is the consideration of mountainous terrain: it allows for heat input from slopes, and considers vertical advection compensating the mass transport in the convection elements, effects which are important in Alpine valleys. The model is entirely numerical, one-dimensional (but using the area-height-distribution of the terrain), and makes use of empirical findings about thermals instead of dynamic equations. It is used operationally at the Swiss Meteorological Institute.

2.2.4 Determination of the MH from NWP model output

Dispersion models for the regional scale or for long-range transports often derive the mixing height from NWP model output. This may also be considered for the local scale if suitable measurements are not available at the site under consideration. It is obvious that methods and their reliability depend on the degree of sophistication of the ABL parametrization and on the vertical resolution of the boundary layer within the NWP model. Results reported here thus cannot claim universal validity.

A procedure to determine h from the output of HIRLAM, the limited area model used in the Nordic and some other European countries, is implemented at the Danish Meteorological Institute. It is based on a bulk Richardson number derived from the model level data.

$$Ri_b(h) = \frac{gh}{\Theta_{vl}} \frac{\Theta_v(h) - \Theta_{vl}}{U(h)^2 + V(h)^2}$$

where Θ_{v1} is the virtual potential temperature at the lowest model level (about 30 m above ground). This formula is consecutively applied for $h = z_2, z_3, ...$, where the z_i are the model levels. The actual value of h is chosen as the height where Ri_b reaches a critical value. A value of 0.25 was selected after applying the method to radiosoundings with a clear convective lid.

The performance of the method in situations without convective lid, especially when the mixing height is determined by purely mechanical turbulence, has not yet been investigated.

At the U. K. Met. Office, a study to determine the boundary layer height h from vertical profiles obtained form NWP for use in NAME (the Met. Office's long range transport, dispersion and deposition model for nuclear accidents) was undertaken by Maryon and Best (1992). Model boundary layer heights as diagnosed by six different methods were tested against radiosonde measurements at noon and midnight from continental Europe and Izmir in Turkey over the period 13 October to 6 November 1992. In total, 51 profiles with a well defined boundary layer height were studied.

Four of the methods, based on identifying the level at which a critical gradient *Ri*-number equal 1.3 is reached, gave generally poor results, underestimating h particularly for the daytime boundary layer. The four methods differed in their interpolation schemes between sub- and super-critical levels. The critical value is usually taken as 0.25, but for the diagnosis from NWP model output a value or 1.30 was assumed in this study. A best-fit procedure yielded a value Ri_c=7.20, but the improvement was limited. The 5th method (Middleton , 1993) was also unsatisfactory.

On the other hand, a simple parcel method (see also below and Section 3.8) gave large improvements: for noon soundings, the rms error was reduced from about 450 m to about 340 m and the bias was reduced from about 270 m to 70 m. The MH was defined as the lowest model level with a potential temperature exceeding the surface value. An addition of +1.2K to the surface temperature minimized the error.

The EMEP MSC-W model has recently introduced another method to derive mixing heights from HIRLAM output (Jakobsen et al., 1995). The mechanical mixing height is defined as the lowest level where the vertical turbulent diffusion co-efficient K_M is less than 1 m^2s^{-1}, with K_M determined by the method of Blackadar (1979) from the Richardson number. The convective mixing height is the height of the adiabatic layer, after the sensible heat input of one hour has been distributed via dry-adiabatic adjustment. The largest one of the two values is used as the mixing height.

Another method has been applied by Wotawa et al. (1996) for their Lagrangian ozone prediction model which is based on ECMWF output. They determined a mechanical mixing height from the friction velocity provided by the model, using Eq. A1.1.3. However, one has to take into account that the model turbulent drag contains also a parameterized component representing the pressure drag exerted by subgrid orography. The proportionality factor c_1 between $u*/f$ and h must therefore be chosen adequately (0.07 instead of the typical values around 0.25). This applies to the ECMWF model version which was used in 1994; in the new parametrization of the mountain drag introduced in 1995, $u*$ seems to be comparable to its common range of values. A convective mixing height was computed by Wotawa et al. (1996) from the temperature and humidity profiles and the respective surface fluxes with the parcel method of Beljaars

and Betts (1992; see also Section 3.7). Under unstable conditions, the maximum of the mechanical and the convective mixing height was used.

2.3 Critical evaluation of existing methods for mixing height estimation

Strictly following our definition given in Section 1.2, the MH should be determined by investigating the dispersion process of non-reactive tracer gases. However, this is a very expensive task and therefore not possible for operational purposes. The analysis of concentration profiles of atmospheric trace constituents may be considered as the best approach for MH estimation. On the other hand, vertical mixing is not the only process determining such profiles. A misinterpretation is therefore possible in certain cases, that may be avoided by a close sequence of vertical soundings. Nevertheless, concentration profiles are not generally available on a routine basis.

Considering turbulent diffusion as the most relevant mixing process, profile measurements of any turbulent parameter should therefore be the next choice of data for mixing height estimation, but these are not performed at most places. Thus, MH determination is based in most cases on profile measurements of mean meteorological variables such as wind, temperature and humidity.

In any case, MH determination from measurements requires vertical profiles of atmospheric parameters within the lower troposphere. These profiles should satisfy the following conditions:

- They should cover the layer between a few tens of meters above the earth's surface and about 2-3 km above ground, considering the typical height range over which the MH varies during its annual and diurnal cycles in Europe.
- The profile measurements should be available with a time resolution of about 1 h or less in order to properly describe the non-stationary evolution of the mixing height, especially during the morning and evening transition phases.
- The measured profiles must have a vertical resolution of about 10-30 m to avoid relative uncertainties of more than 10-20 %, especially for low MH values (< 250 m).
- The measured parameters should be linked physically to the process of dispersion and vertical mixing of pollutants.

The most widespread methods and algorithms to derive the MH from sounding data were briefly summarized in Tables 1 and 2 (see Section 2.2.1). The advantages and shortcomings of the different sounding systems were summarized in Table 3.

Table 4 indicates which of the above-mentioned requirements are fulfilled by the different sounding systems. It clearly appears that none of the systems meets all the requirements, i.e., the *"MH-meter"* does not exist. Reliable mixing height determination under all conditions is therefore still an unsolved problem (e.g., Berkowicz, 1992).

Table 4: Critical assessment of different methods to determine the MH.
✓ fulfilled; (✓) partly fulfilled; — not fulfilled.

	Continuous data output	Lowest level close to the ground, high resolution < 200..500 m	Range of 2-3 km covered	Determination of turbulence parameters or trace gas conc.
In-situ measurements:				
Radiosonde	—	(✓)	✓	—
Tethered balloon	—	✓	—	(✓)
Mast	✓	(✓)	—	✓
Aircraft	—	—	✓	✓
Remote sounding:				
Lidar	(✓)	(✓)	✓	✓
Sodar	✓	✓	—	✓
Radar	✓	—	✓	✓
RASS	(✓)	(✓)	—	(✓)
Numer. models	(✓)	(✓)	✓	✓

3. Computer routines to derive mixing height values

3.1 The OML meteorological preprocessor

The meteorological preprocessor of the Danish dispersion model OML contains a module for the mixing height calculation. It is described in detail in Olesen et al. (1987, 1992). Each hour, the module computes a mechanical and, during daytime, a convective mixing height and selects the larger one as the actual value. A minimum value of 150 m is applied, however.

The mechanical mixing height is calculated as $h = 0.25\ u*/f$ (Eq. A1.1.3 in Appendix A1).

The convective mixing height is obtained from the integration of the prognostic equations (A2.8b) and (A2.9) with the numerical values $A = 0.2$ and $B = 5$ for the constants. It starts with the observed temperature profile, normally from the 00 UTC radiosounding, and uses observed or parameterized hourly values of $u*$ and H_0. The initial values of the mixing height and the temperature jump through the entrainment layer are determined from the heat flux during the hour in which the heat flux first becomes positive and from the temperature gradient near the ground, respectively. If a so-called convective lid is found in the noon sounding, the calculated convective mixing heights before noon are multiplied by the ratio of the base height of this lid to the calculated mixing height for 11 UTC. The integration in the afternoon is continued with the profile from the noon sounding. If a so-called sustained lid is found also in the following midnight sounding, the interpolated lid height is used as an upper bound for the mixing height.

3.2 The HPDM meteorological preprocessor

The role of the meteorological preprocessor of the Hybrid Plume Dispersion Model (HPDM) is to produce time series of hourly values of the surface heat and momentum fluxes and of the mixing depth, using observations of wind speed, cloudiness, surface roughness length, surface moisture availability and albedo. This preprocessor accepts a wide variety of possible input data. It uses boundary layer theory to solve the surface energy balance, determines the mixing depth using upper air data, and derives vertical profiles of wind, temperature and turbulence. If observations of these derived variables, including the mixing depth are available, they can be used directly in the model. However, the preprocessor in its standard form does not accept observed fluxes. The source code had thus to be modified in the present study in order to use measured fluxes.

HPDM uses the following formulae to estimate the mixing height (Hanna and Chang, 1991):

- *Night-time*: The interpolation formula of Nieuwstadt (1981), based on $u*$, $L*$ and f is used (A1.1.2).
- *Daytime*: During daytime, two separate mixing heights are calculated. One is obtained with Carson's (1973) prognostic formula (A2.8) which parameterizes the entrainment heat flux as a fraction A of the surface heat flux ($A = 0.2$). A second MH is calculated, according to a suggestion of Weil and Brower (1983), considering solely the growth rate of the CBL due to mechanical turbulence. This MH is obtained from the relation

$$h^2\,\Theta_{t_0}(h) - 2\int_0^h z\Theta_{t_0}(z)\,dz = 2\frac{B}{\beta}\int_0^t u_*^3(t')\,dt',$$

where $\Theta_{t_0}(z)$ is the initial potential temperature profile, and a value of 2.5 is used for the constant B. Finally, the larger value is taken as the convective mixing height.

- *Neutral conditions (irrespective of the time of the day)*: The u_*/f formula (A1.1.3) is used with the constant $c = 0.3$; neutral conditions are defined as Pasquill-Gifford stability category D. The stability category is computed from L_* and z_0 using Golder's (1972) relations.

Details of HPDM (version 4) and its meteorological preprocessor are described in a set of three papers (Hanna and Paine, 1989; Hanna and Chang, 1992 and 1993). The 1992 paper presents improvements of the meteorological parameterizations (version 4.2). The present study was based on version 4.4 which, however, is identical to version 4.2 with respect to the parameterizations used in the meteorological preprocessor.

3.3 The meteorological preprocessor library of Servizi Territorio

The HPDM and OML meteorological preprocessors were developed in connection with specific dispersion models and also specific data organization. The idea of Servizi Territorio was to offer a library of subroutines as a flexible tool which can be applied in different environments. One set of subroutines is provided for the computation of the ABL parameters. The following alternative routines are included for MH computation:

a) convective mixing height (daytime):

- the so-called encroachment model (Stull, 1989) - Eq. (A2.4) in Appendix A2;
- the mixed-layer growth model proposed by Gryning and Batchvarova (1990) - Eq. (A2.12a) in Appendix A2.

Both routines assume a constant lapse rate above the top of the ML (single value which will be used throughout the day), to be taken from an early morning temperature sounding. The other input parameters are the time history of the air temperature, the friction velocity and the sensible heat flux near the surface. The number of time steps for the calculation can be chosen.

b) neutral and stable mixing height (night-time)

- Nieuwstadt (1981) - Eq. (A1.1.2a) in Appendix A1
- Zilitinkevich (1972) - Eq. (A1.1.6) in Appendix A1 with $c = 0.4$
- Clarke (1970) - Eq. (A1.1.3) in Appendix A1

If $L_* < 0$, only the Clarke's formula (u_*/f) can be used. In all the formulae, f is set to 10^{-4} s^{-1}, but partly absorbed into the constants.

3.4 The FMI Routine

The module used for the evaluation of the boundary layer height h at the Finnish Meteorological Institute (FMI) is described in detail in Karppinen et al. (1996, 1997).

a) Wintertime situations

In wintertime in Finland the boundary layer is mostly stable or near neutral, even during daytime, and h can be estimated as a function of the friction velocity (Deardorff, 1972):

$$h_t = s_t\, u_{*t} \text{ with } s_t = s_0 + (s_{12} - s_{00})\,\frac{t}{12},$$

where the subscript t refers to the sounding times (t = 00 and t = 12). The parameters s_{00} and s_{12} are calculated from the boundary layer heights h_{00} and h_{12} estimated from the respective vertical temperature profiles. The friction velocities (as well as the H_0 and L*) are estimated with an energy balance method according to van Ulden and Holtslag (1985) with slight modifications (see report of Working Group 1).

b) Summer night situations

A summer night is defined as the period when the ABL is stable; in addition there have to be unstable sections at both ends of the nocturnal period. After sunset the thickness of the developing shallow inversion h_{inv} is assumed to keep increasing through the course of the night (see Fig. 8) according to

$$b\, h_t\, (\Theta_M - \Theta_t) = g_t,$$

where g_t is the area under the h vs. Θ curve which is expressed as (Stull, 1983a, 1983b)

$$g_i = \int_o^{t_i} (\Theta_* u_*)\, dt,$$

Assuming the parameter b to be constant during the whole night, h becomes

$$h_t = h_{00}\,\frac{g_t\,(\Theta_M - \Theta_{00})}{g_{00}\,(\Theta_M - \Theta_t)},$$

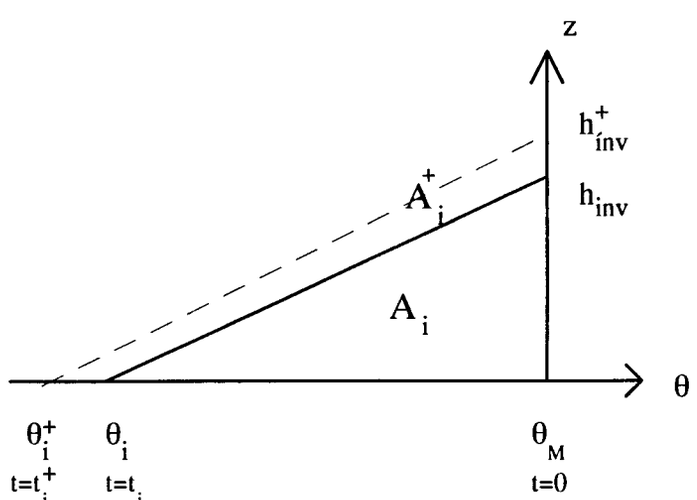

Figure 8: The evolution of nocturnal surface inversion.The boundary layer height is taken to be a linear function of the surface inversion height ($h_{\text{inv}} = bh$)

where Θ_M is the mean potential temperature of the unstable boundary layer during the previous evening (at sunset), Θ_{00} is the respective temperature at 00 UTC, and h_{00} is the boundary layer height estimated from the midnight sounding.

During the first hours after sunset the inversion depth is usually small (< 50 m) and the neutral boundary layer equation A1.1.3 is used with c_1 = 0.2 (van Ulden and Holtslag, 1985). If the height h given by this equation is larger than that of the previous evening's unstable boundary layer prevailing at sunset (t_{00}) the latter value is used in the model.

c) Summer days

Daytime is defined by an upward turbulent heat flux.

The evolution of the unstable boundary layer is simulated by the set of differential equations (A2.1)–(A2.3) (Tennekes, 1973; Driedonks and Tennekes, 1984), to be solved numerically. This system of equations is closed by estimating $\partial h/\partial t$ by

$$\frac{dh}{dt} = C_f w_M / (C_t + Ri_M)$$

where C_f = 0.2 and C_t = 1.5, and $Ri_M = \beta h \Delta\Theta / (w_M{}^2)$. The convective velocity scale w_M is defined by (with c_τ = 25):

$$w_M = (w_*^3 + C_\tau u_*^3)^{1/3}$$

If γ_Θ is very small or if γ_Θ = 0, the solution of the preceeding equations is not physically meaningful. In that case a simple encroachment model (Tennekes, 1973) is used:

$$t_M = \frac{h_0(\Delta\Theta)_0}{g_{\delta t}}, \text{ where } g_{\delta t} = \delta t^{-1} \int_0^{\delta t} (-\Theta_* u_*)\, dt$$

On the other hand, the unstable boundary layer height can be evaluated as

$$h_{\delta t} = \frac{h_0(\Delta\Theta)_0 + g_{\delta t}\delta t}{(\Delta\Theta)_{\delta t}}$$

where the temporal evolution of the inversion strength is assumed to be linear, i.e.

$$(\Delta\Theta)_{\delta t} = (\Delta\Theta)_0 (1 - \delta t / t_M)$$

The initial values of the parameters are calculated using analytical solution for h according to Carson (1973) and Wyngaard (1988) which is Eq. A2.8b in the Appendix with A = 0.2, and

$$\Delta\Theta(t) = \tfrac{1}{7}\gamma_\Theta h(t).$$

After solving the equations for the whole period, the height h is compared to the 12 UTC sounding and corrected if necessary. The solution of the equations is continuously checked against the potential temperature observed at 2 m (Θ_2). If the calculated boundary layer potential temperature $\Theta_b \geq \Theta_2$, and Θ_2 starts to decrease despite the fact that the situation should be unstable, the calculation is stopped (e.g., in the case of a strong cold air advection). The 12 UTC sounding is then used to estimate the mixing height for the remaining period. If the sounding shows that the situation is not unstable as had been suggested by the energy budget method but stable instead, u_*, Θ_*, and L_* are replaced by profile estimates obtained from the lowest layer of the 12 UTC sounding data.

3.5 The RODOS preprocessor

MET-RODOS is a comprehensive atmospheric transport and diffusion module, designed for operational use within the real-time, on-line emergency management system RODOS (Mikkelsen et al., 1996). It contains a sub-system for the computation of local-scale wind fields and micro-meteorological scaling parameters (Deme et al., 1996; Mikkelsen and Desiato, 1993). The mixing height can be calculated from NWP model output utilizing the bulk Richardson number method (Section 2.2.4) with Ri_c = 0.25, or from measurements. The determination of the MH from measurements, which was tested here, is based on the following routines:

During daytime, the mixed-layer growth model proposed by Batchvarora and Gryning (1991; see Eq. A2.14) is used. The integration starts with an initial value of h equal to 50 m; the lapse rate is taken from the previous midnight sounding. Additional input parameters are $u*$, $L*$ and T_0 (the heat flux is implicitly contained in these parameters).

The MH during night is calculated with Nieuwstadt's (1981) formula (Eq. A1.1.2a) from $u*$, $L*$ and f.

In the case of an upward heat flux during night or a downward heat flux during day, the MH is calculated using Eq. A1.1.3 with c = 0.3.

In addition, if a strong inversion (lid) is found above 150 m a.g.l., the MH is calculated using a bulk Richardson number (Eq. A1.1.17) with 3.0 as the critical Ri-number. If this lid is lower than the MH calculated otherwise, it is taken as the MH. The lid height is not interpolated in time.

3.6 Methods based on Richardson numbers

Two different methods based on Richardson numbers have been tested both under stable and convective conditions. Richardson number methods are described in the Appendix in the section on SBL methods because they were primarily developed for stable conditions.

3.6.1 Standard method

The method is described in Section 2.2.4 for NWP model output and was applied to significant level radiosonde data in the same way as it would be applied to model level data. Basically, it is the application of A1.1.17 (using virtual potential temperatures) with a value of 0.2 for the critical Ri number.

3.6.2 Vogelezang and Holtslag's method

The method by Vogelezang and Holtslag (1996, hereafter referred to as the VH method) uses a bulk Ri number between the top of the surface layer (or a fixed level such as 20 m or 40 m) and the top of the ML. Shear production in the SL is parameterized by an additional term depending on $u*$. For unstable situations, an excess temperature as suggested by Troen and Mahrt (1986) and described in Section 3.7.2 (with C_1 = 8.5) is added to the near-surface temperature. The formula is included in Appendix A1 as Eq. 1.1.18 (without the excess temperature).

3.7 Parcel methods for the CBL

Parcel methods determine the mixing height as the equilibrium level of a hypothetical rising parcel of air representing a thermal. They differ in how the temperature of this air parcel is found, and in the thermodynamical variable used to define the equilibrium level. In this study, two different methods have been used; they are illustrated in Figure 9.

3.7.1 Simple parcel method

The simple parcel method, introduced in principle by Holzworth (1964), uses the virtual potential temperature at the lowest level (ground level) of a radiosounding without adding any excess temperature. The MH is taken as the equilibrium level of an air parcel with this temperature.

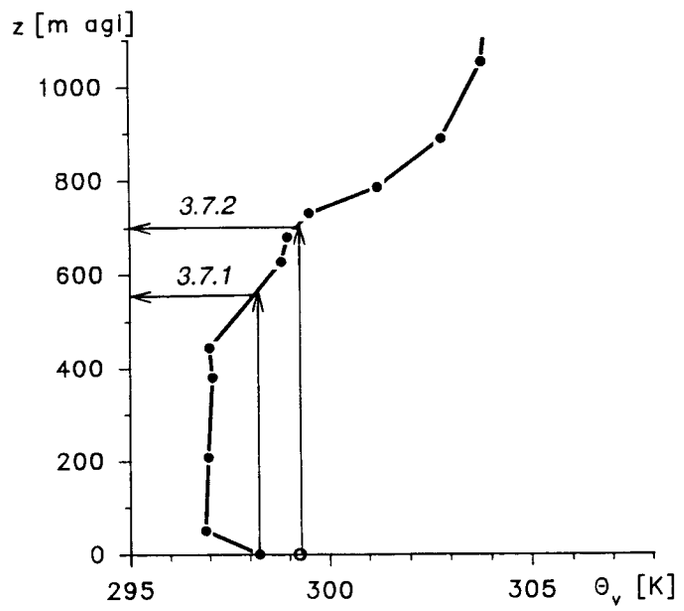

Figure 9: Illustration of the two parcel methods used to derive the MH in the CBL from radiosoundings. The simple parcel method 3.7.1 uses the virtual potential temperature at ground level, while according to the advanced method (3.7.2) an excess temperature is added to this temperature

3.7.2 Advanced parcel method

This method is based on the paper of Beljaars and Betts (1992) and has also been applied (with slightly different values of the constants) by Wotawa et al. (1996). The thermodynamical variable used by these authors is the dry static energy s, defined as $c_p\Theta$, whereas in the present study the virtual potential temperature $\Theta_v = \Theta\,(1 + 0.61r)$ was used. The temperature of the parcel is given as the temperature near the ground plus an excess temperature. This excess temperature is calculated as

$$\delta\Theta_v = \frac{C_1 < w'\Theta'_v >}{\sqrt[3]{u_*^3 + C_2 w_*^3}}$$

This formulation was already used by Holtslag et al. (1990) and Troen and Mahrt (1986). For C_1, values of 5 and 8.5 have been suggested, while for C_2 the value of 0.6 is used throughout.

Since under convective conditions a superadiabatic layer is usually found near the ground in radiosoundings, also the simple parcel method implicitly applies an excess temperature. One may thus wonder whether it is justified to add another excess temperature, especially as the authors who used this concept mainly applied it to NWP model output. Therefore, we plotted both the temperature excess according to the above equation (Fig. 10) and the one found in radiosoundings against the heat flux (which is the dominant term in $\delta\Theta_v$) for the Cabauw / De Bilt data (see Section 4.1). The temperature excess in the radiosounding was defined as the difference between the virtual potential temperature of the lowest level and the first level above which the stratification was neutral or stable. Two features are striking in Fig. 10: the much higher scatter of the observed $\delta\Theta_v$ as compared to the computed one, and its larger magnitude. This observation has two implications. First, it shows that the simple parcel method depends on stochastic influences, as its implicit $\delta\Theta_v$ is not closely related to the heat flux. Secondly, adding $\delta\Theta_v$ according to the similarity formula does not make much sense, as one would add only a small quantity (typically 0.5 K) to much larger (typically 2 K) but stochastically influenced quantity. We suggest that when applying the Beljaars and Betts method to radiosoundings, one should omit the superadiabatic near-surface layer and instead use a larger value of the constant C_1. In order to achieve the same order of magnitude as found in the observed $\delta\Theta_v$, C_1 = 20 was used in this study.

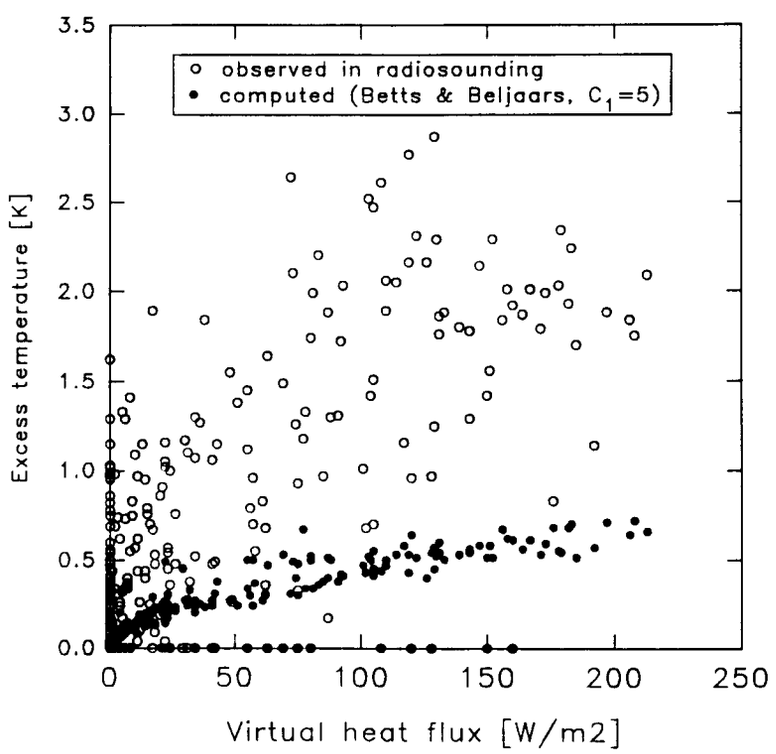

Figure 10: Excess temperatures derived from radiosoundings and computed from the similarity formula used by Beljaars and Betts (1992) plotted against the virtual heat flux. Radiosonde data are from De Bilt and heat flux data from Cabauw.

This reasoning applies to some extent to model data, too, as normal K-type diffusion parameterization requires superadiabatic gradients to produce an upward heat flux and thus also model data will in general contain already a certain excess temperature. This may be the reason why such a small value of the constant C_1 was used. However, one may wonder if this mix of two excess temperatures, one created by the model and another one from similarity theory, is really adequate.

3.8 Methods based on sodar and wind profiler measurements

3.8.1 Sodar measurements during SANA / SADE

The MH determined from sodar measurements was based on the analysis of single-pulse backscatter intensity profiles (usually available with 20 s time resolution). A semi-automatic structure-following algorithm was applied to derive the instantaneous height values using criteria which consider the actual structure of the ABL as described in Beyrich (1993, 1994b, 1996). The decisions on the type of the ABL (stable or convective) and on the layer to be analyzed (in the case of more than one layer of enhanced backscattering being present) were made subjectively. Resulting height values were then averaged over 30 min.

3.8.2 Sodar measurements at Cabauw

At Cabauw, an automatic procedure (described in detail in Beljaars and Agterberg, 1988) is applied to derive the MH from the sodar measurements. Like for the SANA data, it is based on an analysis of the backscatter intensity profiles; however, it uses averaged profiles and also the criteria are slightly different from above (see also Table 2). The decision on the ABL-type and the recognition of the relevant layers is done automatically.

3.8.3 Sodar measurements at Payerne – SMA routine

The algorithm developed at the Swiss Meteorological Institute (SMA) for MH estimation from sodar data at Payerne (see Berger et al., 1996) simply searches for the uppermost local maximum in the averaged backscatter intensity profiles but without differentiating between primary and secondary profile features. It is still in a preliminary test phase. Especially under convective conditions, it tends to place erroneously the MH within the range of the sodar, simply finding weak local maxima within a zone of general decrease. Under stable conditions, the MH may be overestimated if there is more than one layer with small-scale temperature inhomogeneities.

3.8.4 Sodar measurements at Payerne – manufacturer's routine

The sodar manufacturer REMTECH S.A. offers a software option which automatically estimates MH values in real time during the system's operation. According to the manual, it is based on a determination of the peak frequency in the vertical velocity spectrum which is then transformed into a wavelength using the measured wind speed. The manual claims that similarity theory is used to relate this wavelength to the MH. Measurements at different levels are taken into account for the analysis. The method has been suggested in the literature for the convective ABL (e.g., Kaimal et al., 1982), but REMTECH obviously uses this principle under stable conditions, too.

3.8.5 Wind profiler measurements at Payerne

The MH under convective conditions can be derived from the position of an elevated maximum in the backscatter intensity profile obtained from electromagnetic wind profilers as described, e.g., in White et al. (1991) or Angevine et al. (1994). The procedure applied in Payerne and the physics behind it are in principle the same as for the sodar (3.8.3; see also Table 2).

4. Data sets used for testing mixing height routines

We identified the following requirements for data sets in order to allow the testing of MH routines:

- Radiosonde ascents, as frequent as possible
- Continuous profile information (e.g., sodar, electromagnetic profiler, high tower)
- Measurements of turbulent fluxes at the surface
- Sufficiently uniform terrain without too much orographic influence

Searching for such data sets, it turned out that their number is rather limited. As can be seen from the following sections, only data sets of less than a full year were available. Some of the data sets, such as Payerne and Cabauw, will continue to grow (Cabauw: until the end of 1996), and a new data set will be built up at Lindenberg, a major meteorological observatory and aerological station of the German Weather Service DWD. Future work should be based on these more extensive data sets.

4.1 Cabauw (1995/96)

Cabauw is a boundary layer study site operated by the Royal Netherlands Meteorological Institute KNMI (Monna and van der Vliet, 1987). It is located between Utrecht and Rotterdam (51°58´N, 4°56´E, 2 m), surrounded mainly by pastures and meadows with interspersed small water channels. There are also some small woods nearby. Data used in this study comprise turbulent fluxes of sensible and latent heat as derived by different methods from the energy balance measurements and a 20 m mast providing profiles of wind, temperature and humidity at several levels. A sodar without Doppler capabilites (manufactured by Aerovironment Inc.) is operated on the site since the 1970s; it is used to derive mixing height from the backscatter profile. Recently, a Radian LAP-3000 1290 MHz wind profiler has been installed. The data used in this study cover the period from July 1995 until January 1996. In addition to the on-site data, regular aerological soundings from the station De Bilt, which is about 25 km north-east of Cabauw, have been used.

4.2 Payerne 1995/96

Payerne is the aerological station of the Swiss Meteorological Institute located in the western part of the Swiss Midland (46°49´N, 6°57´E, 491 m). The Swiss Midland is a hilly basin surrounded to the north by the Jura mountains and to the south by the Alps. There are interspersed flat plains of the size of a few to several tens of square kilometres. Payerne is a town of 7000 inhabitants, situated in the south-western part of such a plain. Thus, in the north of the station there is a plain of several square kilometres. In the south and west the terrain is hilly and rises 100-200 m above the plain. The aerological station is located south of the town, on a shelf 50m above. The distance to the first buildings around the measurement field is 60 m.

The data relevant for this study comprise routine aerological soundings, measurements of the sensible heat flux, and data obtained from a Remtech PA1 Doppler sodar and a Radian LAP-3000 1290 MHz wind profiler.

The sensible heat flux and the friction velocity were measured at 3 m above ground by eddy-correlation technique using the Solent sonic anemometer / thermometer of the manufacturer Gill. The measurements were started in August 1995, but continuous operation was not achieved before April 1996. In addition, soil heat flux and net radiation were measured. Some periods between August 1995 and June 1996 with more or less clear days have been chosen for the investigation. Their dates are:

August 1995: 22, 23, 31;
September 1995: 1, 5-7, 22, 29;
October 1995: 2, 17-19;
November 1995: 6-8;
January 1996: 16-18;
April 1996: 5, 6, 19, 20;
May 1996: 5-7, 15-18, 24, 28-31;
June 1996: 4-6

4.3 SADE (1993/94)

The SADE-93 and SADE-94 experiments were carried out within the SANA programme (study of changing air pollution situation and its impacts on highly sensitive ecosystems over Eastern Germany) at the SANA field station Melpitz (51°32' N, 12° 54' E, 87 m) about 40 km NE of the city of Leipzig. Melpitz is a flat-terrain site situated within relatively large agricultural fields and pastures. The basic goals of the two field campaigns were:

1) to determine experimentally the dry deposition of non-reactive and reactive trace gases over grass in order to verify models that have been developed to simulate these processes, and

2) to study the influence of certain boundary-layer processes on the observed concentration patterns at this monitoring site.

Therefore, intensive micrometeorological and chemical measurements were performed, supplemented by local boundary layer studies using different profiling techniques. The analysis within this study focused on the three intensive observation periods:

SADE-93: 18 – 23 September 1993
SADE-94: 20 – 30 September 1994, and 6 – 11 October 1994

With respect to the mixing height determination, data from the Doppler-Sodar ECHO-1D and from frequent radiosoundings (64 soundings during SADE-93 and 103 soundings during SADE-1994) were used. The Doppler sodar was operated by the Fraunhofer Institute for Atmospheric Environmental Research (Berlin division), and the radiosoundings and wind profiler measurements were performed by the Institute of Meteorology and Climate Research at the University and Research Centre of Karlsruhe. During both experiments, surface fluxes were derived from gradient measurements (8 levels) and from eddy-correlation measurements (Kaijo-Denki sonic anemometers) at 5.5 m and 10 m above ground. They have been provided by the micrometeorology group of the Meteorological Institute of the University of Munich.

5. Intercomparison of methods

5.1 Introduction

Testing methods for the determination of the MH is difficult because there are no direct measurements and except in situations with a well-defined convective lid different methods usually give different results, without a possibility to recognize clearly one as being correct. One is therefore limited to an intercomparison of methods. By looking simultaneously at results based on different measuring systems, obtained by different data evaluation methods (or different preprocessors), and applying one's expert knowledge about the behaviour of the atmosphere as well as about the methods, it is nevertheless possible to arrive at conclusions. Considering these difficulties, and also the limited amount of data that could be used in this study (see Section 4), results should not be seen as final answers.

5.2 Intercomparison of empirical methods

5.2.1 Time series from SADE

Figure 11 shows the mixing heights derived from frequent radiosoundings, sodar and wind profiler data during four undisturbed days of the SADE-94 field campaign. Radiosoundings were analyzed using the advanced parcel method (see Section 3.7.2), while sodar and wind profiler MHs were obtained semi-objectively from the backscatter intensity by the method described in Section 3.8.1. Excellent agreement between the different results was found with the exception of 7 Oct 1996; on the afternoon of this day, there were differences in the MH derived from the wind profiler and the radiosonde. The ascents at 10 o' clock local time on September 26 and 29 indicate that both remote sensors (sodar and radar) are well capable of reproducing the rise of the convective MH. This can also be seen on other days in the Figures shown in Section 5.3.

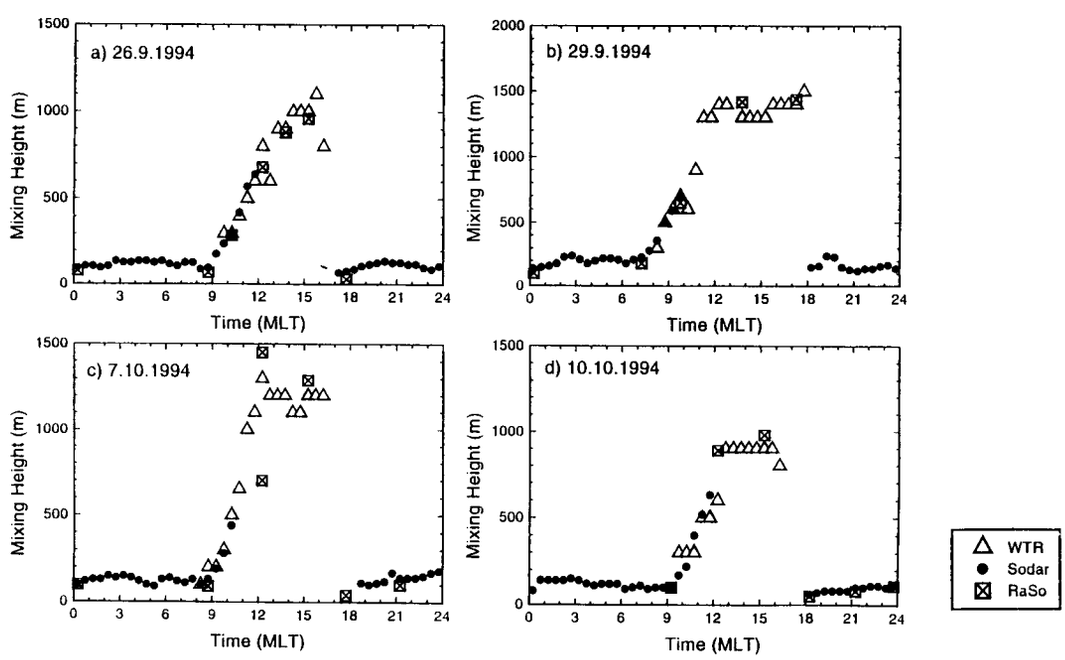

Figure 11: Mixing heights during selected days of SADE 94, as derived from different measurement systems (WTR – wind-temperature-radar, sodar, RaSo – special radiosoundings).

5.2.2 Stable situations

The sodar-derived MH during stable situations was compared with different analyses of radiosoundings for all days of the SADE-93 and SADE-94 intensive observation periods (Fig. 12). The radiosoundings were subjectively analysed with respect to the temperature profile (taking into account the typical shapes as discussed in Section 1.1), and with *Ri*-number methods. The relationships between MHs derived from sodar and with the *Ri*-methods are characterized by a lot of scatter, whereas MHs from the sodar and the temperature profile agree much better. This demonstrates that during stable situations sodar-derived MHs are strongly influenced by the shape of the temperature profile which, however, reflects the effects of mechanical turbulence production for SBL types (a) and (b) only (see Section 1.1 for the definition of these types). The *Ri*-method based on the ground level temperatures yields a number of cases with very shallow MHs (< 50 m) whereas the sodar gives values between 50 m and 200 m. It is hard to check the validity of the value of Ri_c for these circumstances, and they were derived using radiosonde winds which are not well resolved and sometimes inaccurate near the ground. Thus, the reliability of these extremely small MHs is difficult to judge, but it appears possible that they are overestimated by the sodar, also because MHs of less than 50 m are below the range of the sodar. On the other hand, if the temperature at the 20 m level is used instead of the ground-level temperature in the *Ri*-number (similar to the VH method), this results in a number of cases with *Ri*-number-derived MHs exceeding the sodar-derived ones, which means that the VH method tends to overpredict the stable MH.

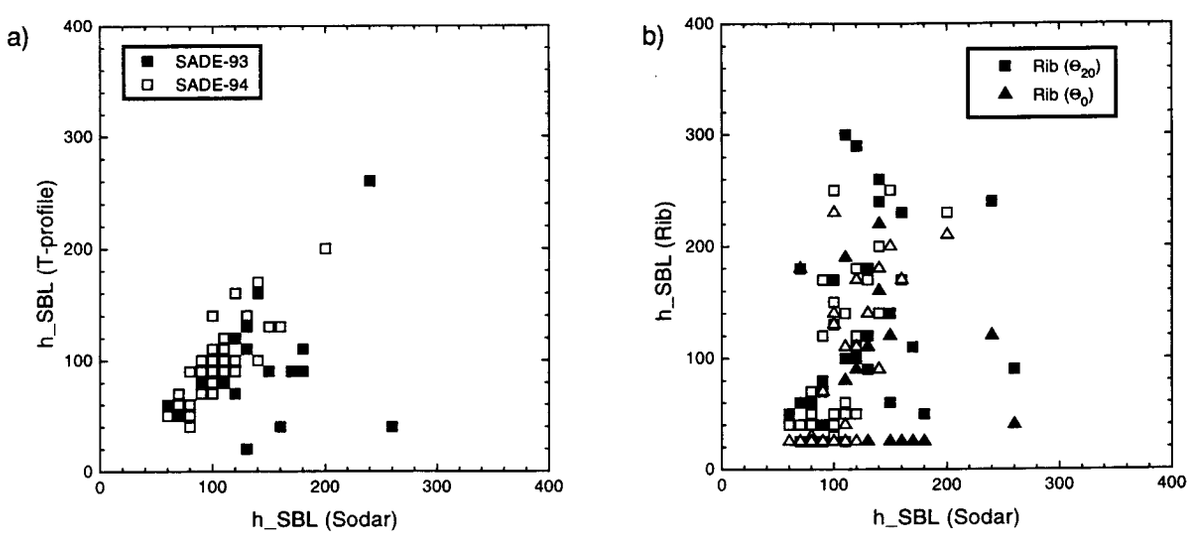

Figure 12: Scatter plots of mixing heights derived (a) from temperature profiles and (b) with the standard *Ri*-number method (squares: standard method; triangles: with temperature in 20 m above ground) versus sodar-derived mixing heights for stable situations during SADE-93 (filled symbols) and SADE-94 (open symbols).

A comparison between MHs under stable conditions in Cabauw, derived from the sodar and from *Ri*-number analyses, is shown in Fig. 13a. In contrast to SADE, the sodar MHs were derived here with a completely automatic algorithm. It has also to be kept in mind that the *Ri*-numbers were analyzed from radiosoundings only, not using the detailed wind and temperature profile from the Cabauw mast. Like in the SADE data, *Ri*-

number derived mixing heights tend to be lower than those indicated by the sodar. The number of extremely shallow MLs is much lower with the VH method than with the standard *Ri*-number method. In some cases the *Ri*-number methods indicate mixing heights around 1000 m while according to the sodar it should be below 300 m; these cases belong to the evening transition period, where the Ri methods can pick up the height of the residual layer. This can be seen from Fig. 13b which contains only midnight data. For the bulk of the data, the agreement between sodar-derived MHs and those obtained with the VH method is not too bad, though the sodar data tend to be somewhat higher. The correlation between MHs obtained with the standard *Ri*-number and from the sodar does not differ much from the correlation obtained for the VH method, but the standard *Ri*-number method leads to systematically lower MHs.

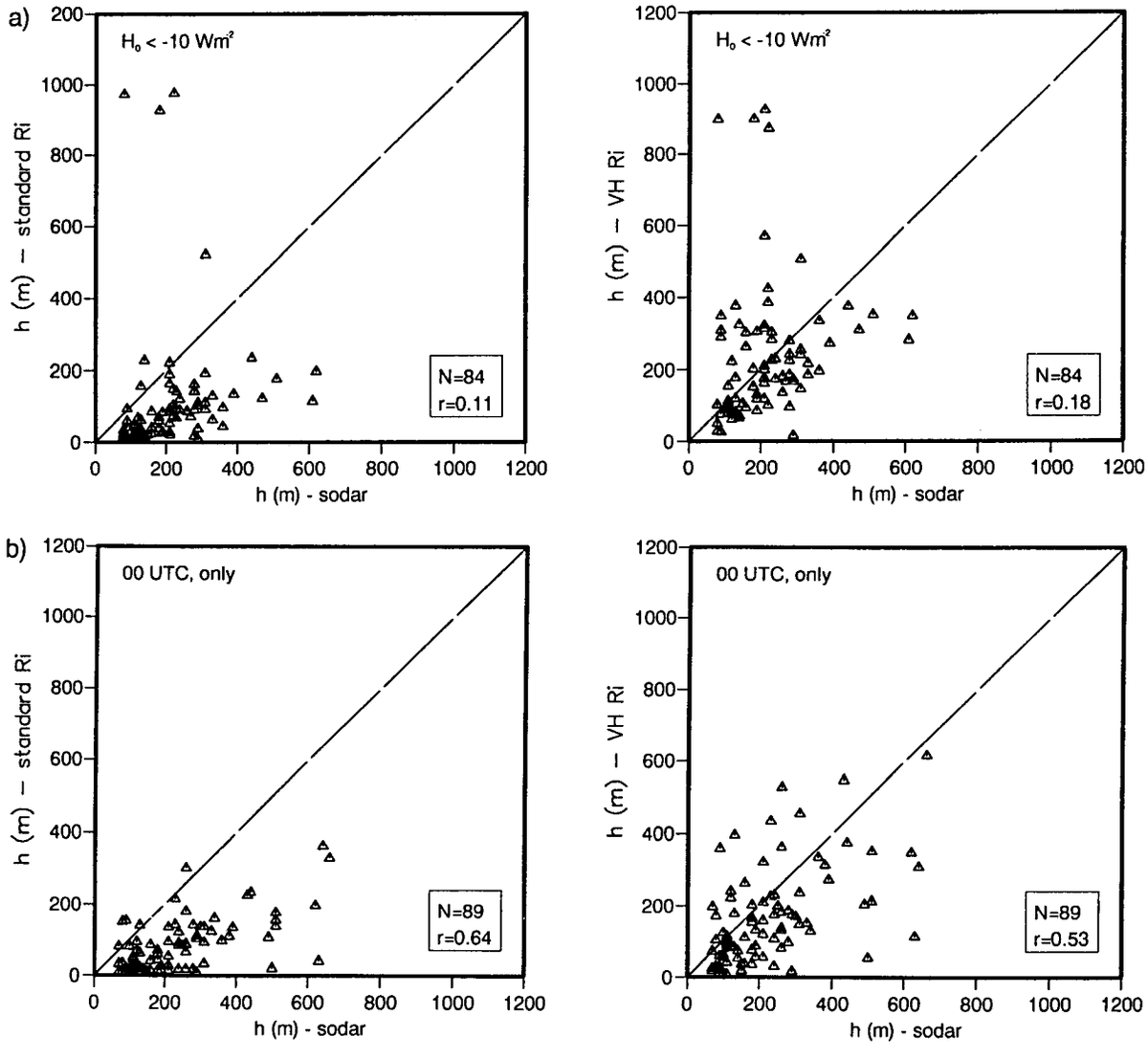

Figure 13: Scatter plots of mixing heights derived by different *Ri*-number methods (standard method and VH method) versus sodar-derived mixing heights in Cabauw. a) all stable hours (H_0 < -10 Wm^{-2}); b) 00 UTC only.

Vogelezang and Holtslag (1996) have already shown that their method is superior to $u*/f$; Fig. 14 compares the RODOS preprocessor results (which means mainly the Nieuwstadt formula (A1.1.13) and only in a few cases the $u*/f$ formula, see Section 3.5) with sodar-derived MHs. For the midnight soundings, RODOS output has about the same quality as the *Ri*-number methods while for all stable hours it appears even to be superior. The latter impression, however, is merely caused by the higher weight of the few outliers from the ETP in the *Ri*-number data, whereas in RODOS (which could be applied every hour as it needs only surface data) many regular night hours contribute to the correlation. In this plot, the artifical cut-off of the sodar-derived MHs at 50 m is clearly visible. Thus, in spite of the physical weakness of the similarity formula used in RODOS, it yields useful results in midlatitudes and appears to be superior to $u*/f$. However, a comparison using a well-resolved temperature and wind profile in the VH method and sodar data with manual quality control is still missing, and these results also do not jusitify the inclusion of f in the similarity formula.

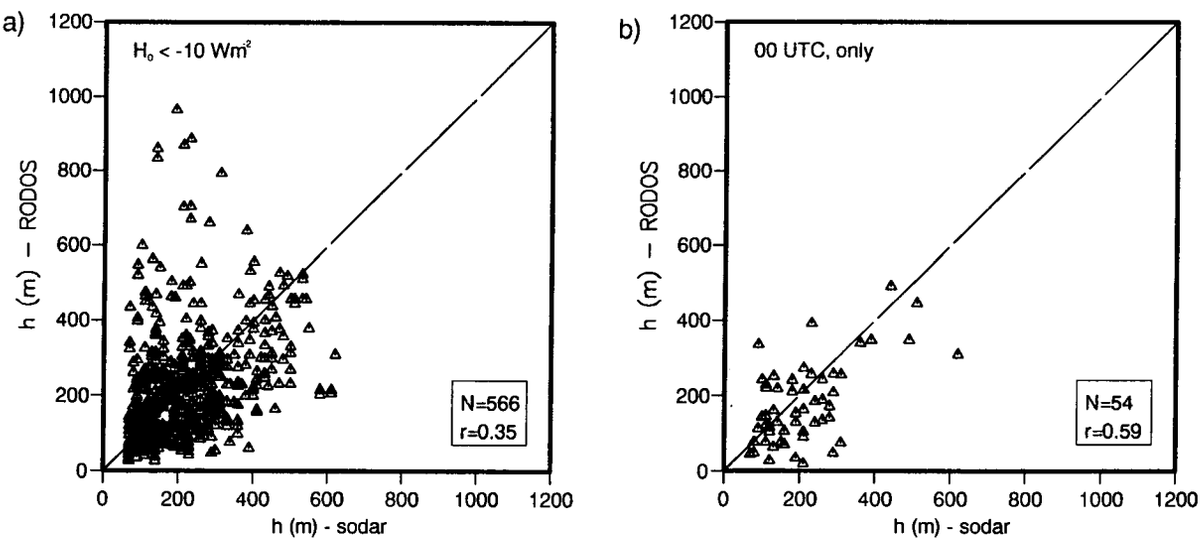

Figure 14: Scatter plots of mixing heights from RODOS (mainly Nieuwstadt's formula A1.1.2) versus sodar-derived mixing heights in Cabauw. a) all stable hours (H_0 < –10 Wm^{-2}); b) 00 UTC only.

5.2.3 Unstable situations

Comparisons of different methods based on empirical data of the SADE campaigns during daytime are shown in Fig. 15. There is a very good agreement between the results of the parcel method on one hand and sodar-derived MHs as well as MHs evaluated subjectively from radiosoundings on the other hand, except for a small number of outliers. The agreement between the parcel method and the *Ri*-number method is also very good, only the SADE-1993 data include a few outliers. The comparison between the standard and the advanced parcel method shows rather small scatter while the MH obtained with the standard parcel method are slightly lower than those from the advanced method. From the other comparisons, it appears that the advanced method is unbiased.

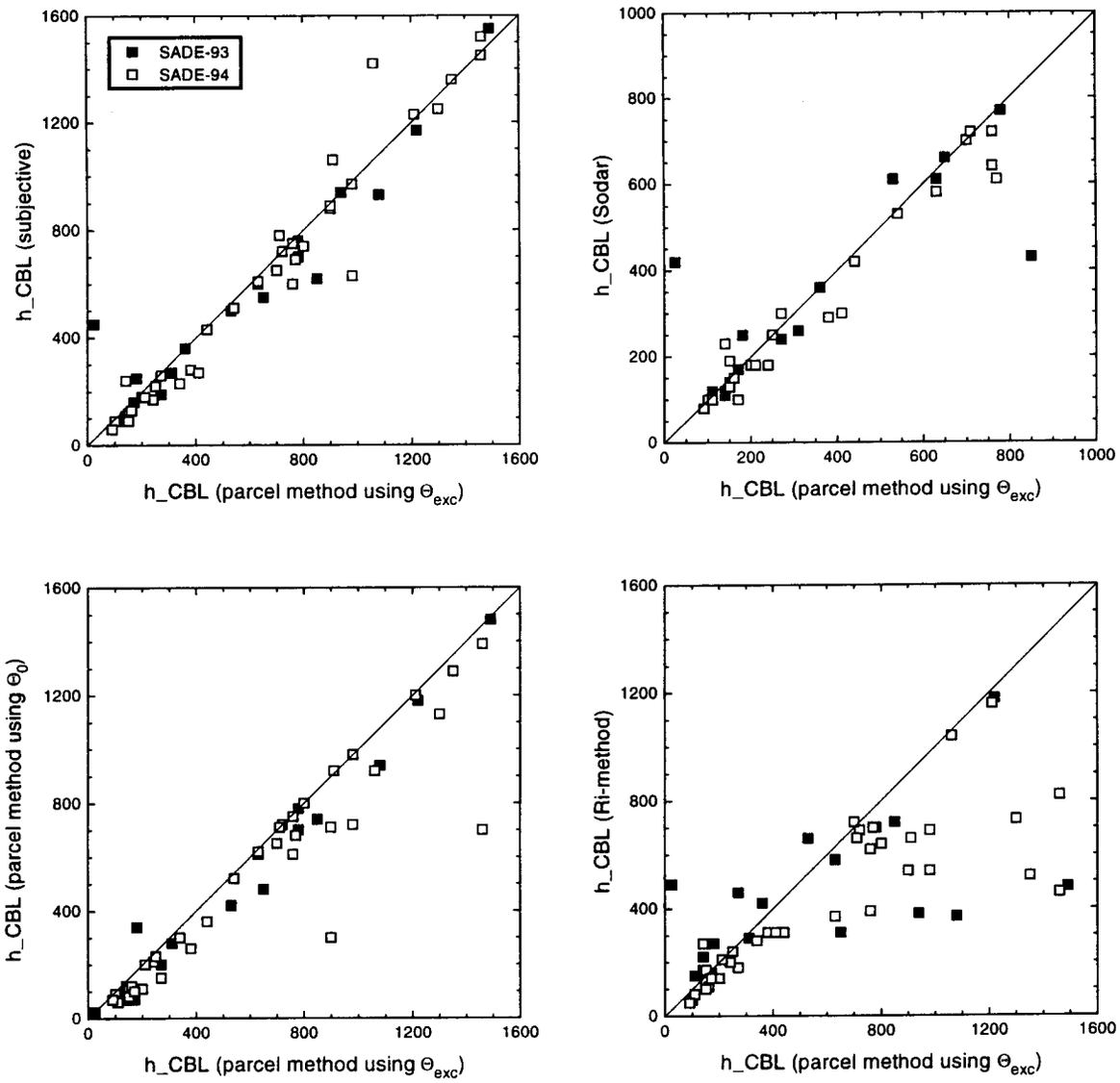

Figure 15: Scatter plot comparing a subjective evaluation of the MH based on radiosoundings (temperature, humidity, wind), a semi-objective evaluation of sodar backscatter data, the simple parcel method and the standard *Ri*-number method with the advanced parcel method. Data sets from SADE-93 (full symbols) and SADE-94 (open symbols), unstable hours only.

Fig. 16 shows results from Cabauw (cases with $H_0 > +10$ Wm^{-2}). All the methods (simple parcel, advanced parcel, standard *Ri*-number, VH *Ri*-number) correlated well ($r > 0.9$) with each other, and without significant biases. The standard *Ri*-number method and the simple parcel methods yield almost equal results. The reason for this is that under convective conditions, where the wind shear is usually small, *Ri*-number and parcel methods are almost equivalent. Especially, the simple parcel method is equivalent to the standard *Ri*-number method if $Ri_c = 0$ were used.

The comparison between the standard and the VH *Ri*-number method (Fig. 16) shows that the VH method overpredicts low MHs (< 500 m, according to the standard method) as compared to the standard method, and has a weak tendency to underpredict for high MHs. If both methods are compared to the advanced parcel method, a better correlation (0.82 instead of 0.75) is found for the standard method than for the VH method.

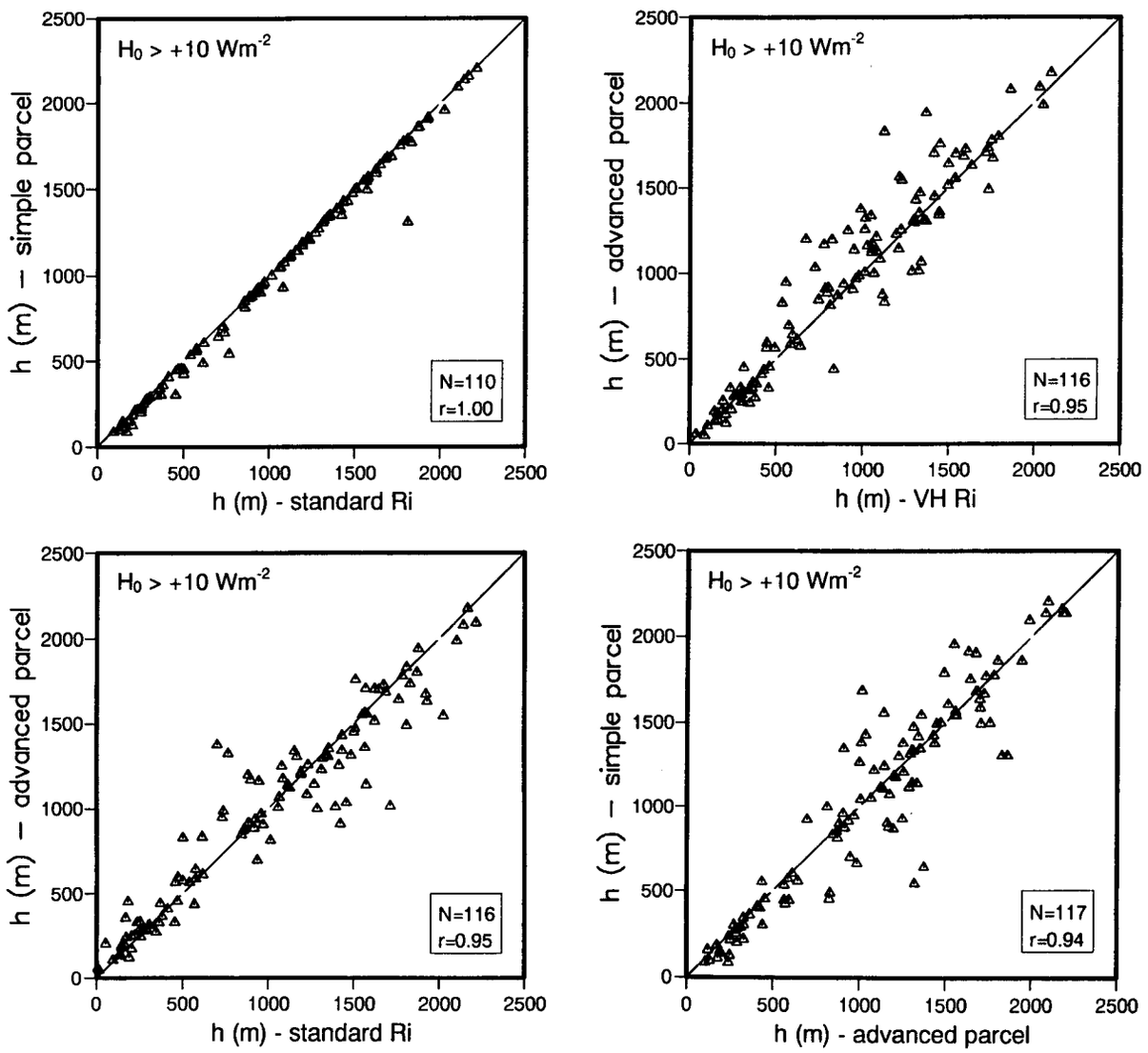

Figure 16: Scatter plots of mixing heights derived by the standard and the VH *Ri*-number and the simple and advanced parcel method at Cabauw, unstable cases.

5.2.4 Conclusions

In the CBL, the *Ri*-number methods give very similar results to the parcel methods when the same near-ground temperature is used. Thus we can recommend to use either the advanced parcel method or a *Ri*-number method where the near-ground temperature contains an excess temperature as in the advanced parcel method (this has also been suggested by Vogelezang and Holtslag, 1996). For boundary layers where shear-produced turbulence is important, *Ri*-number methods should be preferred to the parcel method even if the ABL is unstable. From the limited data available in this study, it

appears difficult to judge the relative performance of the standard and the VH *Ri*-number method. The development of the VH method was based on the sodar mixing height data in Cabauw. As the critical *Ri*-number in the VH method has been determined from Cabauw sodar data (obtained with an automatic routine), evaluations with other, independant data sets are necessary before final conclusions can be drawn.

During stable situations, sodars give a reasonable magnitude of the MH though sometimes they may overestimate it. During the morning of well-developed convective days, there is usually a period when the rise of the CBL is very well captured by the sodar. However, sodars cannot locate the MH if it exceeds the range of the instrument[1] . Hence, a large part of the convective hours are not covered by sodar MH data. This can be seen, e.g., in the time series plots shown in Section 5.3. The problem of the automatic routines (Cabauw, Payerne, Remtech) is to recognize when they can give a useful MH and when the MH is beyond the sodar range. The routine of Remtech shows a lot of unexplainable variability during all times of the day. The limited number of MHs derived from the wind profiler in Payerne indicates that presently this automatic method either is not able to produce useful results (Fig. 17).

There is no doubt that the minimum MH of 150 m applied in the OML preprocessor is not corroborated by observations over rural terrain.

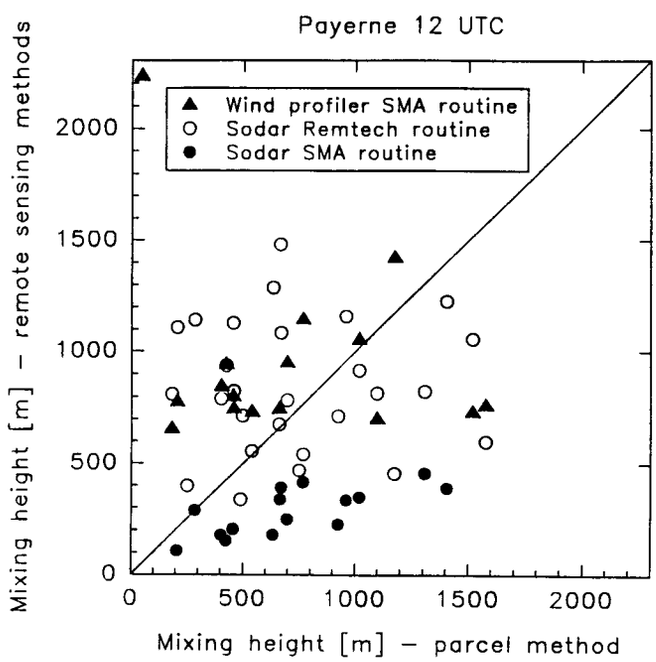

Figure 17: Scatter plot comparing the mixing height as detected by different remote sensing systems using automatic routines with results of the advanced parcel method in Payerne (12 UTC soundings).

[1] In principle, similarity methods allow the determination of the MH even in this case, but in practice they do not work well enough.

5.3 Intercomparison of preprocessor modules

In the following, the behaviour of the MH modules included in different preprocessors (OML, HPDM, ST [= Servizio Territorio library], FMI and RODOS) is discussed and compared with each other and with the results of empirical methods for selected days. The empirical methods are based on radiosoundings and sodar measurements. The radiosoundings were analyzed with the *Ri*-number method and – for hours with positive heat flux – the parcel method. Sodar-derived MHs are the only empirical method available which gave continuous information, but they are limited to night-time and shallow convective boundary layers. We believe that in general these empirical methods reflect the real evolution of the MH in a reliable way. Looking at a number of different methods together may produce somewhat confusing figures (especially in black and white), but it enhances the understanding of the situation and the possibility of identifying unrealistic results. In this way, a number of specific problems of certain preprocessors could be identified. In some cases we could identify the cause of these problems whereas for other problems this was not possible, and it will be a major task for the model developers to investigate them more in depth.

As all the preprocessors have severe problems in certain situations, it seems to be premature to compare their results in the form of scatter diagrams.

a) 28-29 May 1996, Payerne (Fig. 18)

OML and HPDM gave similar results during the night. However, during the convective period of the first day, OML used all the time the MH given by $u*/f$, while HPDM produced a convective growth of the ML during the day. Note the difference between the convective MHs produced by HPDM and ST on the first day, which is probably due to different initializations. On the second day, HPDM and ST agree well as they both start from low initial values. OML again uses $u*/f$, indicating that the convective MH calculated in OML is lower than the one obtained by $u*/f$. During the second night, OML gave its minimum height of 150 m while other methods indicate lower MHs. During daytime, the sodar/based MHs are erroneously placed within the CBL; the reason for this behaviour is discussed in Section 3.8.3.

b) 6-7 July 1995, Cabauw (Fig. 19)

On these days, OML produced a growing ML during the daytime, at first determined by $u*/f$ (growing $u*$) and then by the convective model. Compared with the sodar, the early phase of this growth is overestimated by OML (because it uses the $u*/f$ formula which is not appropriate for this situation) while it is correct in the ST and FMI models. Later on the day, OML gives MHs which co-incide with the radiosounding while the ST and RODOS model values remain lower. We cannot explain the behaviour of HPDM on the first day. The plateau of the MH given by HPDM on the second day is not shown by other models. During the second day, the FMI model produces an unexplained, unrealistic growth in the afternoon. We consider the sodar values of the night from July 6 to 7 too high, but they show nicely the growth of the ML on the morning of the second day, co-inciding with the ST convective slab model and the morning radiosounding. However, while OML reaches the correct MH at noon, ST and RODOS MHs again remain too low.

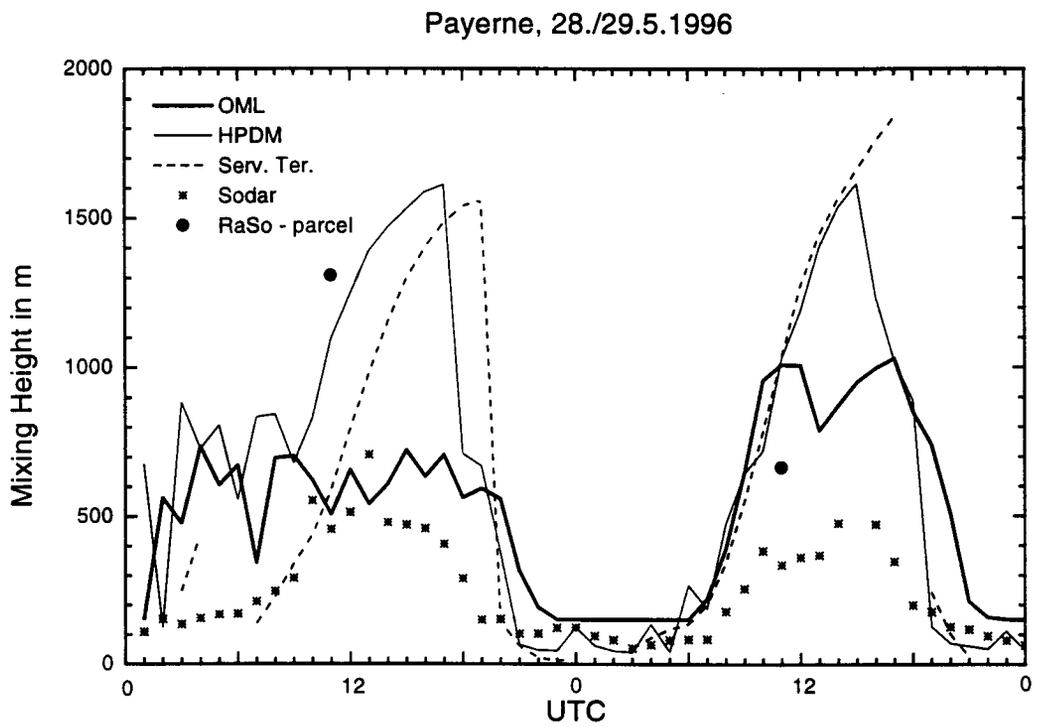

Figure 18: Evolution of the MH in Payerne, 28-29 May 1996, as computed by different preprocessors (lines) and as derived with empirical methods (symbols).

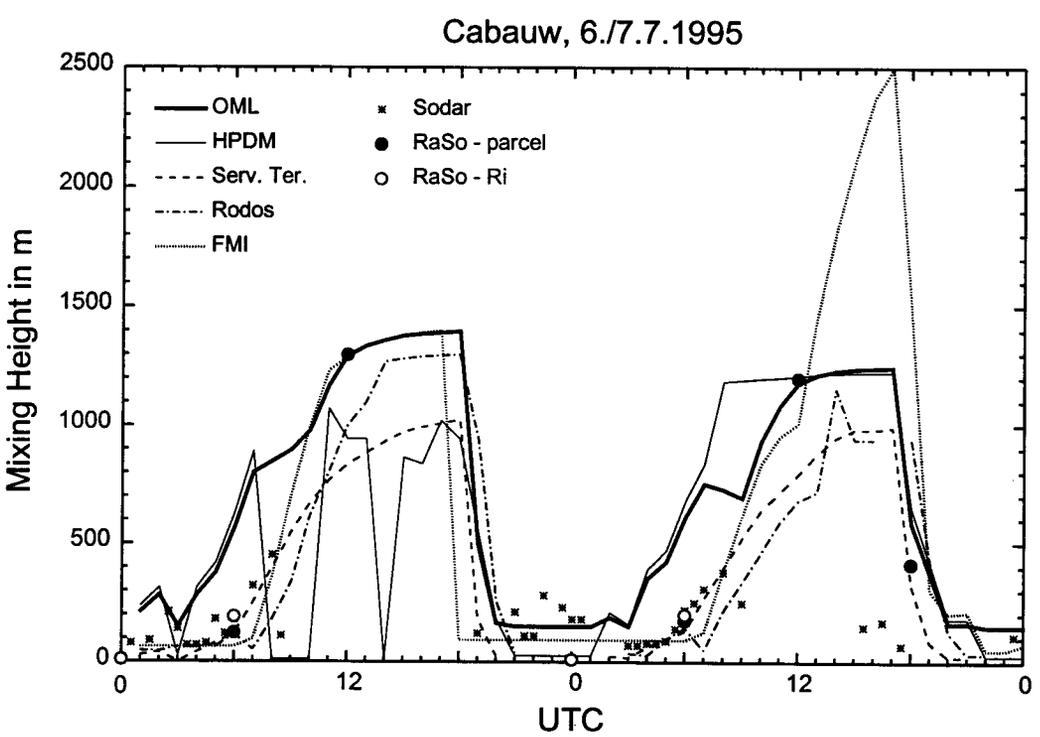

Figure 19: Evolution of the MH in Cabauw, 6-7 July 1995, as computed by different preprocessors (lines) and as derived with empirical methods (symbols).

c) 14-15 July 1995, Cabauw (Fig. 20)

On the first day, ST produced a too high MH which is attributed to the uniform potential temperature gradient used by this model, thus not taking into account the stable layer present above 1300 m. Though the mixing height found by the parcel methods at noon (1200 m and 1600 m) clearly indicates a well-developed CBL, OML and HPDM used the mechanical MH for almost the whole day (both days). Again we observe some unrealistic spikes in the HPDM output. FMI and RODOS start the convective growth of the ML rather late and thus fail to reach the observed 12 UTC value in time. On the second day, ST performes reasonably while in the FMI model the MH grows excessively, and the development in RODOS is again too weak.

d) 12-13 November 1995, Cabauw (Fig. 21)

The sodar was able to detect the mixing height throughout this period, obviously connected with a strong inversion, and also picked up by the parcel method. OML detected this inversion as a "sustained lid" and just interpolated the height of this lid linearly between the radiosoundings. There was a positive heat flux only for a few hours on each of the two days, as indicated in ST slab model. In contrast to OML, strong winds with associated high $u*$ cause the HPDM to yield much too high MHs in the first 30 hours. The other models fluctuated around the values observed with the sodar during the whole period. With the exception of 12 UTC on the second day, the *Ri*-number method always yielded MHs considerably lower than obtained by all other methods; the reasons for this behaviour are not clear at the moment.

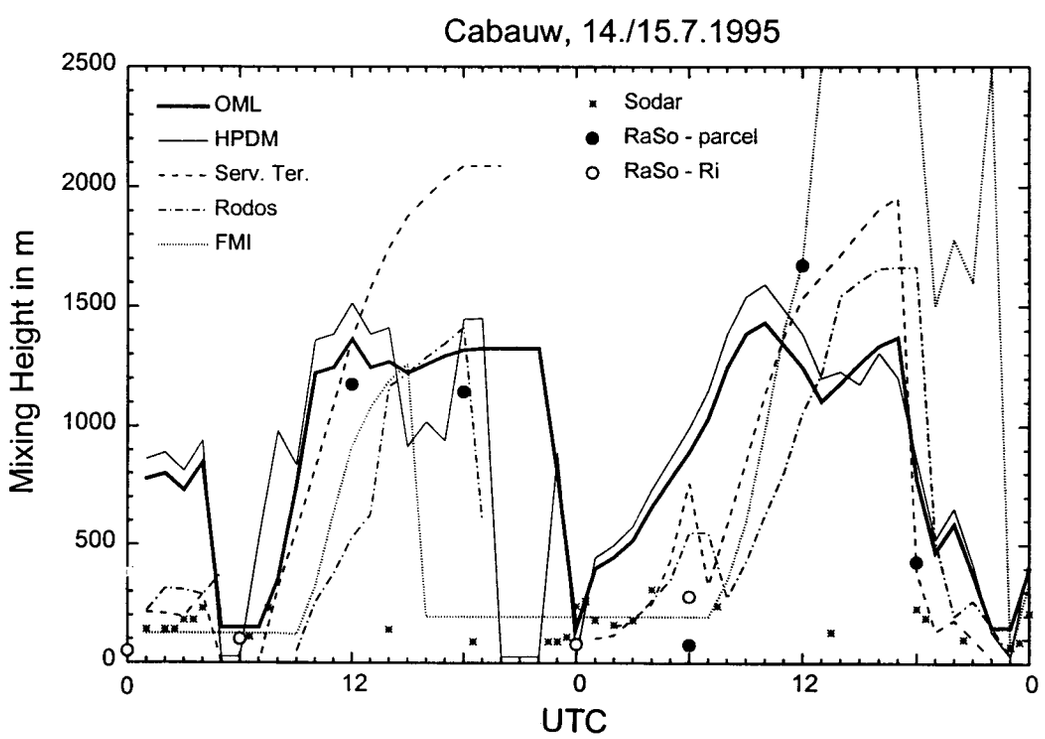

Figure 20: Evolution of the MH in Cabauw, 14-15 July 1995, as computed by different preprocessors (lines) and as derived with empirical methods (symbols).

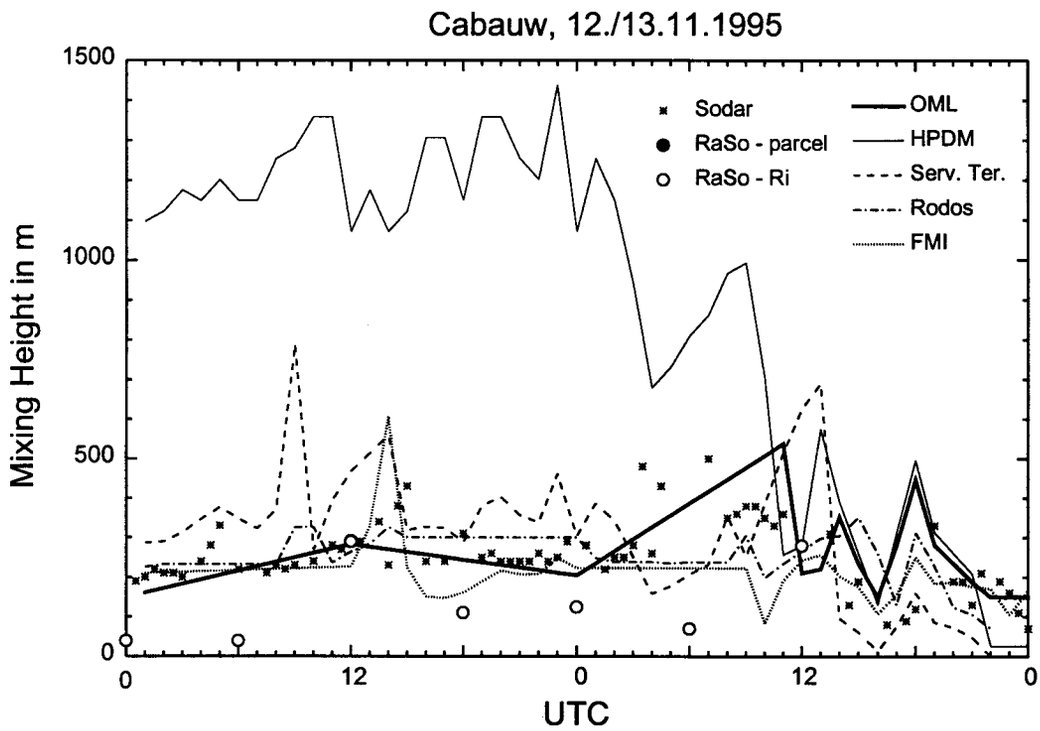

Fig. 21: Evolution of the MH in Cabauw, 12-13 Nov 1995, as computed by different preprocessors (lines) and as derived with empirical methods (symbols).

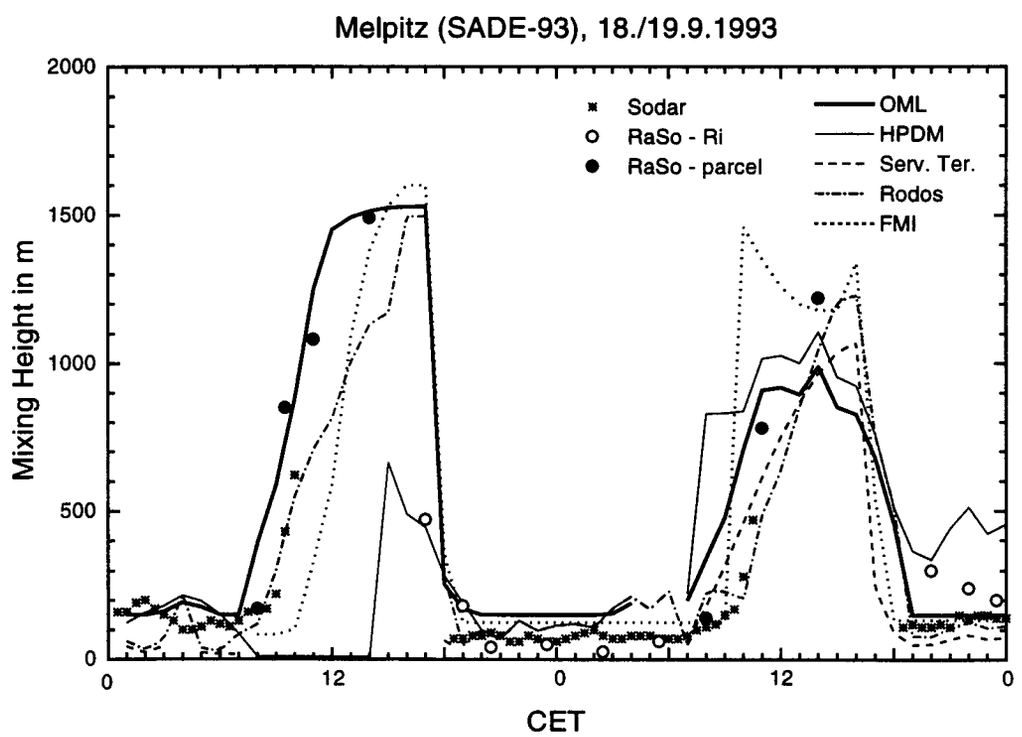

Figure 22: Evolution of the MH in Melpitz, 18-19 Sept 1993, as computed by different preprocessors (lines) and as derived with empirical methods (symbols).

e) 18-19 September 1993, Melpitz / SANA (Fig. 22)

The OML, the FMI and the RODOS models produced a strong development of the CBL up to about 1500 m, but there are differences in the onset of the growth, probably related to the initialization. The ST slab model was not activated during daytime because there was a short time with slightly positive heat flux already during the night. HPDM selected its minimum value of 10 m when the heat flux became positive in the morning until shortly after noon, for unknown reasons. On the second day, we can see that the FMI model adjusted the MH downward to the observed values of the noon sounding, but did not correct previous hours or its growth rate. HPDM displayed a very high growth rate during the second morning, which is higher than the one given by the slab model of ST and the $u*/f$ formula used by OML. During the second night, $u*$ was quite high and HPDM gave MHs exceeding those obtained by the other methods. OML found a lid in the next morning sounding that limited its MH.

f) 20-21 September 1993, Melpitz / SANA (Fig. 23)

On both days, the MH did not exceed 1000 m and was detected by the sodar most of the time. OML and HPDM again showed a too fast growth of the ML because they used the mechanical formulae. The FMI model started the growth of the ML at the right time, but with a too high rate, and adjusted downward at noon. The slab model of ST suffers from the fact that the temperature gradient was taken from the layer 1000-1500 m which in this case was inappropriate. The RODOS model started the convective growth much too late, though it reached finally a correct maximum. These two days are examples where the *Ri*-number method is equally useful for stable and slightly convective situations, while the parcel method cannot be used at noon of the second day as there was a negative heat flux. Due to this negative heat flux, the FMI model switched from the daytime to the nighttime mode already at noon. On both days, the RODOS model produced much too low MH from forenoon until the early afternoon. The shrinking ML during the first half of the night from September 20 to 21 is only picked up by the HPDM model, while the other preprocessors gave too low values.

g) 7-8 October 1994, Melpitz / SANA (Fig. 24)

The OML and HPDM models showed an explosive growth of the ML in the morning of the first day, while FMI, ST and RODOS started the ML growth later and at a slower pace. Sodar and radiosonde data show that HPDM and OML are not realistic. Their behaviour cannot be explained by $u*$ either, in contrast to some other cases. The behaviour of HPDM is even more unexpected than that of OML, which at least shows a normal convective growth phase between 1100 and 1500 m. The slab model of ST did not reach a sufficient height, due to its constant temperature gradient, while all the other models reach the correct maximum MH as indicated by the radiosoundings. On the morning of the second day, OML, FMI, RODOS and ST all create a very similar growth of the CBL which is also supported by the sodar data. However, in HPDM the MH rose until its maximum values of 3000 m, for unknown reasons. During the night between the first and the second day, all the methods and the sodar measurements are in the same range, with exception of the ST and RODOS models which lead to considerably smaller values.

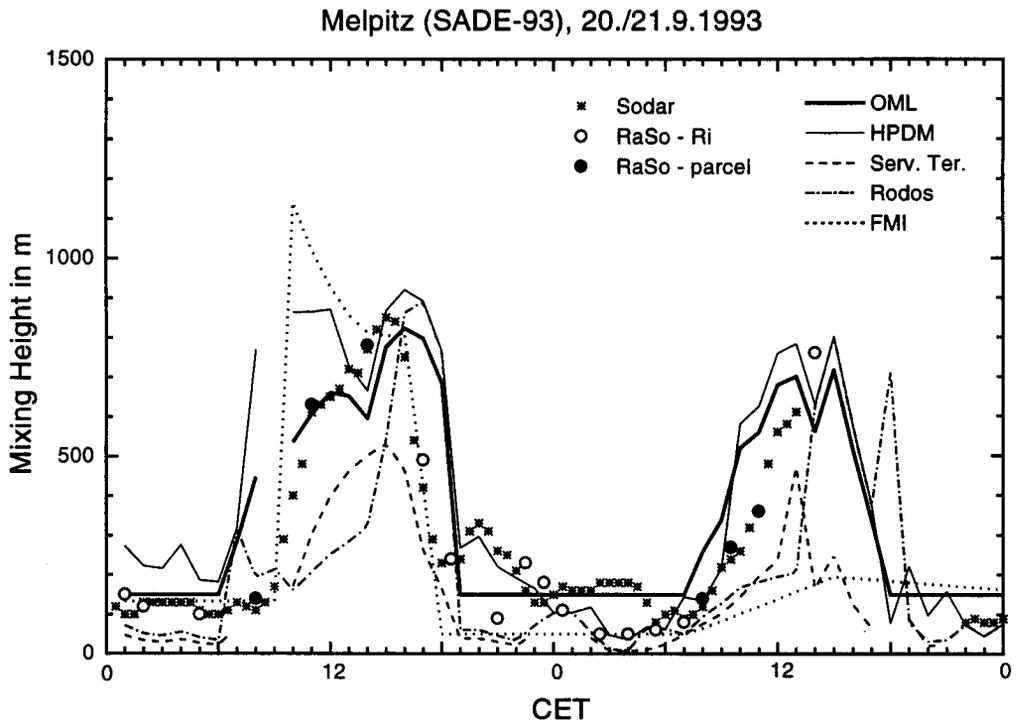

Figure 23: Evolution of the MH in Melpitz, 20-21 Sept 1993, as computed by different preprocessors (lines) and as derived with empirical methods (symbols).

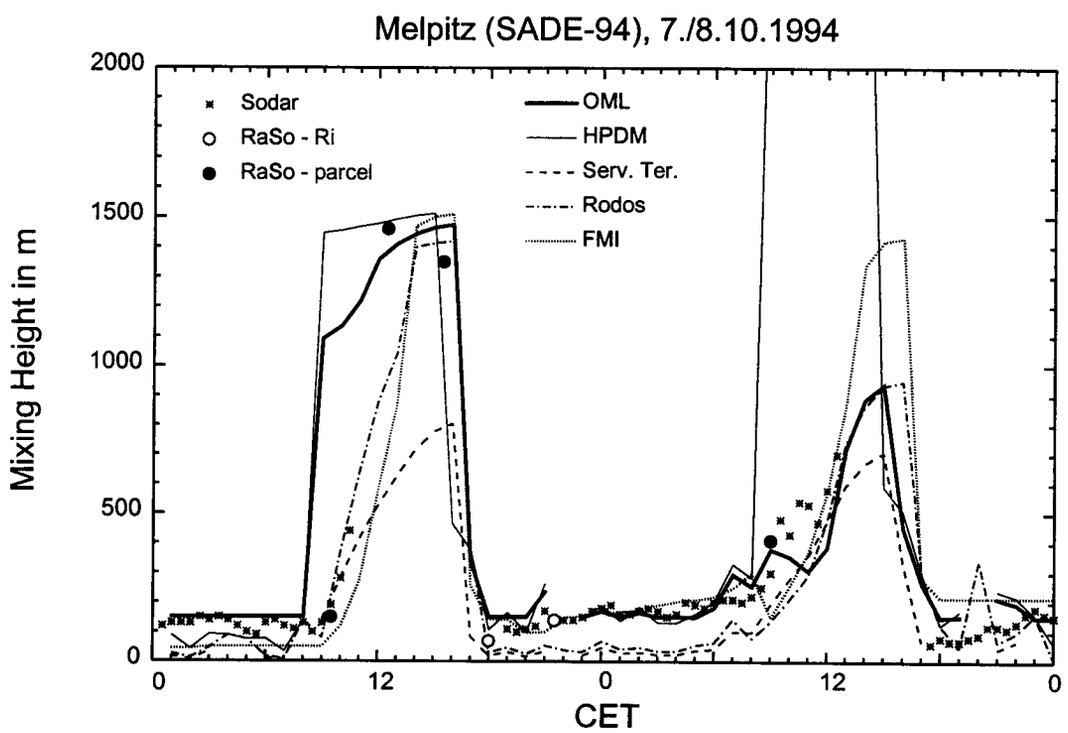

Figure 24: Evolution of the MH in Melpitz, 7-8 Oct 1994, as computed by different preprocessors (lines) and as derived with empirical methods (symbols).

6. Conclusions and recommendations

There are two general possibilities for operational MH determination, namely the analysis of profile measurements on the one hand and the application of parameterizations or models based on operationally available data on the other hand. If suitable data are available, the first option is to be preferred. In convective situations, the most reliable method at present is the parcel method applied to temperature profiles. The determination of the MH in situations where mechanically produced turbulence is important is much more difficult. Given the fact that temperature and wind profiles are the most widespread information, we consider Richardson number methods to be the most appropriate ones under such conditions. In many situations, remote sounding data (sodar, wind profiler, RASS, lidar) can give good results, but it appears premature at present to recommend them for operational purposes.

It is also possible to substitute NWP model output for measurements, but then the results strongly depend on the characteristics of the model, especially its ABL formulation. Therefore, no general recommendations can be made here. High-resolution mesoscale models with good ABL formulation can be useful especially in complex terrain.

For convective boundary layers, the numerical slab model is appropriate, taking into account the specific recommendations listed below.

In situations characterized by a mechanically determined MH, all the current preprocessors rely on similarity formulae involving $u*$ and f, and partly also $L*$. We regard this as not satisfactory from a physical point of view (see Section 2.2.3). Richardson number methods appear to be better in this respect, and also according to some published studies. However, the necessary input for these methods is often not available. Using numerical models (see Section 6.3, 7)) may become a solution in the future. In the meantime, the similarity methods will probably still be used if continuous profile data are not available, but one should be aware that the implied dependence on f is probably unrealistic, especially towards low latitudes. For stable conditions, the formula of Nieuwstadt (1981; A1.1.2) is to be preferred to the simple $u*/f$ approach (A1.1.3).

Since none of the methods and models are perfect, it is recommended to have the results checked by a qualified scientist, considering the basic data.

We list below a number of specific findings and recommendations which should be taken into account for the analyses of measurements and the application and development of preprocessors. In addition, we provide suggestions for future research which appears desirable to provide a more reliable basis for MH determination under different conditions.

6.1 Findings and recommendations concerning the analysis of measurements

1) Parcel methods (for the detection of the convective MH) should be based on the virtual potential temperature whenever possible. The simple parcel method already gives reasonable results. If a similarity method is used to calculate an excess temperature, attention has to be paid to the value to which it is added. If this is the temperature of the well-mixed CBL, a value of the constant C_1 (see Section 3.7.2) around 20 appears to be more appropriate than the values 5 or 8.5 which have been suggested so far. See also recommendation for future research (6.3.1).

2) Methods using a Richardson number can also be applied to convective boundary layers, but then they should use an excess temperature like in the parcel methods to compute the temperature differences.

3) Under stable situations with low MH, methods using a Richardson number give questionable results if the wind profile is available from radiosondes only, as such wind data may be inaccurate and / or not sufficiently well resolved near the ground. Forming a composite with wind information from other measurement systems (sodar, mast) might help to overcome this problem.

4) The use of profiles obtained with tethersondes requires a careful preprocessing including smoothing and removal of trends (substantial local temperature changes may occur during the ascent or descent of the tethersonde) under the control of a qualified scientist. This applies also to thethersonde profiles to be used as input in preprocessors.

5) Direct determination of the MH from sodar data (see Section 2.2.1b) is possible only if the MH is well within the range of the sodar. This range is typically between about 50 m and 500 m. MHs exceeding the sodar range can theoretically be derived using similarity methods, but these methods are not sufficiently reliable for operational use. The preferred method for direct MH determination is to use the backscatter intensity profile. Problems may occur if it is not known whether the MH really falls into the range of the sodar, and erroneous conclusions are easily possible in such cases.

6) MH detection routines currently implemented on commercial sodars by manufacturers appear to be not reliable. As we did not perform in-depth studies of all such routines, and as they may be altered in the future, the recommendation we give to end-users is to have the performance of any routine they want to use carefully checked on their site, using other reliable methods for comparison.

7) The backscatter intensity profiles obtained from electromagnetic wind profilers (operation frequency around 1 GHz) are a promising basis for MH determination in well-developed, cloudless CBLs, as has been shown in a number of published case studies. However, algorithms developed so far appear not to be reliable enough for operational use.

8) There are also other remote sensing systems which can be helpful for the determination of the MH, such as the lidar and the RASS (radio-acoustic sounding systems). However, they were not considered in detail in this study.

6.2 Findings and recommendations concerning the application and improvement of preprocessors

1) The numerical integration of a slab model for the CBL should use the actual initial temperature profile with reasonable vertical resolution. It is not advisable to use a single or predetermined value(s) of the potential temperature gradient above the ML. Rate equations in such models should include also the mechanical contribution to ML growth, parameterized by $u*$.

2) Preprocessors should allow the substitution of measured data for parameterized ones at any stage. This requires both that the technical possibility is provided for in the code, and that the algorithms are able to deal correctly with measured data, even if they do not follow idealized parameterizations. Preprocessors have to be able to deal

correctly with such special conditions. For example, measurements include sometimes cases in which the heat flux reverses its sign more than twice a day, i.e., there are periods of downward heat flux during the day or upward heat flux during the night.

3) Preprocessors should be able to use all soundings available, not just those at the standard hours 00 and 12 UTC. Even in the case of standard soundings, the real launching time of the sounding should be considered, as it may vary by about one hour around the standard time (see Appendix A3).

4) Preprocessors should be able to work with high-resolution radiosonde data (e.g., readings every 10 seconds) and not only with significant levels as reported in the TEMP part B. This requires appropriate dimensioning of the arrays in the code as well as taking into account the presence of small fluctuations in the high-resolution data, which may, e.g., lead to relatively strong positive or negative potential temperature gradients over small layers in a well-mixed CBL. The preferred solution would be, in addition to the archival of full resolution data, to provide TEMP part B data with enhanced resolution in the lower atmospheric layers; some meteorological services have already started to do so (see Appendix A3).

5) Constants and parameters specific to a certain climatic region (e.g., absolute maxima or minima of the MH, or criteria to find convective lids) should be clearly documented in preprocessors, and the users should have the possibility to change such values.

6.3 Recommendations for future research

1) The parcel method is a suitable method for the analysis of measured or modelled temperature profiles in the CBL. It would be desirable to use the mean temperature of the well-mixed part of the CBL as a base value, adding an excess temperature depending on the heat flux and a scaling velocity. Both the practical determination of the mean temperature from an arbitrary sounding (including cases where the ABL is not really well-mixed) and the determination of the constants in the calculation of the excess temperature should receive attention.

2) There is a general need for more work on the SBL. Formulae for the mechanical mixing height, especially those based on Richardson numbers, should be tested on a number of data sets. The validity of the MH concepts originating from boundary layer studies to describe the dispersion of pollutants should be studied, especially with respect to the effects of intermittent turbulence and of waves in the outer SBL.

3) The development of routines to derive the MH in deep CBLs from the backscatter intensity profile of electromagnetic wind profilers should be continued with the aim of operational applicability. Such work would ideally include sodar data to detect the MH below the lowest profiler range gates, especially under stable conditions. Supplementing this chain of profilers with minisodars for very shallow MHs should be considered.

4) The spatial and temporal representativity of mixing heights derived from measurements (including indirect effects, such as those of the initial profile and the heat flux in CBL slab models, for example) should be studied.

5) It should be investigated whether subsidence velocities and horizontal advection at the top of the CBL obtained from NWP model output (presently the only practical source) are reliable enough to improve the performance of CBL models.

6) There is still a lack of appropriate scaling for the entrainment layer. The role of waves at the CBL top and of wind shear across the inversion layer for the turbulent transport of constituents at the top of the CBL is not completely understood.

7) Numerical boundary layer models with a good turbulence parameterization, using at least a prognostic equation for the TKE (closure of the order 1.5), should be considered as an alternative to simple parameterizations in the future. Especially one-dimensional models are fast enough to be used operationally even for long data series.

8) Using NWP models to provide input for dispersion modelling, specific data requirements which are different from those of weather forecasting applications should be taken into account. For example, better temporal resolution of the NWP model output or providing additional variables such as TKE, K_H or parameters describing deep convection (venting of the ABL) can be considered.

9) Techniques to fit parameterizations and models to observed data, such as variational methods, should be developed and implemented. We believe that this is the most important improvement which can be made to CBL slab models.

10) We recommend to establish long-term monitoring programmes for the ABL in different climatic regions, including measurements of the surface energy budget components, turbulence parameters at several levels, at least two continuous profiling systems, and radiosoundings on the site or nearby. This goal could be accomplished by supplementing existing field sites, e.g. sites of national meteorological or environmental services.

11) Further development of remote sounding systems in order to measure turbulence parameters accurately would bring considerable benefits for MH determination.

Acknowledgements

The authors of this report acknowledge the support given by COST through the European Commission, the Swiss Government (Philippe Tercier), the Austrian Government (Petra Seibert), Technical University Cottbus (Frank Beyrich) and Risø National Laboratory. Data for the comparisons have kindly been supplied by the KNMI (Cabauw data set), the Institute of Meteorology and Climate Research at the Research Centre of Karlsruhe (radiosonde and wind profiler data during SADE 93/94), the micrometeorological group at the Meteorological Institute of the University of Munich (surface measurements during SADE-94/94), and the Institute of Troposphere Research in Leipzig (management of the Melpitz field site). Ari Karppinen from the Finnish Meteorological Institute ran the FMI model for the computations of Section 5.3. Special thanks go to Ernst Dittmann, Bert Holtslag and David Thomson for reviewing a draft of the report.

Appendices

A1 Equations for the parameterization of the SBL height

A1.1 Diagnostic Relations

The following basic starting points have been used to derive diagnostic equations for the parameterization of the SBL height:

- the equation for the Ekman-layer depth $h = \pi\,(2\,K_M / |f|)^{1/2}$,
- scaling arguments,
- formulation of a criterion for $Ri > Ri_c$ at the SBL top
- integration of the hydro-dynamic equations of motion[2)].

Based on the equation for the Ekman-layer depth and with $K_M = u_* \kappa\, z_r$ one arrives at

(A1.1.1) $$h = \pi \sqrt{\frac{2\kappa\, u_* z_r}{f}}$$ with z_r=1.25 m Malcher and Kraus (1983)

The Ekman-layer depth equation with $K_M = [z/h\,(1 - z/h)^{3/2} / (1+4.7\,z/L_*)]\,\kappa\, u_*\, h$ may be transformed into

(A1.1.2) $$h = 0.3\,\frac{u_* / f}{1 + 1.9\,h / L_*}$$ Nieuwstadt (1981)

Derbyshire (1990)

As this formulation contains h also on the right-hand side, it is not well suited for practical application. One of the possible transformations into a closed solution for h is

(A1.1.2a) $$h = \frac{L_*}{3.8}\left(-1 + \sqrt{1 + 2.28\,\frac{u_*}{f\,L_*}}\right).$$

The asymptotic behaviour of (A1.1.2) for $h/L_* \rightarrow 0$ (neutral stability) provides

(A1.1.3) $$h = c_1\,\frac{u_*}{f}$$

$c_1 = 0.2$	radiosonde data	Clarke (1970)
$c_1 = 0.185$		Benkley and Schulman (1979)
$c_1 = 0.06$	h_{Ri} from radiosonde data	Mahrt et al. (1982)
$c_1 = 0.14$	sodar data	Arya (1981)
$c_1 = 0.07$	sodar data	Koracin and Berkowicz (1988)
$c_1 = 0.04$	numerical model	Delage (1974)

which has also been suggested from scaling arguments.

---

2) In what follows, generally f is used instead of $|f|$; this has to be considered for applications in the southern hemisphere.

Using a 1-dimensional numerical model with k-ε-closure, Estournel and Guedalia (1990) have argued, that the value for the constant c in (A1.1.3) depends on external conditions, the following modification is proposed:

(A1.1.4) $h = (1.4\ L_* \frac{f}{u_*} + b) \frac{u_*}{f}$ Estournel and Guedalia (1990)

However, the authors did not specify b. From their Figure 4 it comes out that b is a time-dependent function of z_0 and V_g. This makes operational application of (A1.1.4) quite difficult.

Assuming a logarithmic wind profile for a given site (fixed values of f, z_0 and z_r), (A1.1.3) is reduced to

(A.1.1.5)	$h = c\ U_{10}$	c = 125 s	Benkley and Schulman (1979)
		c = 60 s	Koracin and Berkowicz (1988)

Similarity considerations and scaling arguments were used to derive the "classical" diagnostic relation for the parameterization of the SBL height:

(A1.1.6) $h = c_2 \sqrt{\frac{u_* L_*}{f}}$

			Zilitinkevich (1972)
	c_2 = 0.72	comparison with $h_{0.01\tau}$	Businger and Arya (1974)
	c_2 = 0.7	non-stationary conditions (ETP)	Caughey et al. (1979)
	c_2 = 0.74	sodar observations	Arya (1981)
revised:	c_2 = 0.37..0.43		Garratt (1982a)
	c_2 = 0.13	non-stationary conditions, low latitude	Garratt (1982a)
	c_2 = 0.35		Joffre (1981)
	c_2 = 0.6	h_{Ri} from radiosonde data	Mahrt et al. (1982)
	c_2 = 0.37..0.46	} numerical model	Brost and Wyngaard (1978)
	c_2 = 0.27	} stationary	Rao and Snodgrass (1979)
	c_2 = 0.33..0.40	} solution	Dörnbrack (1989)

(A1.1.6) also follows from (A1.1.2) for the asymptotic limit $h/L_* >> 1$ (very stable conditions).

Venkatram (1980) has proposed the relationship $L_* = Au_*^2$ with $A = 1.1 \times 10^3$ s^{2}m^{-1} for stable conditions in the absence of any information on the surface heat flux. Using this formula and $f = 10^{-4}$ s^{-1}, (A1.1.6) can be written as

(A1.1.7) $h = c_* u_*^{3/2}$ with $c_* = 3.3 \times 10^3$ s^{2}m^{-1} c_2,
where c_2 is one of the values given in A1.1.6.

Replacing again, as in (A1.1.5) u_* with U_{10} , (A1.1.7) can be written as

(A1.1.8)	$h = c\ U_{10}^{3/2}$	c = 28		Nieuwstadt (1984b)
		c = 25	sodar observations	Gera and Singal (1990)

From similarity considerations and scaling arguments, also the following diagnostic relations have been proposed in the literature:

(A1.1.9)	$h = c\ L_*$	$c \approx 10$	for very stable conditions	Arya (1981)
		$c \approx 6$		Mahrt et al. (1982)

$c \approx 2..4$ Kitaigorodskii and Joffre (1988)

(A1.1.10) $h = c\,u_* / N_{BV}$ $c \approx 4..13$ Kitaigorodskii and Joffre (1988)

(A1.1.11) $h = c\,V_g / N_{BV}$ Rossby and Montgomery (1935)
Laikhtman (1961)
$c = 0.75$ Hanna (1969)

(A1.1.12) $h = c\,\dfrac{u_*}{\sqrt{f\,N_{BV}}}$ $c = \sqrt{2}$ Venkatram (1980)

$c = 1.2$ Neff and Coulter (1986)

The following equations are interpolation formulae between (A1.1.3) (for near-neutral stability) and (A1.1.6) or (A1.1.9) (for very stable conditions):

(A1.1.13) $$h = \frac{u_*}{f}\left(\frac{1}{\Lambda_0} + \frac{\sqrt{\mu}}{\kappa\,C_h}\right)^{-1}$$

$\mu = \kappa\,u_*/(f\,L_*)$, $\Lambda_0 = 0.3$ and $C_h = 0.85$ Zilitinkevich (1989b)

as well as

(A1.1.14) $$h = \left(\frac{1}{30\,L_*} + \frac{f}{0.35\,u_*}\right)^{-1}$$ Deardorff (1972)

(A1.1.15) $$\left(\frac{h\,f}{C_h\,u_*}\right)^2 + \frac{h}{C_s\,L_*} + \frac{h\,N_{BV}}{C_i\,u_*} + \frac{h}{C_{sr}}\sqrt{\frac{|f|}{u_*L_*}} + \frac{h\sqrt{N_{BV}|f|}}{C_{ir}\,u_*} = 1$$ Zilitinkevich and Mironov (1996)

$C_h = 0.5$; $C_s = 10$; $C_i = 20$;
$C_{sr} = (1.0)$; $C_{ir} = (1.7)$.

(A1.1.16) $$\frac{h\,f}{C_h\,u_*} + \frac{1}{C_{sr}^{\,2}}\,\frac{h^2 f}{C_s\,L_*u_*} + \frac{h^2\,N_{BV}\,f}{C_{ir}^{\,2}\,u_*^{\,2}} = 1$$ Handorf (1996)

$C_h = 0.5$; $C_{sr}^2 = \frac{\sqrt{3}}{2}\kappa$; $C_{ir}^2 = 0.125$.

From the assumption that turbulence production vanishes at the SBL top and the Richardson number therefore exceeds its critical value, the following equations have been derived (in all the equations, Θ may be replaced by Θ_v):

(A1.1.17) $$h = Ri_c\,\frac{V_h^2}{\beta(\Theta_h - \Theta_0)}$$

$Ri_c = 0.33$ Hanna (1969), Wetzel (1982)
$Ri_c = 0.5$ Mahrt (1981b), Troen and Mahrt (1986)
$Ri_c = 0.25$ Holtslag et al. (1990)

(A1.1.18) $$h = Ri_c \frac{(u_h - u_s)^2 + (v_h - v_s)^2 + bu_*^2}{\beta\,(\Theta_{v,h} - \Theta_{v,s})} + z_s$$ Vogelezang and Holtslag (1996)

Ri_c = 0.25; b ≈ 100; z_s ≈ 20 m

(A1.1.19) $$h = Ri_b \frac{(V_h - \overline{V})^2}{\beta[(\partial\Theta / \partial t)_h - (\partial\Theta / \partial t)_0]\Delta t}$$ Tjemkes and Duynkerke (1989)

(A1.1.20) $$h = c \frac{f V_g^2 \cos\alpha_0 \sin\alpha_0}{\beta\,|\partial\Theta_0 / \partial t|}$$

c = 0.15 Nieuwstadt and Tennekes (1981)

with α_0 being the deviation angle between the surface wind and the geostrophic wind.

Integrating the equations of motion over the whole (barotropic) SBL, Wyngaard (1975) has derived the following equation:

(A1.1.21) $$h = c \frac{u_*^2}{f V_g \sin\alpha_0}$$ with α_0 as in (A1.1.20) and

c = 1.1 Wyngaard (1975)
c = 1.6 Brost and Wyngaard (1978)
c = 1.56 Rao and Snodgrass (1979)

A1.2 Prognostic Relations

Most prognostic relations for the parameterization of the SBL height can be written in the form

(A1.2.0) $$\frac{\partial h}{\partial t} = \frac{h_e - h}{\tau_{SBL}}.$$

In (A1.2.0), h_e is a stationary limit, which is approached by h during the night. This process is governed by the characteristic time-scale T_h. In principle, each of the diagnostic equations given in Appendix A1.1 could be used as a definition equation for h_e.

With h_e according to (A1.1.3) and $1/f$ being the characteristic time-scale, the following equations have been proposed in the literature:

(A.1.2.1) $$\frac{\partial h}{\partial t} = 0.025 u_* \left(1 - \frac{h}{h_e}\right)$$ Deardorff (1971)

(A1.2.2) $$\frac{\partial h}{\partial t} = 1.5 f \left(h_e - h\right)$$ Khakimov (1976)

(A1.2.3) $$\frac{\partial h}{\partial t} = 0.06 \frac{u_*^2}{hf} \left[1 - \left(\frac{h}{h_e}\right)^3\right]$$ Smeda (1979a)

Other parameterizations than in (A1.2.1) .. (A1.2.3) for h_e and T_h are used in (A1.2.4) .. (A1.2.7):

(A1.2.4) $$h_e = \kappa L_* \frac{|\Delta V|^2}{u_*^2} \frac{1 - 4\,Ri_*}{1 + 5h/L_*}\,;\quad \tau_{SBL} = \frac{\kappa L_*}{u_*}\left[45 + \delta\left(\frac{N_{BV}\,h}{u_*}\right)^2\right]$$

with $\Delta V = V_h - \overline{V}$, $\Delta\Theta = \Theta_h - \overline{\Theta}$, $Ri^* = h\beta\Delta\Theta\,|\Delta V|^{-2}$, $\delta = 1$ if $\partial h/\partial t > 0$, and $\delta = 0$ else, and $N_{BV} = \sqrt{\beta\gamma^+}$ with γ^+ being γ_Θ above h. Binkowski (1983)

The combined effect of an increase in h due to entrainment processes and a decrease due to the decay of turbulence is described through

(A1.2.5) $$h_e = Ri_b \frac{|V_h|^2}{\beta\Delta\Theta}\,; \qquad \tau_{SBL} = 330\frac{h}{|V_h|}$$

with $Ri_b = 0.5$ Mahrt (1981b)

From the equations of motion and assuming self-similarity of the vertical profiles of wind and temperature in the SBL, the following parameterization has been derived:

(A1.2.6) $$h_e = \frac{c_v\, f\, V_g^2 \sin\alpha\cos\alpha}{\beta\,|\partial\Theta_0/\partial t|} \qquad T_h = -\frac{3}{4}\frac{(\Theta_h - \Theta_0)}{\partial\Theta_0/\partial t}$$

with $c_v = 0.15$ Nieuwstadt and Tennekes (1981)

The combined effect of the inertial oscillation of the wind vector and nocturnal cooling has been taken into account by Garratt (1982a) who suggested a time scale $1/T_h = 1/T_1 + 1/T_2$ and the use of (A1.1.6) for the parameterization of h_e

(A1.2.7) $$\frac{1}{T_h} = \frac{1}{T_1} + \frac{1}{T_2}\,;\quad \frac{1}{T_1} = \frac{1}{\Delta\Theta}\left(\frac{\partial\Theta_h}{\partial t} - \frac{\partial\Theta_0}{\partial t}\right)\,;\quad \frac{1}{T_2} = \frac{\boldsymbol{V_h}}{V_h^2}\cdot\left(\frac{\partial \boldsymbol{V}}{\partial t}\right)_h$$ Garratt (1982a)

The following relations have been derived from a parameterization of the TKE budget equation:

(A1.2.8)

$$\frac{\partial h}{\partial t} = \frac{3}{2}\frac{u_*}{|\Delta\boldsymbol{V_h}|^2}\left[\frac{0.38(1 - Ri_*)}{1 + 5\,h/L_*}|\Delta\boldsymbol{V_h}|^2 - \frac{2}{3}u_*\,(\Delta u\cos\alpha + \Delta v\sin\alpha)\right] + \frac{h}{|\Delta\boldsymbol{V_h}|^2}(\Delta\boldsymbol{V})\cdot\frac{\partial\boldsymbol{V_h}}{\partial t}$$

with $Ri_* = \beta\, h\,(\Theta_h - \Theta)\,/\,|\Delta V|^2$ and $\Delta\boldsymbol{V} = \boldsymbol{V_h} - \boldsymbol{V}$. Zeman (1979)

To describe the growth of the turbulent SBL during the initial stage of its development ($h << h_e$) Zilitinkevich (1975a) has proposed the following relation (from dimensional considerations):

(A1.2.9) $$\frac{\partial}{\partial t}\left(\frac{c\beta}{u_*^4} < w'\Theta' >_0^2 h^2\right) = - < w'\Theta' >_0$$ Zilitinkevich (1975a)

Assuming $\langle w'\,\Theta'\rangle_0$ and u_* to be roughly constant with time, with $c \approx 7.5$ it follows

(A1.2.9a) $$\frac{\partial h}{\partial t} = 0.027\,\frac{u_* L_*}{h}\,.$$

To describe the time evolution of h for both the CBL and the SBL, Smeda (1979b) used

(A1.2.10) $$\frac{\partial h}{\partial t} = \frac{\langle w'\Theta' \rangle_0}{\Delta\Theta} + \frac{2\,u_*^2\,\overline{V}\,e^{-\eta h}}{\beta h \Delta\Theta}$$

$\eta = 10^{-3}..10^{-2}\ m^{-1}$ Smeda (1979b)

A2 Prognostic equations for the parameterization of the CBL height

The majority of equations proposed in the literature to describe the time evolution of the CBL height has been derived from a parameterization of the heat flux $\langle w'\,\Theta' \rangle_h$ at the CBL top to close the equation system of a simple mixed-layer (slab) model. The basic equations of a mixed-layer model (written here for the mean potential temperature in the bulk of the CBL, $\overline{\Theta}$, are (note that $\overline{\Theta} = \langle\overline{\Theta}\rangle$):

(A2.1) $$\frac{\partial \overline{\Theta}}{\partial t} = \frac{\langle w'\Theta' \rangle_0 - \langle w'\Theta' \rangle_h}{h}$$

(A2.2) $$\frac{\partial\,(\Delta\Theta)}{\partial t} = \gamma_\Theta \frac{\partial h}{\partial t} - \frac{\partial \overline{\Theta}}{\partial t}$$

(A2.3) $$-\langle w'\Theta' \rangle_h = \Delta\Theta \frac{\partial h}{\partial t}$$

Similar equations can be written down for the wind components, u and v, and for the water vapour mixing ratio, q. A large-scale vertical velocity at the CBL top, w_h, has been neglected for convenience, it could be easily taken into account as an additive term to $\partial h/\partial t$. Consideration of a synoptic-scale vertical velocity implies a time dependent lapse rate with $\gamma_\Theta(t) = \gamma_\Theta(0)\ \exp[-w_h(z)t/z]$ (cf. Carson, 1973; Steyn, 1981).

Assuming that the temperature jump at the mixed-layer top is zero, and therefore $\langle w'\Theta' \rangle_h = 0$, (A2.1) and (A2.2) can be combined to:

(A2.4) $$\frac{\partial h}{\partial t} = \frac{\langle w'\Theta' \rangle_0}{\gamma_\Theta\, h}.$$

This so-called "*encroachment*"-relation has been shown to provide a good description of the mixed-layer growth in situations which are clearly dominated by convective heating from the earth's surface. It has been applied, e.g., by Gamo (1985), Glendening (1990) and Lyra et al. (1992).

In general, however, (A2.4) underpredicts mixed-layer growth, since entrainment effects at the top of the CBL cannot be neglected. The heat flux at the mixed-layer top can be parameterized through the surface heat flux (the so-called flux-ratio-method):

(A2.5) $$\langle w'\,\Theta' \rangle_h = -A\,\langle w'\,\Theta' \rangle_0$$

Then (A2.3) can be written as

(A2.6) $$\frac{\partial h}{\partial t} = A\,\frac{\langle w'\Theta' \rangle_0}{\Delta\Theta}$$

$A = 1$ Ball (1960)

$A = 0.1$ Lilly (1968), Deardorff (1972)

$A = 0.2$ Tennekes (1973)
$A = 0 .. 0.5$ Carson (1973)

Assuming $\partial(\Delta\Theta) / \partial t = 0$ and using the flux-ratio-assumption (A2.5), (A2.1) and (A2.2) can be combined into

(A2.7) $$\frac{\partial h}{\partial t} = (1+A)\frac{\langle w'\Theta'\rangle_0}{\gamma_\Theta h}.$$ $A = 0.1$ Deardorff (1972), Stull (1976a)

If one desists from the assumption of a constant temperature jump at the mixed-layer top but assumes that $\Delta\Theta$ immediately adjusts to the changing conditions at the ML-top this results in

(A2.8a) $$\frac{\partial h}{\partial t} = (1+2A)\frac{\langle w'\Theta'\rangle_0}{\gamma_\Theta h}.$$ $A = 0$ or 0.5 Carson (1973)

$A = 0.25$ Betts (1973)

This implies

(A2.8b) $$\Delta\Theta = \frac{A}{1+2A}\gamma_\Theta h$$ Betts (1973), Carson (1973)

Driedonks (1981)

Further relations for $\langle w'\,\Theta'\rangle_h$ have been derived from a parameterization of the TKE budget equation either integrated over the whole mixed layer or specified at the mixed-layer top. They mainly differ in which terms of the TKE budget equation have been neglected and how the remaining terms are parameterized. Considering mechanical turbulence production due to surface friction in addition to the buoyant production from surface heating this results in

(A2.9) $$\frac{\partial h}{\partial t} = A\frac{\langle w'\Theta'\rangle_0}{\Delta\Theta} + B\frac{u_*^3}{\beta h \Delta\Theta} = \frac{Aw_*^3 + Bu_*^3}{\beta h \Delta\Theta}.$$

$A = 0.2$	$B = 2.5$	Tennekes (1973)
$A = 0.2$	$B = 1.6$	Deardorff et al. (1980)
$A = 0.2$	$B = 5$	Driedonks (1981)

This equation has been studied in detail by Driedonks (1981, 1982b) and is broadely used today for simulating the CBL evolution (e.g., Chong, 1985; Olesen et al., 1987; Clarke, 1990; Novak, 1991; Culf, 1992; Zilitinkevich et al., 1992). Thomson (1992) presents an analytical solution of the complete mixed layer model, comprising (A2.1) to (A2.3) and (A2.9), valid under certain additional assumptions.

An equation very similar to (A2.9) has been proposed by Smeda (1979b) in his bulk ABL model to describe ABL height evolution for both stable and unstable conditions:

(A2.10) $$\frac{\partial h}{\partial t} = A\frac{\langle w'\Theta'\rangle_0}{\Delta\Theta} + 2\frac{u_*^2\,\overline{V}\,e^{-\eta h}}{\beta h \Delta\Theta}.$$ $\eta = 10^{-2}..10^{-3}\ m^{-1}$

Smeda (1979b)

Assuming again $\partial(\Delta\Theta)/\partial t = 0$ [as for (A2.7)], (A2.1) and (A2.2) can be combined to

(A2.11) $$\frac{\partial h}{\partial t} = (1+A)\frac{\langle w'\Theta'\rangle_0}{\gamma_\Theta h} + B\frac{u_*^3}{\gamma_\Theta \beta h^2}.$$

$A = 0.1$	$B = 8..12$	Garratt and Francey (1978)
$A = 0.2$	$B = 2.5$	Kolarova et al. (1989)

If one again assumes that $\Delta\Theta$ is in equilibrium with the actual meteorological conditions, the alternative equation reads

(A2.12a) $$\frac{\partial h}{\partial t} = (1+2A)\frac{\langle w'\Theta'\rangle_0}{\gamma_\Theta h} + 2B\frac{u_*^3}{\gamma_\Theta \beta h^2} = \frac{(1+2A)w_*^3 + 2Bu_*^3}{\gamma_\Theta \beta h^2}.$$

$A = 0.2$	$B = 2.5$	Gryning and Batchvarova (1990a)

For $\Delta\Theta$ this implies

(A2.12b) $$\Delta\Theta = \frac{Ah - \kappa B L_*}{(1+2A)h - \kappa B L_*}\gamma_\Theta h.$$

Zilitinkevich (1975b) suggests to consider also temporal changes of the local TKE-level at the CBL top. These are attributed to the fact that the air which is entrained from the free atmosphere into the mixed layer has to adjust to the mean energetic level within the mixed layer (so-called "*spin-up*"-effect). The "*spin-up*"-term is of special importance for near-neutral stability and low values of h. Thus, (A2.9) is modified to

(A2.13) $$\frac{\partial h}{\partial t} = \frac{Aw_*^3 + Bu_*^3}{\beta h \Delta\Theta + c_T \sigma_w^2}.$$

$A = 0.2$	$B = 0$	$c_T \approx 1$	Zilitinkevich (1975b)
$A = 0.25$	$B = 0$	$c_T = 1.66$	Zeman and Tennekes (1977)
$A = 0.2$	$B = 5$	$c_T = 1.5$	Driedonks (1981)
$A = 0.2$	$B = 0$	$c_T = 1$	Wetzel (1983)

In (A2.13), $\sigma_w{}^2$is given as $\sigma_w{}^2 = w_*{}^2+\eta^2 u_*{}^2$, the value for η is normally assumed in the range $\eta = 1..2$ (Zeman and Tennekes, 1977; Tennekes and Driedonks, 1981; Byun and Arya, 1990). More recent papers describe the relationship between w_* and u_* with a cubic equation, i.e. $\sigma_w{}^3 = w_*{}^3+\eta^3 u_*{}^3$ (Driedonks, 1981, Clarke, 1990, Rayner and Watson, 1991). Driedonks (1981) points out that this σ_w is not identical to a measured standard deviation of the vertical wind velocity component but is "*a scaling velocity for turbulent fluctuations in the bulk of the mixed layer*".

The analogous equation to (A2.12a) considering the "*spin-up*" term reads

(A2.14) $$\frac{\partial h}{\partial t} = \langle w'\Theta'\rangle_0 \left[\frac{\gamma_\Theta h^2}{(1+2A)h - 2\kappa B L_*} + \frac{c_T u_*{}^2}{\beta(1+A)h - \kappa B L_*}\right]^{-1}.$$

$A = 0.2$	$B = 2.5$	$c_T = 8$	Batchvarova and Gryning (1991)

Although the introduction and theoretical justification of the "spin-up" term is mainly attributed to Zilitinkevich (1975b), it can already be found in an equation proposed by

Deardorff (1974). The following relation was derived based on experiments in a water tank and numerical simulations with a three-dimensional boundary-layer model:

(A2.15) $$\frac{\partial h}{\partial t} = \frac{1.8 w_*^3 + 2u_*^3 (1 - 3f h / u_*)}{\gamma_\Theta \beta h^2 + 9(w_*^2 + 0.8 u_*^2)}$$ Deardorff (1974)

The second term in the numerator of (A2.15) represents a relaxation process during which h approaches an equilibrium value $h_e = 0.33\, u_*/f$ similar to some of the prognostic equations for the stable boundary layer height. Operational application of (A2.15) was proposed, e.g., by Smeda (1979a), Wetzel (1983) and Ossing (1987).

An equation quite similar to (A2.15) is

(A2.16) $$\frac{\partial h}{\partial t} = \frac{w_*^3 + u_* (V_h - \overline{V})^2}{\gamma_\Theta \beta h^2 + 5(w_*^2 + 9u_*^2)}$$ Binkowski (1983)

where V_h is the wind velocity at the top of the EL, while $\overline{V}$ is the wind velocity averaged over the ML.
Binkowski (1983) has used (A2.16) to simulate the time evolution of the ABL height for both stable and unstable conditions with only slight modifications.

Mechanical turbulence production due to wind shear at the CBL top is additionally considered in:

(A2.16a) $$\frac{\partial h}{\partial t} = \frac{A w_*^3 + B u_*^3}{\beta h \Delta\Theta - C|\Delta V|^2 + c_T \sigma_w^2}$$

$A = 0.2$	$B = 5$	$C = 0.7$	$c_T = 1.5$	Driedonks (1981)
$A = 0.32$	$B = 7.5$	$C = 1$	$c_T = 0.75$	Boers et al. (1984)
$A = 0.18$	$B = 0.42$	$C = 0.2$	$c_T = 0.8$	Rayner & Watson (1991)

Driedonks (1982b) as well as Driedonks and Tennekes (1984) pointed out that the shear term in the denominator might occasionally cause numerical instabilities when integrating (A2.16a). Rayner and Watson (1991) therefore propose not only a much smaller value for the constant C but also a dynamic adaptation of the integration time-step or the use of (A2.16) in an implicit form:

(A2.16b) $$\frac{\partial h}{\partial t} = \frac{A w_*^3 + B u_*^3 + C|\Delta V|^2 (\partial h / \partial t)_{t-\Delta t}}{\beta h \Delta\Theta + c_T \sigma_w^2}$$

with $(\partial h/\partial t)_{t-\Delta t}$ being the entrainment rate from the previous time step.

An additive correction term to account for wind shear effects at the CBL top is used in:

(A2.17) $$\frac{\partial h}{\partial t} = \frac{A w_*^3 + B u_*^3}{\beta h \Delta\Theta} \left[1 + \frac{0.7 Ri_f^{-1} (2 + 0.7) Ri_f^{-1}}{1 + 2 (1 + 0.7 Ri_f^{-1}) (1.1 - 0.7 Ri_f^{-1})} \right]$$

with $Ri_f^{-1} = \frac{7}{6} |\Delta V|^2 \gamma_\Theta / [\beta (\Delta\Theta)^2]$ Fairall (1984)

Generally, the parameterization of wind shear across the entrainment layer is still an unsolved problem. Due to the inherent uncertainties, most authors do not consider this effect or even dissuade from taking it into account (Driedonks, 1981; Driedonks and Tennekes, 1984; Deardorff, 1985; Arya and Byun, 1987).

Furthermore, Zeman and Tennekes (1977) explicitly parameterized the dissipation term in the TKE budget equation which results in:

(A2.18) $$\frac{\partial h}{\partial t} = \frac{A w_*^3 + B u_*^3 - C_2\, h N_{BV}\, \sigma_w^2}{\beta h \Delta\Theta - C_1 |\Delta V|^2 + c_T \sigma_w^2}$$

$A = 0.5$	B~4	$C_1 = 0$	$c_T = 3.55$	$C_2 = 0.024$	Zeman and Tennekes (1977)
$A = 0.6$	$B = 4.8$	$C_1 = 0.7 c_T = 4.3$		$C_2 = 0.030$	Driedonks (1981)
$A = 0.4$	$B = 0$	$C_1 = 0$	$c_T = 2$	$C_2 = 0.020$	Arya and Byun (1987)

Equation A2.18 was also used by Benkley (1977) as well as Byun and Arya (1990) with the same values for the constants as proposed by Zeman and Tennekes (1977). Looking at the values for the constants in (A2.18) applied by different authors, it becomes evident that those for A and c_T differ considerably from the values proposed for use in connection with most of the other equations. This is explained by Driedonks (1981) by the fact that in all equations not explicitly parameterizing the dissipation of TKE, this is achieved by considering dissipation as a constant fraction of TKE-production, yielding thus different values for most of the constants.

The CBL growth is parameterized implicitly in

(A2.19) $$(c_2 + Ri_1) E + c_3 Ri_2^{3/2} \left(\frac{Ri_1 E}{1 + Ri_1 E} \right)^3 = c_1 - \frac{2}{5} c_2 De$$

$c_1 = 0.2$ $c_2 = 0.8$ $c_3 = 0.1$ Zilitinkevich (1989a)

with $E = \frac{1}{w_*} \frac{\partial h}{\partial t}$, $Ri_1 = \frac{\beta h \Delta\Theta}{w_*^2}$, $Ri_2 = \frac{N_{BV}^2 h^2}{2 w_*^2}$, $De = \frac{h}{\langle w'\Theta' \rangle_0 w_*} \frac{\partial \langle w'\Theta' \rangle_0}{\partial t}$

Note that mechanical turbulence production is completely neglected in (A2.19). On the other hand, (2.19) contains a parameterization of the energy loss to the free atmosphere associated with gravity wave activity.

Some parameterizations do not consider h itself as the relevant length scale but introduce the entrainment layer depth Δh_E, e.g. in

(A2.20) $$\frac{\partial h}{\partial t} = \frac{A \langle w'\Theta' \rangle_0}{\Delta\Theta} + \frac{B u_*^2 \overline{V} + C |\Delta V|^3}{\beta \Delta h_E \Delta\Theta}$$

$A = 0.1$ $B = 0.05$ $C = 0.001$ Stull (1976a,b)

or

(A2.21) $$\frac{\partial h}{\partial t} = \frac{2}{\beta \Delta\Theta \Delta h_E} (A w_*^3 + B u_*^3 + C |\Delta V|^3)$$

$A = 0.0167$ $B = 0.5$ $C = 0.0006$ Stull (1988)

Here Δh_E is given through $\frac{\Delta h_E}{h} = \frac{-\langle w'\Theta' \rangle_h}{- < w'\Theta' >_h + \langle w'\Theta' \rangle_0}$.

The typical range for the values of the constants A, B and C in (A2.20) was given by Stull (1976a) as follows: A = 0.1..0.3, B = 0.01..0.22, and C = 0.0008..0.01.

The entrainment layer depth as a relevant length scale in addition to h also appears in

(A2.22) $$\frac{\partial h}{\partial t} = \left[1+2A-2E\left(1+\frac{\Delta h_E}{2h}\right)\right] \frac{\langle w'\Theta' \rangle_0}{\Delta\Theta\left(1+\frac{\Delta h_E}{h}\right) - \frac{|\Delta V|^2}{\beta h}}$$

$A = 0$ $E = 0.4$ Mahrt and Lenschow (1976)

with $\Delta h_E = \frac{Ri_b\ |\Delta V|^2}{\beta\ \Delta\Theta}$ and $Ri_b = 0.25$.

A length scale L_c which is assumed proportional to the typical wavelength λ of the convective eddies is used in

(A2.23) $$\frac{\partial h}{\partial t} = \frac{A w_*^3}{C_\Theta\, \beta L_c\, \Delta\Theta + c_T w_*^2} + C_e w_* \frac{\Delta h_E}{L_c}$$

$A = 0.25$ $c_T = L_c/h$ $C_\Theta = 0.5$ $C_e = 0.15$ Mahrt (1979)

with $\Delta h_E = \partial h/\partial t\ N_{BV}$

Advection is taken into account in addition to local heating in the following equation:

(A2.24) $$\frac{\partial h}{\partial t} = A \frac{< w'\Theta' >_0}{\Delta\Theta} - \sqrt{\frac{(1+2A)\ \overline{V}_h \langle w'\Theta' \rangle_0}{2\gamma_\Theta\, x}}$$ Steyn and Oke (1982)

with x being the advective fetch.

More generalized but much more complicated equations for $\partial h/\partial t$ have been proposed, e.g., by Deardorff (1979), Fedorovich (1995) and Fedorovich and Mironov (1995). They partly even consider horizontal inhomogeneity or the internal structure of the EL. However, these equations are not suitable for operational application, since they contain additional constants and parameters which are not really known or at least very uncertain.

A3 Questionnaire on the resolution of operational radiosoundings in WMO Regional Association VI (Europe) countries

A3.1 Text of the questionnaire

Questionnaire
"Vertical Resolution of Operational Radiosonde Ascents"

issued by COST-710 (Preprocessing of Meteorological Data for Dispersion Models) - Working Group II (Determination of Mixing Heights)

If the situation is not the same for all of your TEMP stations, please copy this sheet and fill in separately for each group of stations. If the space provided is insufficient, please use additional sheets!

1) Name and address of agency filling in this form (if possible, including fax and electronic mail):

2) Contact Person:

3) TEMP stations operated by agency (WMO station code and name, nominal and real launching hours [UTC] of pTU-soundings):

4) How are significant levels to be reported in TEMP part B selected?

o manually, by personal judgement
o manually, using graphical instruments
o by a computer programme of your own
o by a computer programme of the radiosonde supplier
o _____

5) Which are the criteria for selecting the significant levels in TEMP part B?

o just to meet the WMO requirements

o resolution usually higher than required by WMO
(please specify your criteria below, separately for wind and temperature!)

6) Do you archive radiosonde data with a vertical resolution higher than transmitted via GT.?

o yes, on electronic media (please continue with question no. 8)
o yes, in form of diagrammes or written tables (please continue with question no. 7)
o no (please continue with question no. 7)

7) Do you consider, or would it be feasible for you, to archive data with higher resolution in electronic form?

o yes, with a resolution of _____
o no, because _____
(please continue with question 10)

8) When did you start archiving the high-resolution data in electronic form, and what is their resolution (if specified in seconds, please give also typical rising speed of balloon in the lower troposphere?

9) Are you able to deliver sets of high-resolution data on electronic media for periods of several years? (This question refers to the technical possibility only and not to commercial aspects such as fees charged for data.)

o yes
o no

10) Would you be in favour of an internationally agreed format for the archiving of high-resolution radiosonde data?

o yes
o no

11) Considering the technical progress in radiosonde technology, data handling and transmission, what is your opinion concerning an enhanced minimum standard for the vertical resolution of TEMP part B data (at least in the lower troposphere)?

o I would welcome that
o I would welcome that, but our agency is not yet technically prepared for
o I do not think that this is important, but we could change / have already changed our practices
o I do not think that this is important, and it would not be easily possible for us to change the current practice
o other: _____

Space for additional remarks:

A3.2 Results

Abbreviations used in the table:

Significant level selection method (S.L. selection method):
CO ... own computer programme
CS ... computer programme of radiosonde supplier
MG ... manually, using graphical instruments

High resolution data archive (high res.d. arch.):
C ... computerized archive
P ... archived on paper (charts or tables)

Improved WMO standards for TEMP part B (imp'd WMO stnd.):
Y-NP ... yes, but not yet technically prepared for that
NI ... not important, but better standards already implemented

The present WMO regulation on the selection of the significant levels for TEMP part B

Countries which provide resolution better than WMO standards are shaded.

Country	# of sta-tions	# of asc. / day	real ascent time	S.L.sel-ection method	S.L. sel. criteria (GTS)	high res.d. arch.	h.r.d. arch. since	h.r.d. resol.	able to deliver hrd	intern. format archive	impr'd WMO stnd.
Austria 035	1	2	-0:40	CO	WMO	C	1987	(21)	Yes	Yes	Yes
010,120,240	3	1	?	CS	WMO	C	1994	(22)	No	Yes	-
Azerbaijan	1	1	-	MG	WMO	P	?	?	No	Yes	No
Belgium	2	2	-	CS	WMO	C	(11)	10s	Yes	No	Y-NP
Bulgaria	1	2	-0:30	CO	WMO	C	1960	30s	Yes	Yes	Y-NP
Croatia	1	2	-0:45	(13)	WMO	C	1985	?	Yes	Yes	Yes
Cyprus	1	1	-0:45	MG	WMO	No	-	-	No	Yes	Y-NP
Czech Rep.	1	4	(12)	CS	WMO	C	1971		Yes	Yes	Y-NP
Denmark	7	2	-	CS	better (14)	C	1991	?	Yes	Yes	Yes
Finland	3	2	-	CS	WMO	C	1961	10s	Yes	Yes	Yes
France											
- 07...	7	2	-	CO	better (3)	C	1989	?	Yes	Yes	-
-not in RA VI	15	1-2(2)	-	CO	better (3)	C	1989	?	Yes	Yes	-
Germany											
10184,10393	2	4	-1:15	-	better (1)	C	1992	10s	Yes	Yes	Yes
- all other	7	2	-1:15	-	better (1)	C	1992	10s	Yes	Yes	Yes
Greece	1	2	-	CS	-	C	1956	(15)	Yes	Yes	Y-NP
Ireland	1	3	-0:45	CS	WMO	C	1994	10s	No	Yes	Yes
Italy	6	4	-1:00	CS	better	No	-	10s	?	Yes	Yes
Jordan	1	1	-1:00	MG	WMO	No	-	-	?	Yes	Y-NP
Latvia	1	1	-	C	better (4)	P	?	?	No	Yes	Y-NP
Lithunia	1	2	-	CS	WMO	No	1978	?	Yes	?	Y-NP
Macedonia	1	1	?	CS	WMO	C	1995	?	Yes	Yes	Yes
Netherlands	1	4	-	CS	better (5)	C	1993	10s	Yes	Yes	Yes
Norway (16)											
- 01661	1	4	-0:45	CS	WMO	C	1995	2s	No	?	Yes
- 01384	1	1	-1:00	CS	WMO	C	1995	2s	No	?	Yes
- all other	6	2	-0:55	CS	WMO	C	1995	2s	No	?	Yes
Portugal	2	2	-1:00	CS	?	C	1992	?	(10)	Yes	Yes
- Acores	1	1	-1:30	CS (8)	(9)	No	-	-	No	Yes	
Romania 420	1	2	?	CS	(17)	(18)	1994	10s	Yes	Yes	Yes
15120,	1	2	?	MG	better	No	1994	10s	No	Yes	Y-NP
15480	1	2	?	MG	WMO	No	-	-	No	Yes	Y-NP
Russia	116	-	-		WMO	No	-	-	No	Yes	Y-NP
Slowakia	1	2	-0:45	CS	WMO	C	1991	10s	Yes	Yes	Y-NP
Spain	7	2	-0:45	CS	WMO	P	?	?	?	Yes	Yes
Sweden	4	-	-	CS	WMO	C	1995	(19)	No	?	-
Switzerland	1	2	-1:00	MG	better (7)	C	1990	10s	Yes	Yes	NI
Syria	2	2	?	?	?	?	?	?	?	?	Yes
Turkey	7	2	-	CS	better	?	?	?	?	Yes	Y-NP
Ukrainia	8	2	-	(20)	better (8)	P	?	?	No	Yes	Y-NP
- Kyiev	1	4		(20)	better (8)	P	?	?	No	Yes	Y-NP
Un. Kingdom	8	4	-0:45	CS	better (23)	C	1991	2s	Yes	Yes	-
- Gibraltar	1	2	-0:45	CS	better (23)	C	1991	2s	Yes	Yes	
Yugoslavia	1	1	+0:15	CS	WMO	No	-	-	No	Yes	Y-NP

Footnotes

(1) surface - 700 hPa: 0.3 K, 10°, 2.5 m/s (T, dd, ff)
700 hPa - tropopause: 0.6 K, 10°, 5 m/s

(2) different sondes are used

(3) surface - 700 hPa: 0.8 K; 15 % (rh); 700 hPa - 300 hPa: 1 K; >300 hPa: 2 K

(4) Troposphere: 1 K, 10°, 5 m/s, 15 % (T, dd, ff, rh); Stratosphere: 2 K

(5) 0.5 K, 5m/s, 5% (T, ff, rh)

(6) > 10 kt: 0.5 K, 10°, 10 kt, 10 % (T, dd, ff, rh)
< 10 kt: 30° (dd)

(7) Troposphere: 1 K, 10°, 5 m/s; Stratosphere: 2 K

(8) station 08508: by Vaisala Digicora MW11

(9) station 08508: better: T: specified under FM 35-V Temp

(10) station 08522, 08579: Yes, only for two years (1992, 1993)
station 08508: No

(11) station 06476: 1993; station 06447: 1990

(12) 00 UTC and 12 UTC: -0:45; 06 UTC and 18 UTC: -0:30

(13) CO, GMD-A1 with our programm for PC; CS, Vaisala Microcora, from 1.8.1995

(14) better for domestic distribution only

(15) every 50 hPa up to 200 hPa

(16) stations 01400: -0:45 real launching time

(17) better (00 UTC), WMO (12 UTC)

(18) C (00UTC), No (12 UTC)

(19) 10 s (first 5 min.), 30 s (5 - 15 min.), 1 min. from 15 min.

(20) MG: stations 33658, 33393, 33837, 33946, 33791;
CS: stations 33345, 33317, 33631, 34300

(21) 50% of WMO criteria

(22) 30 s - 2 min., depending on height .

(23) T 0.5 K; u,v 2 m/s; computer programme allows manual interaction to control reported structure

T temperature
dd wind direction
ff wind velocity
rh relative humidity

A4 Bibliography on mixing layer height in the atmosphere

A4.1 Introductory remarks to the bibliography:

The bibliography (consisting of the literature list A4.2 and the cross-reference table A4.3) contains references to literature dealing with the following topics:

- determination of the MH on the basis of measurements
- parameterization and modelling of the MH or the ABL height
- regional variability and climatology of the MH
- dependence of trace constituent concentrations on the MH

Literature on the following subjects is *not* included:

- oceanic mixing layer
- results of laboratory (water tank, wind tunnel) experiments
- internal boundary layer height
- (nocturnal) surface inversion height (if MH / ABL height is not discussed)
- entrainment zone depth (if MH / ABL height is not discussed)

Certainly, the list is far from being complete. Any additional hints or corrections are welcome and should be sent to Frank Beyrich.

In addition, the literature list (but not the cross-reference table) should contain all papers quoted in this report, whether they fulfill the above criteria or not. On the other hand, not all the literature listed in the bibliography is necessarily quoted in the text of the report.

A4.2 Literature list

André, J.C. (1983): On the variability of the nocturnal boundary layer depth. *J. Atmos. Sci.* **40**, 2309-2311

André, J.C.; G. De Moor; P. Lacarrere; G. Therry; R. du Vachat (1978): Modeling the 24 hour evolution of the mean and turbulent structures of the planetary boundary layer. *J. Atmos. Sci.* **35**, 1861-1883.

André, J.C.; L. Mahrt (1982): The nocturnal surface inversion and influence of clear-air radiative cooling. *J. Atmos. Sci.* **39**, 864-878.

Anfossi, D. (1989): A discussion on nocturnal temperature profiles. *Atmos. Environm.* **23**, 1177-1186.

Anfossi, D.; P. Bacci; A. Longhetto (1976): Forecasting of vertical temperature profiles in the atmosphere during nocturnal radiation inversions from air temperature trend at screen height. *Quart. J. Roy. Meteorol. Soc.* **102**, 173-180.

Angevine, W.M.; A.B. White; S.K. Avery (1994a): Boundary layer depth and entrainment zone characterization with a boundary-layer profiler. *Boundary-Layer Meteorol.* **68**, 375-385

Angevine, W.M.; M. Trainer; D.D. Parrish; M.P. Buhr; F.C. Fehsenfeld; G.L. Kok (1994b): Wind profiler mixing depth and entrainment measurements with chemical applications. *Proc. 8th AMS Conf. Air Poll. Meteorol. & AWMA, Nashville*, 32-34

Angevine, W.M.; W.L. Clark; T.E. VanZandt (1995): Boundary layer height climatology measured with the 915-MHz radar wind profiler at the Flatland Atmospheric Observatory. *Proc. 11th AMS Symp. Boundary Layers & Turb., Charlotteville*, 130-131

Aron, R. (1983): Mixing height - an inconsistent indicator of potential air pollution concentrations. *Atmos. Environm.* **17**, 2193-2197

Arya, S.P.S. (1981): Parameterizing the height of the stable atmospheric boundary layer. *J. Appl. Meteorol.* **20**, 1192-1202

Arya, S.P.S. (1984): Parametric relations for the atmospheric boundary layer. *Boundary-Layer Meteorol.* **30**, 57-73

Arya, S.P.S. (1988): *Introduction to Micrometeorology*. San Diego: Academic Press. xxi + 307 pp.

Arya, S.P.S.; D.W. Byun (1987): Rate equations for the planetary boundary layer depth (urban vs. rural). *in: Modeling the urban boundary layer. Boston: Amer. Meteorol. Soc.*, 215-251

Bacci, P.; C. Giraud; A. Longhetto; R. Richiardone (1984): Acoustic sounding of land and sea breezes. *Boundary-Layer Meteorol.* **28**, 187-192.

Ball, F.K. (1960): Control of inversion height by surface heating. *Quart. J. Roy. Meteorol. Soc.* **86**, 483-494

Batchvarova, E.; S.E. Gryning (1991): Applied model for the growth of the daytime mixed layer. *Boundary-Layer Meteorol.* **56**, 261-274

Batchvarova, E.; S.E. Gryning (1994): Applied model for the height of the daytime mixed layer and the entrainment zone. *Boundary-Layer Meteorol.* **71**, 311-323

Baxter, R.A. (1991): Determination of mixing heights from data collected during the 1985 SCCCAMP field program. *J. Appl. Meteorol.* **30**, 598-606

Beljaars, A.C.M.; R. Agterberg (1988): Automatische detektie van inversies met sodar. *De Bilt - KNMI Techn. Rep. TR-106*, 17 pp.

Beljaars, A.C.M.; A.K. Betts (1992): Validation of the boundary layer representation in the ECMWF model. *ECMWF Seminar Proceedings: Validation of Models over Europe, Vol.II, Reading (UK), 7-11 September 1992.*

Benkley, C.W. (1977): Model of the planetary boundary layer growth using sodar validation: Applications to pollutant dispersion. *M.S. Thesis, Penn. State Univ.*, 110 pp.

Benkley, C.W.; L.L. Schulman (1979): Estimating mixing depths from historical meteorological data. *J. Appl. Meteorol.* **18**, 772-780

Berger, H.; D. Ruffieux; R. Stübi (1996): Time evolution of the planetary boundary layer estimated by merging sodar, wind profiler and soundings data. *In: M.A. Kallistratova (Ed.): Proc. 8th Internat. Symp. on Acoustic Remote Sensing, Moscow*, 6.41-6.46

Bernhardt, K.; B. Klose; H. Pethe (1982): Grenzschichthöhen und Windprofile nach Radiosonden-Daten. *Abh. MD der DDR* **Bd. XVII** Nr.28, 41-52

Bes'chastnov, S.P. (1984): Prognosticheskie uravneniya dlya masshtabov pogranichnogo sloya atmosfery v usloviakh ustoichivoi stratifikatsii. *Trudy IEM* **33(108)**, 3-13

Betts, A.K. (1973): Non-precipitating cumulus convection and its parameterization. *Quart. J. Roy. Meteorol. Soc.* **99**, 178-196

Betts, A.K. (1992): FIFE atmospheric boundary layer budget methods. *J. Geophys. Res.* **97**, 18,523-18,531

Betts, A.K.; Albrecht B.A. (1987): Conserved variable analysis of the convective boundary layer thermodynamic structure over tropical oceans. *J. Atmos.Sci.* **44**, 83-99

Beyrich, F. (1990): The diurnal cycle of mixing height - Sodar observations and model calculations: A status report from Heinrich-Hertz-Institute. *in: J. Walczewski (Ed.): Proc. EURASAP-Symp. on Applic. of Sodar & Lidar Techn. in Air Poll. Meteorol., Cracow*, III.1-III.11

Beyrich, F. (1992): Some additional remarks on 'Sodar estimates of heat flux and mixed layer depth compared with direct measurements'. *Atmos. Environm.* **26A**, 2459-2461

Beyrich, F. (1993): On the use of sodar data to estimate mixing height. *Appl. Phys. B* **57**, 27-35

Beyrich, F. (1994a): Sodar observations of the stable boundary layer height in relation to the nocturnal low-level jet. *Meteorol. Z. (N.F.)* **3**, 29-34

Beyrich, F. (1994b): Bestimmung der Mischungsschichthöhe aus Sodar-Daten unter Verwendung numerischer Modellrechnungen. *Frankfurt/M.: Wiss.-Verlag Dr. W. Maraun (ISBN 3-927548-67-7), Schriftenreihe des FhI für Atmosphärische Umweltforschung Garmisch-Partenkirchen*, **Bd. 28**, 161 pp. + Anh.

Beyrich, F. (1995): Mixing height estimation in the convective boundary layer using sodar data. *Boundary-Layer Meteorol.* **74**, 1-18.

Beyrich, F. (1996): Mixing height estimation from sodar data - a review. *in: M.A. Kallistratova (Ed.): Proc. 8th Internat. Symp. on Acoustic Remote Sensing, Moscow*, 6.8-6.18

Beyrich, F.; B. Klose (1988): Some aspects of modeling low-level jets. *Boundary-Layer Meteorol.* **43**, 1-14

Beyrich, F.; A. Weill (1993): Some aspects of determining the stable boundary layer depth from sodar data. *Boundary-Layer Meteorol.* **63**, 97-116

Beyrich, F.; V. Kotroni (1993): Estimation of surface stress over a forest from sodar measurements and its use to parameterize the stable boundary layer height. *Boundary-Layer Meteorol.* **66**, 93-103

Beyrich, F.; U. Görsdorf (1995): Composing the diurnal cycle of mixing height from simultaneous sodar and wind profiler measurements. *Boundary-Layer Meteorol.* **76**, 387-394

Beyrich, F.; H. Güsten; D. Sprung; U. Weisensee (1996): Comparative analysis of sodar and ozone profile measurements in a complex structured boundary layer and implications for mixing height estimation. *Boundary-Layer Meteorol.* **81**, 1-9

Binkowski, F.S. (1983): A simple model for the diurnal variation of the mixing depth and transport flow. *Boundary-Layer Meteorol.* **27**, 217-236

Blackadar, A.K. (1957): Boundary-layer wind maxima and their significance for the growth of nocturnal inversions. *Bull. Amer. Meteorol. Soc.* **38**, 283-290.

Blackadar, A.K. (1979): High resolution models of the planetary boundary layer. *In J.R. Pfafflin and E.N. Zeigler (Eds.): Advances in Environmental Science and Engineering*, Vol. **1**, New York: Gordon and Breach, pp. 50-85.

Blumenthal, D.L.; J.A. McDonald; W.S. Keifer; J.B. Tommerdahl; M.L. Saeger; J.H. White (1984): Three-dimensional pollutant distribution and mixing layer structure in the northeast U.S., summary of sulfate regional experiment (SURE) aircraft measurements. *Atmos. Environm.* **18**, 733-749

Boers, R.; E.W. Eloranta; R.L. Coulter (1984): Lidar observations of mixed layer dynamics: Test of parameterized entrainment models of mixed layer growth rate. *J. Clim. Appl. Meteorol.* **23**, 247-266

Boers, R.; S.H. Melfi (1987): Cold-air outbreak during MASEX: Lidar observations and boundary layer model test. *Boundary-Layer Meteorol.* **39**, 41-51

Boers, R.; S.H. Melfi; S.P. Palm (1991): Cold-air outbreak during GALE: Lidar observations and modeling of boundary layer dynamics. *Mon. Wea. Rev.* **119**, 1132-1150

Boers, R.; S.H. Melfi; S.P. Palm (1995): Fractal nature of the planetary boundary layer depth in the trade wind Cumulus regime. *Geophys. Res. Let.* **22**, 1705-1708

Bonino, G.; A. Longhetto; P. Trivero; G. Elisei; A. Marzorati (1989): Evolution of the atmospheric convective boundary layer monitored by the metric RASS. *Il Nuovo Cimento* **12C**, 163-171

Brost, R.A.; J.C. Wyngaard (1978): A model study of the stably stratified planetary boundary layer. *J. Atmos. Sci.* **35**, 1427-1440

Businger, J.A.; S.P.S. Arya (1974): Height of the mixed layer in the stably stratified planetary boundary layer. *Adv. Geophys.* **18A**, 73-92

Byun, D.W.; S.P.S. Arya (1990): A two-dimensional mesoscale numerical model of an urban mixed layer - I. Model formulation, surface energy budget and mixed layer dynamics. *Atmos. Environm.* **24A**, 829-844

Cappellani, F.; A. Bielli (1995): Correlation between SO_2 and NO_2 measured in an atmospheric column by a Brewer spectrophotometer and at ground level by photochemical techniques. *Environm. Monitoring & Assessm.* **35**, 77-84

Carson, D.J. (1973): The development of a dry inversion-capped convectively unstable boundary layer. *Quart. J. Roy. Meteorol. Soc.* **99**, 450-467

Carson, D.J.; F.B. Smith (1974): Thermodynamic model for the development of a convectively unstable boundary layer. *Adv. Geophys.* **18A**, 111-129

Cats, G.J.; J. Reiff; C.A. Engeldal (1985): Procedures used in the boundary-layer height and wind analysis for the PHOXA-project. *De Bilt: KNMI Techn. Rep.* TR-64

Caughey, S.J. (1982): Observed characteristics of the atmospheric boundary layer. In: F.T.M. Nieuwstadt and H. van Dop (eds.): *Atmospheric Turbulence and Air Pollution Modeling*. Dordrecht-Boston-London: Reidel Publ. Co., 107-158.

Chang, W.L.; S. Lau (1990): Estimating mixing heights from acoustic sounding. *in: S.P. Singal (Ed.): Acoustic remote sensing.* New Delhi: Tata McGraw-Hill, 500-505

Chaudhury, B.B.; A.K. De; A. Ganguli; J. Das (1992): Automatic recognition and interpretation of sodar records. *Ind. J. Radio & Space Phys.* **21**, 123-128

Chong, B.L. (1985): Modeling and climatological aspects of the convective boundary layer. *Tsukuba: Environm. Res. Center Pap.* No.7, 63 pp.

Clarke, R.H. (1970): Observational studies in the atmospheric boundary layer. *Quart. J. Roy. Meteorol. Soc.* **96**, 91-114.

Clarke, R.H. (1990): Modeling mixed layer growth in the Koorin experiment. *Austral. Meteorol. Mag.* **38**, 227- 234

Clifford, S.F.; J.C. Kaimal; R.J. Lataitis; R.G. Strauch (1994): Ground-Based Remote Profiling in Atmospheric Studies: An Overview. *Proc. IEEE* **82**, 313-355

Connolly, S.T.; W.R. Dagle (1991): A Doppler radar for the measurement of mixing layer height. *Proc. AMS Conf. Meteorol. Instrum. & Obs. Methods, New Orleans,* J234-J237

Cooper, D.I.; W.E. Eichinger (1994): Structure of the atmosphere in an urban planetary boundary layer from lidar and radiosonde observations. *J. Geophys. Res.* **99**, 22,937-22,948

Coulter, R.L. (1979): A comparison of three methods for measuring mixing layer height. *J. Appl. Meteorol.* **18**, 1495-1499

Coulter, R.L. (1990): A case study of turbulence in the stable nocturnal boundary layer. *Boundary-Layer Meteorol.* **52**, 75-91.

Crespi, S.N.; B. Artinano; H. Cabal (1995): Synoptic classification of the mixed-layer height evolution. *J. Appl. Meteorol.* **34**, 1666-1677

Culf, A. (1992): An application of simple models to Sahelian convective boundary layer growth. *Boundary-Layer Meteorol.* **58**, 1-18

Dayan, U.; R. Shenhav; M. Graber (1988): The spatial and temporal behavior of the mixed layer in Israel. *J. Appl. Meteorol.* **27**, 1382-1394

Deardorff, J.W. (1971): Rate of growth of the nocturnal boundary layer. *Proc. AMS Conf. Air Poll., Turb. & Diff., Las Cruces*, 246

Deardorff, J.W. (1972): Parameterization of the planetary boundary layer for use in General Circulation Models. *Mon. Wea. Rev.* **100**, 93-106

Deardorff, J.W. (1974): Three-dimensional numerical study of the height and mean structure of a heated planetary boundary layer. *Boundary-Layer Meteorol.* **7**, 81-106

Deardorff, J.W. (1979): Prediction of convective mixed-layer entrainment for realistic capping inversion structure. J. *Atmos. Sci.* **36**, 424-436

Deardorff, J.W. (1980): Stratocumulus-capped mixed layers derived from three-dimensional models. *Boundary-Layer Meteorol.* **18**, 495-527.

Deardorff, J.W.; G.E. Willis (1982): Ground-level concentrations due to fumigation into an entraining mixed layer. *Atmos. Environm.* **16**, 1159-1170

Delage, Y. (1974): A numerical study of the nocturnal boundary layer. *Quart. J. Roy. Meteorol. Soc.* **100**, 351-364

Demchenko, P.F. (1993): Integral'naya model' planetarnogo pogranichnogo sloya atmosfery s nestatsionarnymi uravnenyami dlya kineticheskoi energii turbulentnosti i skorosti ee dissipatsii. *Fiz. Atmos. i Okeana* **29**, 315-320

Deme, S.; T. Mikkelsen; S. Thykier-Nielsen (1996): Local Scale Preprocessor (LSP) for atmospheric dispersion: description and users guide. *RODOS(WG2)-TN(96)01* (can be obtained from Risø National Laboratory, DK-4000 Roskilde, Denmark).

Deng, J. P.; R.H. Aron (1985): Further investigations into mixing heights. *Atmos. Environm.* **19**, 1563-1564

Derbyshire, S.H. (1990): Nieuwstadt's stable boundary layer revisited. *Quart. J. Roy. Meteorol. Soc.* **116**, 127-158

Derbyshire, S.H. (1995): Stable boundary layers: Observations, models and variability - Part I: Modelling and measurements. *Boundary-Layer Meteorol.* **74**, 19-54

Devara, P.C.S.; P.E. Raj; B.S. Murthy; G. Pandithurai; S. Sharma; K.G. Vernekar (1995): Intercomparison of nocturnal lower-atmospheric structure observed with lidar and sodar techniques at Pune, India. *J. Appl. Meteorol.* **34**, 1375-1383

Dohrn, R.; E. Raschke; A. Bujnoch; G. Warmbier (1982): Inversion structure heights above the city of Cologne (Germany) and a rural station nearby as measured with two sodars. *Meteorol. Rdsch.* **35**, 133-144

Donev, E.; K. Zeller; I. Kolev (1992): The morning boundary layer transition in response to the surface heat flux. *Proc. 10th AMS Symp. Turb. & Diff., Portland*, 242-243

Donev, E.; K. Zeller; St. Panchev; I. Kolev (1995): Boundary layer growth and lapse rate changes determined by lidar and surface heat flux in Sofia. *Acta Meteorol. Sin.* **9**, 101-111

Dörnbrack, A. (1989): Approximative Berechnung turbulenter Flüsse und des Tensors der turbulenten Diffusion auf der Grundlage einer Schließung 2. Ordnung. *Dissertation, Humboldt-Univ. Berlin*, 138 S.

van Dop, H. (1986): The CCMS air pollution model intercomparison study. *Atmos. Environm.* **20**, 1261-1271

van Dop, H.; R. Steenkist; D. Altena; R. Scholten (1978): The use of acoustic methods for boundary layer studies near the coast of the Netherlands. *Proc. 4th AMS Symp. Meteorol. Instrum. & Obs. Methods, Denver*, 326-329

Driedonks, A.G.M. (1981): Dynamics of the well-mixed atmospheric boundary layer. *De Bilt KNMI Sci. Rep. WR 81-2*, 189 pp.

Driedonks, A.G.M. (1982a): Sensitivity analysis of the equations for a convective mixed layer. *Boundary-Layer Meteorol.* **22**, 475-480

Driedonks, A.G.M. (1982b): Models and observations of the growth of the atmospheric boundary layer. *Boundary-Layer Meteorol.* **23**, 283-306

Driedonks, A.G.M.; H. Tennekes (1984): Entrainment effects in the well-mixed atmospheric boundary layer. *Boundary-Layer Meteorol.* **30**, 75-105

Druilhet, A.; J.P. Frangi; D. Guedalia; J. Fontan (1983): Experimental studies of the turbulence structure parameters of the convective boundary layer. *J. Clim. Appl. Meteorol.* **22**, 594-608.

Dubosclard, G. (1980): A comparison between observed and predicted values for the entrainment coefficient in the planetary boundary layer. *Boundary-Layer Meteorol.* **18**, 473-483

Dubosclard, G.; Ch. Mazaudier; A. Weill (1985): Sodar network observations of the mixed layer growth in complex terrain. *Proc. 3rd ISARS, Issy-les-Moulineaux*, 171-184

Dupont, E. (1991): Étude méthodologique et expérimentale de la couche limite atmosphérique par télédetection laser. *Ph.D. Thesis, Univ. Paris VI*, 220 pp.

Dye, T.S.; C.G. Lindsay; J.A. Anderson (1995): Estimates of mixing depth from boundary layer radar profilers. *Proc. 9th AMS Symp. Meteorol. Instrum. & Obs., Charlotteville*, 156-160

Eberhard, W.L.; W.R. Moninger; G.A. Briggs (1988): Plume dispersion in the convective boundary layer. Part I: CONDORS Field experiment and example measurements. *J. Appl. Meteorol.* **27**, 599-616

Elsom, D.M.; T.J. Chandler (1978): Meteorological controls upon ground level concentrations of smoke and sulphur dioxide in two urban areas of the United Kingdom. *Atmos. Environm.* **12**, 1543-1554

Endlich, T.M.; F.L. Ludwig; E.E. Uthe (1979): An automatic method for determining the mixing depth from lidar observations. *Atmos. Environm.* **13**, 1051-1056

Estournel, C. (1988): Étude de la phase nocturne de la couche limite atmosphérique. *Ph.D. Thesis, Univ. P. Sabatier Toulouse*, 161 pp.

Estournel, C.; D. Guedalia (1990): Improving the diagnostic relation for the nocturnal boundary layer height. *Boundary-Layer Meteorol.* **53**, 191-198

Etling, D.; F. Wippermann (1975): The height of the planetary boundary layer and of the surface layer. *Beitr. Phys. Atmos.* **48**, 250-254

Fairall, C.W. (1984): Wind-shear enhancement of entrainment and refractive index structure parameter at the top of the turbulent mixed layer. *J. Atmos. Sci.* **41**, 3472-3484.

Fanaki, F. (1986): Simultaneous acoustic sounder measurements at two locations. *Boundary-Layer Meteorol.* **37**, 197-207

Fedorovich, E.E. (1995): Modeling the atmospheric convective boundary layer within a zero-order jump approach: An extended theoretical framework. *J. Appl. Meteorol.* **34**, 1916-1928

Fedorovich, E.E.; D.V. Mironov (1995): A model for the shear-free convective boundary layer with parameterized capping inversion structure. *J. Atmos. Sci.* **52**, 83-95

Fitzharris, B.B.; A. Turner; W. McKinley (1983): Cold season inversion frequencies as measured with acoustic sounder in the Cromwell Basin. *New Zeal. J. Sci.* **26**, 307-313

Fitzjarrald, D.R. (1982): New applications of a simple mixed layer model. *Boundary-Layer Meteorol.* **22**, 431-451

Fitzjarrald, D.R.; M. Garstang (1981): Boundary layer growth over the tropical ocean. *Mon. Wea. Rev.* **109**, 762-1772

Frisch, A.S.; S.F. Clifford (1974): A study of convection capped by a stable layer using Doppler radar and acoustic echo sounders. *J. Atmos. Sci.* **31**, 1622-1628.

Galadzhii, N.M.; I.J. Melentyeva; A.V. Tkatchenko (1963): Opredelenie vysoty pogranichnogo sloya atmosfery razlichnymi metodami. *Trudy GGO / Ukrainsk. NIGMI* **No. 144/40**, 96-101

Gamo, M. (1985): Seasonal change of mixed layer structure at Tsukuba. *J. Meteorol. Soc. Jap.* **63**, 60-74

Gamo, M. (1988): Diurnal variations of the mixed layer characteristics at Tsukuba. *J. Meteorol. Soc. Jap.* **66**, 691-701

Gamo, M.; O. Yokoyama (1979): Growth of the mixing depth and the diurnal variation of vertical profiles of temperature and turbulence characteristics in the mixing layer. *J. Meteorol. Soc. Jap.* **57**, 159-171

Gamo, M.; P. Goyal; M. Kumari; U.C. Mohanhy (1994): Mixed-layer characteristics as related to the Monsoon climate of New-Delhi, India. *Boundary-Layer Meteorol.* **67**, 213-227

Garland, J.A.; J.R. Branson (1976): The mixing height and mass balance of SO_2 in the atmosphere above Great Britain. *Atmos. Environm.* **10**, 353-362

Garratt, J.R. (1982a): Observations in the nocturnal boundary layer. *Boundary-Layer Meteorol.* **22**, 21-48

Garratt, J.R. (1982b): Surface fluxes and the nocturnal boundary layer height. *J. Appl. Meteorol.* **21**, 725-729

Garratt, J.R. (1992): *The Atmospheric Boundary Layer.* Cambridge: University Press, 316 pp.

Garratt, J.R.; R.A. Brost (1981): Radiative cooling effects within and above the nocturnal boundary layer. *J. Atmos. Sci.* **30**, 2730-2746.

Garrett, A.J. (1981): Comparison of observed mixed layer depth to model estimates using observed temperature and winds, and MOS forecasts. *J. Appl. Meteorol.* **20**, 1277-1283

Gaynor, J.E.; Ye Jin Ping; A.B. White (1994): Determining mixing depths in complex terrain near a power plant with radar profiler reflectivities. *Proc. 8th AMS Conf. Air Poll. Meteorol. & AWMA, Nashville*, 335-339

Gera, B.S.; S.P. Singal (1990): Tropical boundary layer studies during monsoon period using sodar. *in: S.P. Singal (Ed.): Acoustic remote sensing.* New Delhi: Tata McGraw-Hill, 390-394.

Gerasimov, A.V.; V.S. Maksimyuk; S.V. Tat'yanin (1988): O vliyanii meteorologicheskikh kharakteristik na opredelenie tolshchiny pogranichnogo sloya atmosfery metodami opticheskogo zondirovaniya. *Meteorol. i Gidrol.*, No.2, 25-33

Gland, H. (1981): Qualifying test on a three-dimensional Doppler-sodar (Satolas: July-December 1980). *Report EDF HE/32 - 81.9*, 36 pp.

Glendening, J.W. (1990): A mixed-layer simulation of daytime boundary-layer variations within the Los Angeles basin. *Mon. Wea. Rev.* **118**, 1531-1550

Godowitch, J.M.; K.S. Ching; J.F. Clarke (1985): Evolution of the nocturnal inversion layer at an urban and nonurban location. *J. Clim. Appl. Meteorol.* **24**, 791-804

van Gogh, R.G.; P. Zib (1978): Comparison of simultaneous tethered balloon and monostatic acoustic sounder records of the statically stable lower atmosphere. *J. Appl. Meteorol.* **17**, 34-39

Golder, D. (1972): Relations among stability parameters in the surface layer. *Boundary-Layer Meteorol.* **3**, 47-58.

Goroch, A.K. (1976): Comparison of radiosonde and acoustic echo sounder measurements of atmospheric thermal strata. *J. Appl. Meteorol.* **15**, 520-521

Grechko, E.I.; V.S. Rakitin; E.V. Fokeeva; A.V. Dzhola; M.S. Pekour; N.S. Time (1993): Izuchenie vliyaniya parametrov atmosfernogo pogranichnogo sloya na izmenchivost' soderzhaniya okisi ugleroda v tsentre Moskvy. *Fiz. Atmos. i Okeana* **29**, 11-18

Gryning, S.E.; A.A.M. Holtslag; J.S. Irwin; B. Sivertsen (1987): Applied dispersion modelling based on meteorological scaling paramters. *Atmos. Environ.*, **21**, 79-89.

Gryning, S.E.; E. Batchvarova (1990): Simple model of the daytime boundary layer height. *Proc. 9th AMS Symp. Turb. & Diff., Roskilde*, 379-382

Guedalia, D.; A. Ntsila; A. Druilhet; J. Fontan (1980): Monitoring of the atmospheric stability above an urban and suburban site using sodar and radon measurements. *J. Appl. Meteorol.*, **19**, 839-848.

Gutsche, A.; C. Lefebvre (1981): Statistik der maximalen Mischungsschichthöhe nach Radiosondenmessungen an den aerologischen Stationen des Deutschen Wetterdienstes im Zeitraum 1957-1973. *Ber. Dt. Wetterdienst, Offenbach,* Nr.154

Handorf, D. (1996): Zur Parameterisierung der stabilen atmosphärischen Grenzschicht über einem antarktischen Schelfeis. *Berlin: Humboldt-Univ. Ph.D. Thesis*, 127 pp.

Hanna, S.R. (1969): The thickness of the planetary boundary layer. *Atmos. Environm.* **3**, 519-536

Hanna, S.R. (1992): Effects of data limitations on hopes for improved short range atmospheric dispersion models. *in: H.R. Olesen and T. Mikkelsen (Eds.): Proc. Workshop "Objectives for next generation of practical short-range atmospheric dispersion models" (Risø 1992). DCAR Roskilde,* 77-85

Hanna, S.R.; C.L. Burkhart; R.J. Paine (1985): Mixing height uncertainties. *Proc. 7th AMS Symp. Turb. & Diff., Boulder*, 82-85

Hanna, S.R.; R.J. Paine (1989): Hybrid Plume Dispersion Model (HPDM) Development and evaluation. *J. Appl. Meteorol.* **28**, 206-224.

Hanna, S.R.; J.C. Chang (1991): *Modification of the Hybrid Plume Dispersion Model (HPDM) for urban conditions and its evaluation using the Indianapolis data set.* Report No. A089-1200, Electric Power Research Institute, 3412 Hillview Av., Palo Alto, CA 94303, USA.

Hanna, S.R.; J.C. Chang (1992): Boundary-Layer Parameterizations for Applied Dispersion Modeling over Urban Areas. *Boundary-Layer Meteorol.* **58**, 229-259

Hanna, S.R.; J.C. Chang (1993): Hybrid Plume Dispersion Model (HPDM) improvements and testing at three field sites. *Atmos. Environm.* **27A**, 1491-1508.

Hashiguchi, H.; M.D. Yamanaka; T. Tsuda; M. Yamamoto; T. Nakamura; T. Adachi; S. Fukao; T. Sato; D.L. Tobing (1995): Diurnal variations of the planetray boundary layer observed with a L-band clear-air Doppler radar. *Boundary-Layer Meteorol.* **74**, 419-424

Hashmonay, R.; A. Cohen; U. Dayan (1991): Lidar observation of the atmospheric boundary layer over Jerusalem. *J. Appl. Meteorol.* **30**, 1228-1236

Hayashi, M. (1980): Acoustic sounding of the lower atmospheric inversion layer. *J. Meteorol. Soc. Jap.* **58**, 194-201

Heidt, F. (1977): The growth of the mixed layer in a stratified fluid due to penetrative convection. *Boundary- Layer Meteorol.* **12**, 439-461

Heinemann, G.; L. Rose (1990): Surface energy balance, parameterizations of boundary layer heights and the application of resistance laws near an Antarctic ice shelf front. *Boundary-Layer Meteorol.* **51**, 123-158

Helfland, H.M.; R. Boers (1990): Numerical simulation of a shear driven well-mixed atmospheric planetary boundary layer. *Proc. 9th AMS Symp. Turb. & Diff., Roskilde*, 192-195

Hicks, R.B.; D. Smith; P.J. Irwin; T. Mathews (1977): Preliminary studies of atmospheric acoustic sounding at Calgary. *Boundary-Layer Meteorol.* **12**, 201-212

Hildebrand, P.H. (1988): Flux and sounding data from the NCAR King Air aircraft during HAPEX. *NCAR / TN 319+STR*, viii+35 pp.

Holets, S.H.; R.N. Swanson (1984): Estimating mixed layer heights from digitized Doppler acoustic sounder data. *Proc. 77th Ann. Meeting Air Poll. Contr. Assoc., San Francisco,* 84-51.4 (1-15)

Holtslag, A.A.M.; F.T.M. Nieuwstadt (1986): Scaling the atmospheric boundary layer. *Boundary-Layer Meteorol.* **36**, 201-209.

Holtslag, A.A.M.; R.M. van Westrhenen (1989): Diagnostic derivation of boundary layer parameters from the outputs of atmospheric models. *De Bilt: KNMI Sci. Rep.* **WR89-04**

Holtslag, A.A.M.; E.I.F. De Bruin; H.-L. Pan (1990): A high resolution air mass transformation model for short range weather forecasting. *Mon. Wea. Rev.* **118**, 1561-1575.

Holzworth, C.G. (1964): Estimates of mean maximum mixing depths in the contiguous United States. *Mon. Wea. Rev.* **92**, 235-242

Holzworth, C.G. (1967): Mixing depths, wind speeds and air pollution potential for selected locations in the United States. *J. Appl. Meteorol.* **6**, 1039-1044

Holzworth, C.G. (1972): *Mixing depths, wind speeds, and potential for urban pollutions throughout the contiguous United States.* EPA, Office of Air Programs Publ. AP-101, 118 pp. (Can be obtained from EPA, Research Triangle Park NC 277711, USA.)

Hsu, S.A. (1979): An operational forecasting model for the variation of mean maximum mixing heights across the coastal zone. *Boundary-Layer Meteorol.* **16**, 93-98

Hsu, S.A.; R.E. Larson; D.J. Bressan (1980): Diurnal variations of radon and mixing heights along the coast: a case study. *J. Geophys. Res.* **85**, 4107-4110

Jakobsen, H.A.; E. Berge; T. Iversen; R. Skålin (1995): Status of the development of the multilayer Eulerian model. *EMEP / MSC-W Note 3 / 95* (can be obtained from: Norwegian Meteorological Institute, P.O. Box 43, N - 0313 Oslo 3, Norway)

Jegede, O.O. (1994): On the variation of the mean convective mixed-layer depth over West Africa. *Meteorol. Z. (N.F.)* **3**, 307-311

Jochum, A.M.; N. Entstrasser; P. Mörl; D. Paffrath; S. Schulz (1991): Observational analysis of mixed layer depth evolution and variability. *Proc. 7th Joint Conf. Applic. Air Poll. Meteorol & AWMA, New Orleans*

Joffre, S.M. (1981): The physics of the mechanically driven atmospheric boundary layer as an example of air-sea ice interaction. *Univ. of Helsinki, Dept. of Meteorol. Rep. No. 20*, 75 pp.

Jones, D.E. (1985): Mixing depth in La Trobe Valley. *Clean Air in Austral.* **19**, 49-51

Jones, D.E.; P.J. Smith; N.A. Shaw; I.A. Bourne (1984): Analysis of acoustic radar wind data. *Proc. 8th Int. Clean Air Conf. Melbourne*, 337-349

Kaimal, J.C.; J.J. Finnigan (1994): *Atmospheric Boundary Layer Flows: Their structure and measurement.* New York - Oxford: University Press Inc.,

Kaimal, J.C.; N.L. Abshire; R.B. Chadwick; M.T. Decker; W.H. Hooke; R.A. Kroepfli; W.D. Neff; F. Pasqualucci; P.H. Hildebrand (1982): Estimating the depth of the daytime convective boundary layer. *J. Appl. Meteorol.* **21**, 1123-1129

Karppinen, A.; J. Kukkonen; G. Nordlund; E. Rantakrans; I. Valkama (1996): A dispersion modelling system for urban air pollution. *Finnish Meteorological Institute: Publications on Air Quality*. Helsinki, 30 pp. (in print).

Karppinen, A.; S. Joffre; P. Vaajama (1997): Boundary layer parametrization for Finnish regulatory dispersion models. *International Journal of Environment and Pollution* (in print).

Kassomenos, P.; V. Kotroni; G. Kallos (1995): Analysis of climatological and air quality observations from the greater Athens area. *Atmos. Environm.* **29**, 3671-3688

Kazanskii, A.B.; Monin, A.S. (1960): The turbulent regime above the surface atmospheric layer. *Izv. Acad. Sci., Ser. Geof.* **1**, 165-168.

Khakimov, I.R. (1976): O profile vetra i tolshchine nejtral'no stratifitsirovannogo pogranichnogo sloya atmosfery. *Fiz. Atmos. i Okeana* **12**, 1020-1023

Kiemle, C.; M. Kästner; G. Ehret (1995): The convective boundary layer structure from lidar and radiosonde measurements during the EFEDA campaign. *J. Atmos. Ocean. Technol.* **12**, 771-782

Kitaigorodskii, S.A. (1988): A note on similarity theory for atmospheric boundary layers in the presence of background stable stratification. *Tellus* **40A**, 434-438

Kitaigorodskii, S.A.; S.M. Joffre (1988): In search of a simple scaling for the height of the stratified atmospheric boundary layer. *Tellus* **40A**, 419-433

Klapisz, C.; A. Weill (1985): Modélisation semi-empirique de la couche limite nocturne. Application au calcul du profil d'indice de réfraction. *Ann. Telecomm.* **40**, 672-679.

Klöppel, M.; G. Stilke; C. Wamser (1978): Experimental investigations into variations of ground based inversions and comparison with results of simple boundary layer models. *Boundary-Layer Meteorol.* **15**, 135-145

Klose, B. (1991): Ausgewählte Charakteristika der stabilen nächtlichen Grenzschicht. *Meteorol. Rdsch.* **44**, 55- 61

Klose, B.; C. Schäke (1991): Empirische Untersuchungen zur akustischen Sondierung der Grenzschicht. *Z. Meteorol.* **41**, 8-17.

Kolarova, M.; D. Yordanov; D. Sirakov; G. Dzholov; D. Karadzhov; L. Aleksandrov (1989): Parametrizatsiya konvektivnogo planetarnogo pogranichnogo sloya. *Fiz. Atmos. i Okeana* **25**, 659-664

Koo, E.; W.L. Chang; C.M. Tam (1983): Comparison of mixing height obtained by using a monostatic acoustic radar and by direct measurement in a tropical coastal enviroment. *76th Ann. Meeting Air Poll. Contr. Assoc. Atlanta*, 83-25.8 (1-15)

Koracin, D.; R. Berkowicz (1988): Nocturnal boundary layer height: observations by acoustic sounders and prediction in terms of surface layer parameters. *Boundary-Layer Meteorol.* **43**, 65-83

Kottmeier, Chr. (1982): Die Vertikalstruktur nächtlicher Grenzschichtstrahlströme. *Ber. Inst. Meteorol. Klimatolog. Univ. Hannover*, Nr. 21, 130 pp.

Kraus, H.; E. Schaller (1978): Steady-state characteristics of inversions capping a well-mixed planetary boundary layer. *Boundary-Layer Meteorol.* **14**, 83-104

Kukharets, V.P.; L.R. Tsvang (1979): Ekstremum vertikalnogo profilya strukturnoi kharakteristiki temperaturnogo polya. *Dokl. AN SSSR* **248**, 832-835

Kurzeja, R.J.; S. Berman; A.H. Weber (1991): A climatological study of the nocturnal planetary boundary layer. *Boundary-Layer Meteorol.* **54**, 105-128

Kuznetsova, I.N. (1989): Vysota sloya peremeshivaniya i koeffitsient turbulentnosti kak pokazatel' vertikal'nogo obmena v pogranichnom sloe atmosfery. *Trudy GMC* **299**, 99-103

Laikhtman, D.L. (1961): *Fizika pogranichnogo sloya atmosfery*. Leningrad: Gidrometeoizdat

Lanicci, J.M.; T.T. Warner (1991): A synoptic climatology of the elevated mixed layer inversion over the southern Great Plains in spring. Part I: Structure, dynamics and seasonal evolution. *Wea. & Forecasting* **6**, 181-197

Lenschow, D.H. (Ed.), (1986): *Probing the Atmospheric Boundary Layer*. Boston: AMS, 269 pp.

Liechti, O.; B. Neiniger (1993): ALPTHERM – a PC-based model for atmospheric convection over complex topography. *Proc. OSTIV Congress*

Lieman, R.; P. Alpert (1993): Investigation of the planetary boundary layer height variations over complex terrain. *Boundary-Layer Meteorol.* **62**, 129-142

Lilly, D.K. (1968): Models of cloud-topped mixed layers under a strong inversion. *Quart. J. Roy. Meteorol. Soc.* **94**, 292-309

Ludwig, F.L.; W.F. Dabberdt (1973): Effects of urbanization on turbulent diffusion and mixing depth. *Int. J. Biometeorol.* **17**, 1-11

Lyra, R.; A. Druilhet; B. Benech; C. Bouka Biona (1992): Dynamics above a dense equatorial rain forest from the surface boundary layer to the free atmosphere. *J. Geophys. Res.* **97**, 12,953-12,965

Mahrt, L. (1979): Penetrative convection at the top of a growing boundary layer. *Quart. J. Roy. Meteorol. Soc.* **105**, 469-485

Mahrt, L. (1981a): The early evening boundary layer transition. *Quart. J. Roy. Meteorol. Soc.* **107**, 329-343

Mahrt, L. (1981b): Modeling the depth of the stable boundary layer. *Boundary-Layer Meteorol.* **21**, 3-19

Mahrt, L.; D.H. Lenschow (1976): Growth dynamics of the convectively mixed layer. *J. Atmos. Sci.* **33**, 41-51

Mahrt, L.; R.C. Heald (1979): Comments on "Determining the height of the nocturnal boundary layer". *J. Appl. Meteorol.* **18**, 383

Mahrt, L.; R.C. Heald; D.H. Lenschow; B.B. Stankow; I. Troen (1979): An observational study of the structure of the nocturnal boundary layer. *Boundary-Layer Meteorol.* **17**, 247-264

Mahrt, L.; J.C. André; R.C. Heald (1982): On the depth of the nocturnal boundary layer. *J. Appl. Meteorol.* **21**, 90-92

Malcher, J.; H. Kraus (1983): Low-level-jet phenomena described by an integrated dynamical planetary boundary layer model. *Boundary-Layer Meteorol.*, 27, 327-343.

Manins, P.C. (1982): The daytime planetary boundary layer: A new interpretation of Wangara data. *Quart. J. Roy. Meteorol. Soc.* **108**, 689-705

Mann, J.; K.J. Davis; D.H. Lenschow; S.P. Oncley; C. Kiemle; G. Ehret; A. Giez; H.G. Schreiber (1995): Airborne observations of the boundary layer top, and associated gravity waves and boundary layer structure. *Proc. 9th AMS Symp. Meteorol. Instrum & Obs., Charlotteville*, 113-116

Manton, M.J. (1978a): On dry penetrative convection. *Boundary-Layer Meteorol.* **14**, 301-322

Manton, M.J. (1978b): Moist penetrative convection and the formation of incipient cloud. *Boundary-Layer Meteorol.* **15**, 265-287

Manton, M.J. (1987): A bulk model of the well-mixed boundary layer. *Boundary-Layer Meteorol.* **40**, 165-178

Marsik, F.J.; K.W. Fischer; T.D. McDonald; P.J. Samson (1995): Comparison of methods for estimating mixing height used during the 1992 Atlanta Field Initiative. *J. Appl. Meteorol.* **34**, 1802-1814

Martin, C.L.; D. Fitzjarrald; M. Garstang; A.P. Oliveira; S. Greco; E. Browell (1988): Structure and growth of the mixing layer over the Amazonian rain forest. *J. Geophys. Res.* **93**, 1361-1375

Maryon, R. H.; Best, M. J. (1992): 'NAME', 'ATMES' and the bounday layer problem. *Met O (APR) Turbulence and Diffusion Note* **No. 204** (U. K. Met. Office)

Marzorati, A.; D. Anfossi (1993): Doppler sodar measurements and evaluations in complex terrain. *Il Nuovo Cimento* **16**, 141-154

Marzorati, A.; G. Mastrantonio; G. Fiocco (1988): Criteria for the automatic classification of micrometeorological situations by the analysis of sodar intensity profiles. *Proc. 4th ISARS, Canberra*, 9(1-8)

Mason, P.J.; S.H. Derbyshire (1990): Large-eddy simulation of the stably stratified atmospheric boundary layer. *Boundary-Layer Meteorol.* **53**, 117-162

Maughan, R.A. (1979): Frequency of potential contributions by major sources to ground-level concentrations of SO_2 in the Forth Valley, Scotland: An application of acoustic sounding. *Atmos. Environm.* **13**, 1697-1706

Maughan, R.A.; A.M. Spanton; M.L. Williams (1982): An analysis of the frequency distribution of sodar derived mixing heights classified by atmospheric stability. *Atmos. Environm.* **16**, 1209-1218

McElroy, J.L.; T.B. Smith (1991): Lidar descriptions of mixed layer thickness characteristics in a complex terrain / coastal enviroment. *J. Appl. Meteorol.* **30**, 585-597

Melas, D. (1990): Sodar estimates of surface heat flux and mixed layer depth compared with direct measurements. *Atmos. Environm.* **24A**, 2847-2854

Melas, D. (1991): Using a simple resistance law to estimate friction velocity from sodar measurement. *Boundary-Layer Meteorol.*, **57**, 275-287.

Melas, D. (1993): Similarity methods to derive turbulence quantities and mixed layer depth from sodar data – a review. *Appl. Phys.* **B57**, 11-17

Melgarejo, J.W.; J.W. Deardorff (1974): Stability functions for the boundary layer resistance laws based upon observed boundary layer heights. *J. Atmos. Sci.* **31**, 1324-1333

Melkaya, I.Yu. (1987): Primenenie modeli nochnogo pogranichnogo sloya k raschyotu strujnykh techenii nizhnego urovnaya. *Trudy GCO* **506**, 40-52.

Middleton, D. R. (1993): Empirical diagnosis of Boundary Layer Depth. *Met O (APR) Turbulence and Diffusion Note* **No. 203**. (U. K. Met. Office)

Mikkelsen, T.; F. Desiato (1993). Atmospheric dispersion models and pre-processing of meteorological data for real-time application. *Rad. Prot. Dosimetry* **50**, 205-218.

Mikkelsen, T.; S. Thykier-Nielsen; P. Astrup; H.E. Jørgensen; J.M. Santabárbara; A. Rasmussen; J. H. Sørensen; L. Robertson; C. Persson; S. Deme; R. Martens, J.G. Bartzis; P. Deligiannis; N. Catsaros; J. Päsler-Sauer (1996): The real-time on-line atmospheric dispersion module Met-Rodos. *RODOS(WG2)-TN(96)08* (can be obtained from Risø National Laboratory, DK-4000 Roskilde, Denmark).

Miller, M.E. (1967): Forecasting afternoon mixing depth's and transport wind speed. *Mon. Wea. Rev.* **95**, 35-44

Monna, W.A.A., J.G. van der Vliet (1987): Facilities for research and weather observations on the 213 m tower at Cabauw and at remote locations. *De Bilt: KNMI Sci. Rep. WR 87-5*, 27pp.

Myrick, R.H.; S.K. Sakiyama; P.R. Angle; A.S. Sandhu (1994): Seasonal mixing heights and inversions at Edmonton, Alberta. *Atmos. Environm.* **28A**, 723-729

Neff, W.D.; R.L. Coulter (1986): Acoustic remote sensing. *in: D.H. Lenschow (Ed.): Probing the atmospheric boundary layer. Boston: AMS*, 201-236

Nicolas, R.M.; J. Gonzalez; J. Casanova (1988): Estudio comparativo de la altura de mezcla equivalente en un medio rural y en medio urbano. *Ann. Fis.* **84B**, 179-184

Nicolas, R.M.; J.L. Cano; M. Castro; J. Gonzalez; J.L. Casanova (1985): Estudio comparativo del calculo de la altura de la capa de mezcla matinal a partir de la onda de Rn y de radiosondeos. *Rev. de Geofis.* **41**, 145-148

Nieuwstadt, F.T.M. (1981): The steady state height and resistance laws of the nocturnal boundary layer: Theory compared with Cabauw observations. *Boundary-Layer Meteorol.* **20**, 3-17

Nieuwstadt, F.T.M. (1984a): The turbulent structure of the stable, nocturnal boundary layer. *J. Atmos. Sci.* **41**, 2202-2216

Nieuwstadt, F.T.M. (1984b): Some aspects of the turbulent stable boundary layer. *Boundary-Layer Meteorol.* **30**, 31-55

Nieuwstadt, F.T.M.; A.G.M. Driedonks (1979): The nocturnal boundary layer - a case study compared with model calculations. *J. Appl. Meteorol.* **18**, 1397-1405

Nieuwstadt, F.T.M.; H. Tennekes (1981): A rate equation for the nocturnal boundary layer height. *J. Atmos. Sci.* **38**, 1418-1428

Nieuwstadt, F.T.M.; J.W. Glendening (1989): Mesoscale dynamics of the depth of a horizontally non-homogeneous, well-mixed boundary layer. *Contr. Atmos. Phys.* **62**, 275-288

Noonkester, V.R. (1976): The evolution of the clear air convective layer revealed by surface based remote sensors. *J. Appl. Meteorol.* **15**, 594-606

Norton, C.L.; G.B. Hoidale (1976): The diurnal variation of mixing height by season over White Sands Missile Range, New Mexico. *Mon. Wea. Rev.* **104**, 1317-1320

Novak, M.D. (1991): Application of a mixed layer model to bare soil surfaces. *Boundary-Layer Meteorol.* **56**, 33-50

O'Brien, J. (1970): On the vertical structure of the eddy exchange coefficient in the planetary boundary layer. *J. Atmos. Sci.*, **27**, 1213-1215.

Økland, H. (1983): Modeling the height, temperature and relative humidity of a well-mixed planetary boundary layer over a water surface. *Boundary-Layer Meteorol.* **25**, 121-141

Olesen, H.R.; A.B. Jensen; N. Brown (1987): An operational procedure for mixing height estimation. *Risø Nat. Lab. MST-Luft-A96*. End edition 1992, 182 pp.

Orlenko, L.P. (1979): Stroenie planetarnogo pogranichnogo sloya. *Leningrad: Gidrometeoizdat*, 270 pp.

Osborne, J.B.; R.E. Peterson (1995): Diurnal evolution of the convectively unstable boundary layer: A computer simulation. *Proc. 11th AMS Symp. Boundary Layers & Turb., Charlotteville*, 132-135

Ossing, F.J. (1987): Ein Ansatz zur Berechnung der Mischungshöhe. *Beilage zur Berliner Wetterkarte 33/87 (SO 7/87)*, 9 S.

Overland, J.E.; K.L. Davidson (1992): Geostrophic drag coefficients over sea ice. *Tellus* **44A**, 54-66.

Pahwa, D.R.; B.S. Gera; S.P. Singal (1990): Study of the evolution of the nocturnal boundary layer at Delhi by acoustic sounding technique. *in: S.P. Singal (Ed.): Acoustic remote sensing. New Delhi: Tata McGraw-Hill*, 363-371

Park, P.M.; M.H. Smith; H.J. Exton (1990): The effect of mixing height on maritime aerosol concentrations over the North Atlantic ocean. *Quart. J. Roy. Meteorol. Soc.* **116**, 461-476

Pekour, M. (1990): Opredelenie parametrov sloya peremeshivaniya po faksimil'nym zapisyam ekho-signala sodara (obzor). *Prepr. Sem. Sekt. Atmos. Akust. AN SSSR ch. 1, Moskva*, 15-24

Pekour, M.S.; M.A. Kallistratova (1993): Sodar study of the boundary layer over Moscow for air pollution application. *Appl. Phys.* **B57**, 49-55

Piringer, M. (1988): The determination of mixing heights by sodar in an urban environment. *In: K. Grefen and J. Löbel (Eds.): Environmental meteorology.* Dordrecht-Boston-London: Kluwer Acad. Publ., 425-444

van Pul, W.A.J.; A.A.M. Holtslag; D.P.J. Swart (1994): A comparison of ABL-heights inferred routinely from lidar and radiosonde at noontime. *Boundary-Layer Meteorol.* **68**, 173-191

Rao, K.S.; H.F. Snodgrass (1979): Some parameterizations of the nocturnal boundary layer. *Boundary-Layer Meteorol.* **17**, 41-55

Rao, S.T.; G. Sistla; J.Y. Ku; N. Zhou; W. Hao (1994): Sensitivity of the urban airshed model to mixing height profiles. *Proc. 8th AMS Conf. Air Poll. Meteorol. & AWMA, Nashville*, 162-167

Rayner, K.N. (1987): Dispersion of atmospheric pollutants from point sources in a coastal environment. *Perth: Environm. Protect. Authority, Techn. Ser. No. 22*, 249 pp.

Rayner, K.N.; D. Watson (1991): Operational prediction of daytime mixed layer heights for dispersion modeling. *Atmos. Environm.* **25A**, 1427-1436

REMTECH (1994): Sodar Manual. *Remtech DT94/003, A.20-A.27*

Rossby, C.G.; R.B. Montgomery (1935): The layer of frictional influence in wind and ocean currents. *Pap. Phys. Oceanogr. Meteorol.* **3**, 101 pp.

Roth, R.; Ch. Kottmeier; D. Lege (1979): Die lokale Feinstruktur eines Grenzschichtstrahlstromes. *Meteorol. Rdsch.* **32**, 65-72.

Russell, P.B.; E.E. Uthe (1978a): Acoustic and direct measurements of atmospheric mixing at three sites during an air pollution incident. *Atmos. Environm.* **12**, 1061-1074

Russell, P.B.; E.E. Uthe (1978b): Regional patterns of mixing depth and stability: Sodar network measurements for input to air quality models. *Bull. Amer. Meteorol. Soc.* **59**, 1275-1287

Russell, P.B.; E.E. Uthe; F.L. Ludwig; N.A. Shaw (1974): A comparison of atmospheric structure as observed with monostatic acoustic sounder and lidar techniques. *J. Geophys. Res.* **79**, 5555-5566

San José, R.; J. Casanova (1988): An empirical method to evaluate the height of the convective boundary layer by using small mast measurements. *Atmos. Res.* **22**, 265-273

Sasano, Y.; H. Shimizu; N. Sugimoto; I. Matsui; N. Takeuchi; M. Okuda (1980): Diurnal variation of the atmospheric planetary boundary layer observed by a computer-controlled laser radar. *J. Meteorol. Soc. Jap.* **58**, 143-148

Sasano, Y.; A. Shigemazu; H. Shimizu; N. Takeuchi; M. Okuda (1982): On the relationship between the aerosol layer height and mixed layer height determined by laser radar and low-level radiosonde observations. *J. Meteorol. Soc. Jap.* **60**, 889-895

Sasano, Y.; I. Matsui; H. Shimizu; N. Takeuchi (1983): Automatic determination of atmospheric mixed layer height in routine measurements by laser radar. *J. Jap. Soc. Air Poll.* **18**, 175-183

Scheele, M.P.; H. van Dop (1989): Menghoogteberekeningen voor het Europese continent – een vergelijkend onderzoek. *De Bilt: KNMI Techn. Rep.* **TR-113**

Schlünzen, K.H (1994): Mesoscale modelling in complex terrein – an overview on the German nonhydrostatic models. *Contr. Atmos. Phys.*, **67**, 243-253.

Scholten, R.D.A.; J.J. Erbrink (1990): Measurements of plume parameters and boundary layer height with a mobile lidar. *in: J. Walczewski (Ed.): Proc. EURASAP-Symp. on Applic. of Sodar & Lidar Techn. in Air Poll. Meteorol., Cracow,* XVI.1-XVI.13

Schwiesow, R.L. (1986): A comparative overview of active remote-sensing techniques. *in: D.H. Lenschow (Ed.): Probing the atmospheric boundary layer. Boston: AMS*, 129-138

Segal, M.; J.R. Garratt; G. Kallos; R.A. Pielke (1989): The impact of wet soil and canopy temperatures on daytime boundary layer growth. *J. Atmos. Sci.* **46**, 3673-3684

Seibert, P.; M. Langer (1996): Deriving characteristic parameters of the convective boundary layer from sodar measurements of the vertical velocity variance. *Boundary-Layer Meteorol.* **81**, 11-22

Shipley, S.T.; I.A. Graffman (1991): ASOS Ceilometer measurements of aerosol and mixed layer height in the lower troposphere. *Boston: AMS Proc. Internat. Symp. on Meteorol. Obs. & Instrum., New Orleans,* J228-J229

Singal, S.P. (1988): The use of an acoustic sounder in air quality studies. *J. Sci. Industr. Res.* **47**, 520-533

Singal, S.P. (1990): Current status of air quality related boundary layer meteorology studies using sodar. *in: S.P. Singal (Ed.) Acoustic remote sensing. New Delhi: Tata McGraw & Hill*, 453-476

Singal, S.P.; S.K. Aggarwal (1979): Sodar and radiosonde studies of thermal structure of the lower atmosphere at Delhi. *Ind. J. Radio Space Phys.* **8**, 76-81

Singal, S.P.; B.S. Gera; S.K. Aggarwal (1983): Studies of the boundary layer at Delhi using sodar. *Proc. 2nd ISARS Rome*, XXIII(1-8)

Singal, S.P.; D.R. Pahwa; S.K. Aggarwal; B.S. Gera (1985): Studies of sodar surface based shear echo structures. *Proc. 3rd ISARS Issy-les-Moulineaux*, 47-63

Singal, S.P.; V.K. Ojha; T. Pal; B.S. Gera; M. Sharma; T.N. Monihan (1989): Studies of the atmospheric boundary layer of Delhi using acoustic sounders at two locations. *Mausam* **40**, 193-196

Smeda, M.S. (1979a): Incorporation of planetary boundary layer processes into numerical forecasting models. *Boundary-Layer Meteorol.* **16**, 115-129

Smeda, M.S. (1979b): A bulk model for the atmospheric planetary boundary layer. *Boundary-Layer Meteorol.* **17**, 411-427

Smedman, A.S. (1988): Observations of multi-level turbulence structure in a very stable atmospheric boundary layer. *Boundary-Layer Meteorol.* **44**, 231-253

Smedman, A.S. (1991): Some turbulence characteristics in stable atmospheric boundary layer flow. *J. Atmos. Sci.* **48**, 856-868.

Soler, M.R.; J. Hinojosa; J. Cuxart (1996): Atmospheric thermic structure studied by acoustic echo sounder, boundary-layer model, and direct measurements. *Boundary-Layer Meteorol.* **81**, 35-47

Sorbjan, Z. (1989): *Structure of the Atmospheric Boundary Layer.* London: Prentice Hall, 317 pp.

Sorbjan, Z.; R.L. Coulter; M.L. Wesely (1991): Similarity scaling applied to sodar observations of the convective boundary layer above an irregular hill. *Boundary-Layer Meteorol.* **56**, 33-50

Spanton, A.M.; M.L. Williams (1988): A comparison of the structure of the atmospheric boundary layers in central London and a rural/sub-urban site using acoustic sounding. *Atmos. Environm.* **22**, 211-223

Steyn, D.G. (1981): The depth of the mixed layer under conditions of advection and subsidence. *Proc. 5th AMS Symp. Turb., Diff. & Air Poll., Atlanta*, 84-85

Steyn, D.G. (1990): An advective mixed layer model for heat and moisture incorporating an analytic expression for moisture entrainment. *Boundary-Layer Meteorol.* **53**, 21-31

Steyn, D.G.; T.R. Oke (1982): The depth of the daytime mixed layer at two coastal sites: a model and it's validation. *Boundary-Layer Meteorol.* **24**, 161-180

Stull, R.B. (1973): Inversion rise model based on penetrative convection. *J. Atmos. Sci.* **30**, 1092-1099

Stull, R.B. (1976a): The energetics of entrainment across a density interface. *J. Atmos. Sci.* **33**, 1260-1267

Stull, R.B. (1976b): Mixed-layer depth model based on turbulent energetics. *J. Atmos. Sci.* **33**, 1268-1278

Stull, R.B. (1976c): Internal gravity waves generated by penetrative convection. *J. Atmos. Sci.* **33**, 1279-1286

Stull, R.B. (1983a): A heat flux history length scale for the nocturnal boundary layer. *Tellus* **35A**, 219-230

Stull, R.B. (1983b): Integral scales for the nocturnal boundary layer. Part I: Empirical depth relationships. *J. Clim. Appl. Meteorol.* **22**, 673-686

Stull, R.B. (1988): *An Introduction to Boundary Layer Meteorology.* Dordrecht - Boston - London: Kluwer Academic Publishers, 665 pp.

Stull, R.B. (1992): A theory for mixed-layer-top levelness over irregular topography. *Proc. 10th AMS Symp. Turb. & Diffus., Portland,* J92-J94

Surridge, A.D.; D.J. Swanepoel (1987): On the evolution of the height and temperature difference across the nocturnal stable boundary layer. *Boundary-Layer Meteorol.* **40**, 87-98.

Tennekes, H. (1970): Free convection in the turbulent Ekman-layer of the atmosphere. *J. Atmos. Sci.* **27**, 1027- 1033.

Tennekes, H. (1973): A model for the dynamics of the inversion above a convective boundary layer. *J. Atmos. Sci.* **30**, 558-567

Tennekes, H.; A.P. van Ulden (1974): Short term forecasts of temperature and mixing height on sunny days. *Proc. 2nd AMS Symp. Atmos Diffus. & Air Poll., Santa Barbara*, 35-40

Tennekes, H.; A.G.M. Driedonks (1981): Basic entrainment equations for the atmospheric boundary layer. *Boundary-Layer Meteorol.* **20**, 515-531

Tercier, Ph.; R. Stübi; Ch. Häberli (1995): Evaluation de la hauteur de la couche limite de mélange dans le cadre du projet POLLUMET. *Report of the Swiss Meteorol. Inst.*, 31 pp.

Thomson, D.J. (1992): An analytical solution of Tennekes' equations for the growth of boundary-layer depth. *Boundary-Layer Meteorol.* **59**, 227-229

Tjemkes, S.A.; P.G. Duynkerke (1989): The nocturnal boundary layer: Model calculations compared with observations. *J. Appl. Meteorol.* **28**, 161-175

Tombach, I.; M. Chan (1976): Estimation of mixing depth and inversion height by acoustic radar - a comparison with in-situ measurements. *Proc. 17th AMS Conf. Radar Meteorol., Seattle*, 313-320

Tombach, I.; D. Ettenheim (1985): Automatic determination of the depth of the atmospheric mixed layer by acoustic sounding. *Proc. 78th Ann. Meet. Air Poll. Contr. Assoc. Detroit* 85-18.6 (1-17)

Troen, I.; L. Mahrt (1986): A simple model of the planetary boundary layer: Sensitivity to surface evaporation. *Boundary-Layer Meteorol.* **37**, 129-148

van Ulden, A.P.; A.A.M. Holtslag (1985): Estimation of atmospheric boundary layer parameters for diffusion applications. *J. Clim. Appl. Meteorol.* **24**, 1196-1207.

Venkatram, A. (1080): Estimating the Monin-Obukhov length in the stable boundary layer for dispersion calculations. *Boundary-Layer Meteorol.*, **19**, 481-485.

Visvanadham, D.V.; K.R. Santosh (1994): On the relation between atmospheric stability, surface turbulence, and mixing height over Southern India. *Theor. Appl. Climatol.* **49**, 19-25

Vogelezang, D.H.P.; A.A.M. Holtslag (1996): Evolution and model impacts of alternative boundary layer formulations. *Boundary-Layer Meteorol.* **81**, 245-269

Walczewski, J. (1989): Development of sodar and acoustic sounding of the atmosphere in Poland. *Z. Meteorol.* **39**, 129-141

Walczewski, J. (1992): Dziesiec lat rozwoju polskiego sodaru i akustycznego sondazu atmosfery w Krakowie. *Wiad. IMGW* **15**, 37-46

Weil, J.C.; R.P. Brower (1983): *Estimating convective boundary layer parameters for diffusion applications.* Report PPSP-MP-48 Prepared by Environmental Center, Martin Marietta Corporation, For Maryland Department of Natural Resources, Armapolis, MD.

Weill, A. (1982): Measurements in the atmospheric boundary layer: techniques and limitations, representativeness. *ECMWF-workshop on PBL-parametrization, Reading, 1981*, 35-57

Weill, A.; F. Baudin; J. P. Goutorbe; P. van Grunderbeeck; P. Leberre (1978): Turbulence structure in temperature inversions and in convective fields as observed by Doppler-sodar. *Boundary-Layer Meteorol.* **15**, 375-390.

Weill, A.; C. Klapisz; B. Strauss; F. Baudin; C. Jaupart; P. van Grunderbeeck; J.P. Goutorbe (1980): Measuring heat flux and structure functions of temperature fluctuations with an acoustic Doppler sodar. *J. Appl. Meteorol.* **19**, 199-205.

Wetzel, P.J. (1982): Toward parameterization of the stable boundary layer. *J. Appl. Meteorol.* **21**, 7-13

Wetzel, P.J. (1983): A simple physical model for the height and thermal structure of the unstable boundary layer. *Proc. 6th AMS Symp. Turb. & Diffus., Boston*, 77-80

White, A.B. (1993): Mixing depth detection using 915-MHz radar reflectivity data. *AMS: Proc. 8th Symp. Meteorol. Instrum. Obs., Anaheim*, 248-250

White, A.B.; C.W. Fairall; D.E. Wolfe (1991): Use of 915-MHz wind profiler data to describe the diurnal variability of the mixed layer. *AMS: Proc. 7th Joint Conf. Applic. Air Poll. Meteorol. & AWMA, New Orleans*, J161-J166

Wotawa, G.; A. Stohl; H. Kromp-Kolb (1996): Parameterization of the planetary boundary layer over Europe: A data comparison between the observation-based OML preprocessor and ECMWF model data. *Contr. Atmos. Phys.* **69**, 273-284

Wratt, D.S.: Air pollution meteorology and acoustic sounding. *in: S.P. Singal (Ed.): Acoustic remote sensing. New Delhi: Tata McGraw-Hill,* 443-452

Wyckoff, R.J.; D.W. Beran; F.F. Hall (1973): A comparison of the low-level radiosonde and the acoustic echo sounder for monitoring atmospheric stability. *J. Appl. Meteorol.* **12**, 1196-1204

Wyngaard, J.C. (1975): Modeling the planetary boundary layer – extension to the stable case. *Boundary-Layer Meteorol.* **9**, 441-460.

Wyngaard, J.C. (1988): Structure of the Planetary Boundary Layer. In: A.Venkatram, J.C.Wyngaard (eds.), *Lectures on Air Pollution*. Boston: American Meteorological Society, p. 9-61.

Wyngaard, J.C.; M. Lemone (1980): Behaviour of the refractive index structure parameter in the entraining convective boundary layer. *J. Atmos. Sci.* **37**, 1573-1585.

Yamada, T.; S. Berman (1979): A critical evaluation of a simple mixed layer model with penetrative convection. *J. Appl. Meteorol.* **18**, 781-786

Yu, T.W. (1978): Determining the height of the nocturnal boundary layer. *J. Appl. Meteorol.* **17**, 28-33

Zeman, O. (1979): Parameterization of the dynamics of stable boundary layers and nocturnal jets. *J. Atmos. Sci.* **36**, 792-804

Zeman, O.; H. Tennekes (1977): Parameterization of the turbulent kinetic energy budget at the top of the daytime boundary layer. *J. Atmos. Sci.* **34**, 111-123

Zilitinkevich, S.S. (1972): On the determination of the height of the Ekman boundary layer. *Boundary-Layer Meteorol.* **3**, 141-145

Zilitinkevich, S.S. (1975a): Resistance laws and prediction equations for the depth of the planetary boundary layer. *J. Atmos. Sci.* **32**, 741-752

Zilitinkevich, S.S. (1975b): Comments on a paper by H. Tennekes. *J. Atmos. Sci.* **32**, 991-992

Zilitinkevich, S.S. (1989a): Pronikayushchaya turbulentnaya konvektsiya. Tallinn: Valgus, 207 pp.

Zilitinkevich, S.S. (1989b): Velocity profiles, the resistance law and the dissipation rate of mean flow kinetic energy in a neutrally and stably stratified planetary boundary layer. *Boundary-Layer Meteorol.* **46**, 367-387

Zilitinkevich, S.S., J.W. Deardorff (1974): Similarity theory for the planetary boundary layer of time-dependent height. *J. Atmos. Sci.*, **31**(5), 1449-1452.

Zilitinkevich, S.S.; E.E. Fedorovich; M.V. Shabalova (1992): Numerical model of a non-steady atmospheric planetary boundary layer, based on similarity theory. *Boundary-Layer Meteorol.* **59**, 387-411

Zilitinkevich, S.S.; D.V. Mironov (1996): A multi-limit formulation for the equilibrium depth of a stably stratified boundary layer. *Boundary-Layer Meteorol.* **81**, 325-351

A4.3 Cross-reference table for the bibliography

The following table is intended to assist in finding the references related to a specific type of problem. Please note that not all the references contained in the literature list (A4.2) are included in the cross-reference table, especially text books and papers outside the subjects defined in A4.1.

Author / Reference	ABL-regime		measurement / experiment							model / parameterization						application				
	CBL	SBL	radio sonde	teth. ball.	mast/ tower	air-craft	radar/ profi-ler	lidar/ ceilo-meter	sodar	diagn.	progn.	slab model	higher order/ LES	indep. model test	algor. devel	NWP /pre-proc.	regio-nal var.	cli-ma-tol.	pollut. conc.
André (1983)		X							X	X	X									
Angevine et al. (1994a)	X		X				X								X					
Angevine et al. (1994b)	X		X				X													X
Angevine et al. (1995)	X						X												X	
Aron (1983)	X		X																	X
Arya (1981)		X			X				X	X				X						
Arya (1984)	X	X								X	X									
Arya and Byun (1987)	X										X	X					X			
Bacci et al. (1984)	x	x	x						x											
Ball (1960)	X		X								X	X							X	
Batchvarova and Gryning (1991)	X			X							X	X		X						
Batchvarova and Gryning (1994)	X							X			X	X		X						
Baxter (1991)	X		X			X			X								X			
Beljaars and Agterberg (1988)	X	X							X						X					
Benkley (1977)	X								X		X	X		X						X
Benkley and Schulman (1979)	X	X	X							X				X					X	
Berger et al. (1996)	X	X	X				X		X						X					
Bernhardt et al. (1982)	X		X														X		X	
Bes'chastnov (1984)		X			X						X									

Author / Reference	ABL-regime		measurement / experiment							model / parameterization					application				
	CBL	SBL	radio sonde	teth. ball.	mast/ tower	air-craft	radar/ profi-ler	lidar/ ceilo-meter	sodar	diagn.	progn.	slab model	higher order/ LES	indep. model test	algor. devel	NWP /pre-proc.	regio-nal ver.	cli-ma-tol.	pollut. conc.
Betts (1973)	X										X	X							
Betts and Albrecht (1987)	X		X												X				
Betts (1992)	X		X			X					X								
Beyrich (1990)	X	X							X		X	X		X					
Beyrich (1992)	X		X						X										
Beyrich (1993)	X	X							X	X	X		X	X					
Beyrich (1994a)		X							X										
Beyrich (1994b)	X	X							X	X	X	X	X	X	X				X
Beyrich (1995)	X								X		X			X	X				
Beyrich (1996)	X	X							X						X				
Beyrich and Klose (1988)		X	X								X	X		X					
Beyrich and Weill (1993)		X							X				X		X				
Beyrich and Kotroni (1994)		X							X	X				X					
Beyrich and Görsdorf (1995)	X	X	X				X		X						X				
Beyrich et al. (1996)	X	X		X					X										X
Binkowski (1983)	X	X									X	X							
Blumenthal et al. (1984)	X	X				X											X		X
Boers et al. (1984)	X							X			X	X		X	X				
Boers & Melfi (1987), - et al. (1991)	X					X		X			X	X		X			X		

Author / Reference	ABL-regime		measurement / experiment							model / parameterization					application				
	CBL	SBL	radio sonde	teth. ball.	mast/ tower	air-craft	radar/ profi-ler	lidar/ ceilo-meter	sodar	diagn.	progn.	slab model	higher order/ LES	indep. model test	algor. devel	NWP /pre-proc.	regio-nal var.	cli-ma-tol.	pollut. conc.
Boers et al. (1995)	X					X		X									X		
Bonino et al. (1989)	X								X		X			X				X	
Brost and Wyngaard (1978)		X								X			X						
Businger and Arya (1974)		X								X									
Byun and Arya (1990)	X										X	X		X					
Cappelani and Bielli (1995)	X	X																	X
Carson (1973), - and Smith (1974)	X										X	X							
Cats et al. (1985)	X	X	X												X	X	X		
Chang and Lau (1990)	X	X							X										
Chaudhury et al. (1992)	X	X							X						X				
Chong (1985)	X		X								X	X						X	
Clarke (1990)	X		X								X	X		X					
Cifford et al. (1994)	X	X					X	X	X										
Connolly and Dagle (1991)	X	X					X								X				
Cooper and Eichinger (1994)	X	X	X					X											
Coulter (1979)	X		X					X	X										
Crespi et al. (1995)	X		X															X	
Culf (1992)	X		X								X	X		X					
Dayan et al. (1988)	X		X	X		X											X		

Author / Reference	ABL-regime		measurement / experiment							model / parameterization					application				
	CBL	SBL	radio sonde	teth. ball.	mast/ tower	air-craft	radar/ profi-ler	lidar/ ceilo-meter	sodar	diagn.	progn.	slab model	higher order/ LES	indep. model test	algor. devel	NWP /pre-proc.	regio-nal var.	cli-ma-tol.	pollut. conc.
Deardorff (1971)		X									X								
Deardorff (1972)	X	X								X	X								
Deardorff (1974)	X		X								X		X	X					
Deardorff (1979)	X										X	X		X					
Deardorff and Willis (1983)	X																		X
Delage (1974)		X								X			X						
Demchenko (1993)	X	X									X	X							
Deme et al. (1996)	X	X								x	x	x				x			
Derbyshire (1990)		X								X			X						
Derbyshire (1995)		X		X															
Devara et al. (1995)		X						X	X										
Dohrn et al. (1982)	X	X	X						X								X		
Donev et al. (1992, 1995)	X			X				X			X			X					
van Dop (1986)	X	X												X		X			X
van Dop et al. (1978)	X	X							X		X						X		
Dörnbrack (1989)	X	X								X			X						X
Driedonks (1981, 1982b)	X		X		X				X		X	X		X					
Driedonks (1982a)	X										X	X							
Driedonks and Tennekes (1984)	X		X		X				X		X	X		X					

Author / Reference	ABL-regime		measurement / experiment							model / parameterization					application				
	CBL	SBL	radio sonde	teth. ball.	mast/ tower	air-craft	radar/ profi-ler	lidar/ ceilo-meter	sodar	diagn.	progn.	slab model	higher order/ LES	indep. model test	algor. devel	NWP /pre-proc.	regio-nal ver.	cli-ma-tol.	pollut. conc.
Druilhet et al. (1983)	X					X													
Dubosclard (1980)	X								X					X					
Dubosclard et al. (1985)	X								X								X		
Dupont (1991)	X	X	X					X	X						X				
Dye et al. (1995)	X						X												
Eberhardt et al. (1988)	X		X		X		X	X	X										
Elsom and Chandler (1978)	X			X											X				X
Endlich et al. (1979)	X							X							X				
Estournel (1988), & Guedalia (1990)		X								X			X	X					
Etling and Wippermann (1975)	X	X								X			X						
Fairall (1984)	X										X								
Fanaki (1984)	X	X	X						X								X		
Fedorovich (1995) , & Mironov (1995)	X										X	X							
Fitzharris et al. (1983)	X	X		X					X										
Fitzjarrald (1982), & Garstang (1981)	X										X	X							
Galactzij et al. (1963)	X		X																
Gamo (1985, 1988)	X		X								X	X							
Gamo et al. (1979, 1994)	X		X								X	X						X	
Garland and Branson (1976)	X	X		X															X

Author / Reference	ABL-regime		measurement / experiment							model / parameterization					application				
	CBL	SBL	radio sonde	teth. ball.	mast/ tower	air-craft	radar/ profi-ler	lidar/ ceilo-meter	sodar	diagn.	progn.	slab model	higher order/ LES	indep. model test	algor. devel	NWP /pre-proc.	regio-nal var.	cli-ma-tol.	pollut. conc.
Garratt (1982a)		X	X	X						X	X								
Garratt (1982b)		X							X	X				X					
Garrett (1981)	X		X								X	X		X		X			
Gaynor et al. (1994)	X						X												
Gerasimov et al. (1988)	X					X		X											
Gland (1981)	X	X	X						X										
Glendening (1990)	X		X								X	X		X			X		
Godovitch et al. (1985)	X	X		X													X		
van Gogh and Zib (1978)	X	X		X					X										
Goroch (1976)	X	X	X						X										
Grechko et al. (1993)	X	X							X										X
Gryning and Batchvarova (1990)	X			X							X	X		X					
Guedalia et al. (1980)	X	X	X						X										X
Gutsche and Lefebrve (1981)	X		X														X	X	
Handorf (1996)		X			X					X			X	X					
Hanna (1969)	X	X								X									
Hanna et al. (1985)	X	X	X					X	X	X	X			X					
Hashiguchi et al. (1995)	X						X												
Hashmonay et al. (1991)	X		X					X							X				

Author / Reference	ABL-regime		measurement / experiment							model / parameterization					application				
	CBL	SBL	radio sonde	teth. bal.	mast/ tower	air-craft	radar/ profi-ler	lidar/ ceilo-meter	sodar	diagn.	progn.	slab model	higher order/ LES	indep. model test	algor. devel	NWP /pre-proc.	regio-nal var.	cli-ma-tol.	pollut. conc.
Hayashi (1980)	X	X	X	X					X										
Heidt (1977)	X										X	X							
Heinemann and Rose (1990)		X	X	X						X				X					
Helfland and Boers (1990)	X							X			X		X						
Hicks et al. (1977)	X	X	X						X										
Hildebrand (1988)	X					X									X		X		
Holets and Swanson (1984)	X	X							X						X				
Holtslag and v. Westrhenen (1989)	X	X								X						X			
Holzworth (1964, 1972)	X		X												X		X	X	
Holzworth (1967)	X		X												X		X	X	X
Hsu (1979)	X		X								X	X					X		
Hsu et al. (1980)	X	X	X						X										X
Jakobsen et al. (1995)	X	X	X													X			
Jegede (1994)	X		X														X	X	
Jochum et al. (1991)	X					X											X		
Joffre (1981)	X	X	X		X					X		X							
Jones (1985)	X	X	X						X									X	
Jones et al. (1984)	X	X							X						X				
Kaimal et al. (1982)	X		X		X	X	X	X	X						X				

Author / Reference	ABL-regime		measurement / experiment							model / parameterization					application				
	CBL	SBL	radio sonde	teth. ball.	mast / tower	air-craft	radar / profi-ler	lidar / ceilo-meter	sodar	diagn.	progn.	slab model	higher order / LES	indep. model test	algor. devel	NWP / pre-proc.	regio-nal var.	cli-ma-tol.	pollut. conc.
Karppinen et al. (1996, 1997)	X	X								X	X					X			
Kassomenos et al. (1995)	X		X														X	X	X
Khakimov (1976)	X	X									X								
Kiemle et al. (1995)	X		X			X		X									X		
Kitaigorodskii and Joffre (1988)	X	X	X		X					X									
Klapisz and Weill (1985)		X							X										
Klöppel et al. (1978)	X	X			X						X			X			X		
Klose (1991)		X							X	X									
Klose and Schäke (1991)	X	X	X						X										
Kolarova et al. (1989)	X		X								X	X		X					
Koo et al. (1983)	X	X							X										
Koracin and Berkowicz (1988)		X							X	X				X			X		
Kraus and Schaller (1978)	X												X						
Kukharets and Tsvang (1979)	X					X													
Kurzeja et al. (1991)		X			X													X	
Kuznetsova (1989)	X	X	X																
Laikhtman (1961)	X	X								X									
Lanicci and Warner (1991)	X		X														X	X	
Lieman and Alpert (1993)	X	X	X					X					X				X		

Author / Reference	ABL-regime		measurement / experiment							model / parameterization					application				
	CBL	SBL	radio sonde	teth. ball.	mast/ tower	air-craft	radar/ profi-ler	lidar/ ceilo-meter	sodar	diagn.	progn.	slab model	higher order/ LES	indep. model test	algor. devel	NWP /pre-proc.	regio-nal var.	cli-ma-tol.	pollut. conc.
Lilly (1968)	X		X								X	X							
Ludwig and Dabberdt (1973)	X	X	X							X							X		
Lyra et al. (1992)	X			X		X					X	X		X					
Mahrt (1979)	X										X								
Mahrt (1981b)		X									X								
Mahrt and Lenschow (1976)	X										X	X		X					
Mahrt and Heald (1979)		X								X				X					
Mahrt et al. (1979)		X	X	X															
Mahrt et al. (1982)		X	X							X				X					
Malcher and Kraus (1983)		X								X									
Manins (1982)	X		X								X	X							
Mann et al. (1995)	X					X		X									X		
Manton (1978a,b)	X		X								X	X							
Manton (1987)	X										X	X					X		
Marsik et al. (1995)	X		X				X	X											
Martin et al. (1988)	X	X	X	X		X		X			X	X		X			X		
Marzorati and Anfossi (1993)	X								X	X									
Marzorati et al. (1988)	X								X						X				
Mason and Derbyshire (1990)		X											X						

Author / Reference	ABL-regime		measurement / experiment							model / parameterization					application				
	CBL	SBL	radio sonde	teth. ball.	mast/ tower	air-craft	radar/ profi-ler	lidar/ ceilo-meter	sodar	diagn.	progn.	slab model	higher order/ LES	indep. model test	algor. devel	NWP /pre-proc.	regio-nal var.	cli-ma-tol.	pollut. conc.
Maughan (1979)	X	X							X									X	X
Maughan et al. (1982)	X	X							X									X	
McElroy and Smith (1991)	X					X		X		X							X		X
Melas (1990)	X		X						X										
Melas (1993)	X								X										
Melgarejo and Deardorff (1974)		X	X												X				
Mikkelsen et al. (1993, 1996)	X	X								X	X					X			
Miller (1967)	X		X												X			X	X
Myrick et al. (1994)	X		X															X	
Nicolas et al. (1985)	X			X															X
Nicolas et al. (1988)	X																X	X	X
Nieuwstadt (1981)		X			X				X	X									
Nieuwstadt (1984a)		X			X				X										
Nieuwstadt (1984b)		X							X	X				X					
Nieuwstadt and Driedonks (1979)		X							X	X			X	X					
Nieuwstadt and Tennekes (1981)		X							X	X	X			X					
Nieuwstadt and Glendening (1989)	X										X	X					X		
Noonkester (1976)	X		X				X		X										
Norton and Hoidale (1976)	X		X															X	

Author / Reference	ABL-regime		measurement / experiment							model / parameterization					application				
	CBL	SBL	radio sonde	teth. ball.	mast/ tower	air-craft	radar/ profi-ler	lidar/ ceilo-meter	sodar	diagn.	progn.	slab model	higher order/ LES	indep. model test	algor. devel	NWP /pre-proc.	regio-nal var.	cli-ma-tol.	pollut. conc.
Novak (1991)	X										X	X							
Olesen et al. (1987)	X	X	X							X	X				X				
Orlenko (1979)	X		X															X	
Osborne and Peterson (1995)	X										X								
Ossing (1987)	X	X								X	X								
Økland (1983)	X										X	X							
Pahwa et al. (1990)		X	X						X	X				X				X	
Park et al. (1990)	X	X				X			X	X									X
Pekour (1990)	X	X							X										
Pekour and Kallistratova (1993)	X	X							X								X	X	X
Piringer (1988)	X	X	X	X					X										X
van Pul et al. (1994)	X		X					X											
Rao and Snodgrass (1979)		X	X							X			X	X					
Rao et al. (1994)	X													X			X		X
Rayner (1987), & Watson (1991)	X		X								X	X		X					X
REMTECH (1994)	X	X							X						X				
Rossby and Montgomery (1935)		X								X									
Russell and Uthe (1978 a)	X	X	X		X	X			X								X		X
Russell and Uthe (1978b)	X	X				X		X	X								X		

Author / Reference	ABL-regime		measurement / experiment							model / parameterization					application				
	CBL	SBL	radio sonde	teth. ball.	mast/ tower	air-craft	radar/ profi-ler	lidar/ ceilo-meter	sodar	diagn.	progn.	slab model	higher order/ LES	indep. model test	algor. devel	NWP /pre-proc.	regio-nal var.	cli-ma-tol.	pollut. conc.
Russell et al. (1974)	X	X	X					X	X										
San Jose and Casanova (1988)	X					X		X		X				X					
Sasano et al. (1980, 1982, 1983)	X		X					X							X				
Scheele and van Dop (1989)	X	X	X							X	X			X			X		
Scholten and Erbrink (1990)	X							X											
Schwiesow (1986)	X	X					X	X	X										
Segal et al. (1989)	X										X	X							
Seibert and Langer (1996)	X		X						X							X			
Shipley and Graffman (1991)	X	X						X											
Singal (1988) , (1990)	X	X							X										X
Singal and Aggarwal (1979)	X	X	X						X								X		
Singal et al. (1983)	X		X						X	X				X					
Singal et al. (1985)		X	X						X										
Singal et al. (1989)	X	X							X								X		
Smeda (1979a)	X	X									X								
Smeda (1979b)	X	X									X	X		X					
Smedman (1988)		X			X				X										
Sorbjan et al. (1991)	X								X										
Soler et al. (1996)	X	X	X						X				X						

Author / Reference	ABL-regime		measurement / experiment							model / parameterization					application				
	CBL	SBL	radio sonde	teth. ball.	mast/ tower	air-craft	radar/ profi-ler	lidar/ ceilo-meter	sodar	diagn.	progn.	slab model	higher order/ LES	indep. model test	algor. devel	NWP /pre-proc.	regio-nal var.	cli-ma-tol.	pollut. conc.
Spanton and Williams (1989)	X	X							X								X	X	X
Steyn (1981)	X										X	X							
Steyn (1990)	X			X							X	X					X		
Steyn and Oke (1982)	X		X						X		X	X							
Stull (1973, 1976a,b,c)	X										X	X							
Stull (1983a,b)		X							X	X									
Stull (1992)	X																X		
Tennekes (1973)	X										X	X							
Tennekes and van Ulden (1974)	X		X								X	X		X					
Tennekes and Driedonks (1981)	X										X	X							
Tercier et al. (1995)	X		X												X				
Thomson (1992)	X										X	X							
Tjemkes and Duynkerke (1989)		X							X				X						
Tombach and Chan (1976)	X	X	X			X			X										
Tombach and Ettenheim (1985)	X	X							X						X				
Troen and Mahrt (1986)	X	X								X		X		X					
Visvanadham and Santosh (1994)	X		X																
Vogelezang and Holtslag (1996)	X	X			X					X				X		X			
Walczewski (1989)	X							X	X										

Author / Reference	ABL-regime		measurement / experiment							model / parameterization					application				
	CBL	SBL	radio sonde	teth. ball.	mast/ tower	air-craft	radar/ profi-ler	lidar/ ceilo-meter	sodar	diagn.	progn.	slab model	higher order/ LES	indep. model test	algor. devel	NWP /pre-proc.	regio-nal var.	cli-ma-tol.	pollut. conc.
Walczewski (1992)	X	X							X									X	
Weill (1982)	X	X	X	X	X				X										
Weill et al. (1978, 1980)	X								X										
Wetzel (1982)		X	X							X				X					
Wetzel (1983)	X		X								X			X					
White (1993), - et al. (1991)	X						X								X				
Wotawa et al. (1996)	X	X	X							X	X	X		X		X			
Wratt (1990)	X	X							X										
Wyckoff et al. (1973)	X	X	X						X										X
Yamada and Berman (1979)	X		X						X		X	X		X					
Yu (1978)		X	X							X	X			X					
Zeman (1979)		X									X	X							
Zeman and Tennekes (1977)	X										X	X							
Zilitinkevich (1972)		X								X									
Zilitinkevich (1975a)		X									X								
Zilitinkevich (1975b)	X										X								
Zilitinkevich (1989a)	X										X	X							
Zilitinkevich (1989b)		X								X									
Zilitinkevich et al. (1992)	X	X								X	X	X							

Author / Reference	ABL-regime		measurement / experiment							model / parameterization					application				
	CBL	SBL	radio sonde	teth. ball.	mast/ tower	air-craft	radar/ profi-ler	lidar/ ceilo-meter	sodar	diagn.	progn.	slab model	higher order/ LES	indep. model test	algor. devel	NWP /pre-proc.	regio-nal ver.	cli-ma-tol.	pollut. conc.
Zilitinkevich and Mironov (1996)		X								X									

Authors' affiliations and addresses

Frank Beyrich
Lehrstuhl für Umweltmeteorologie –
Fakultät IV
Brandenburgische Technische Universität
(BTU) Cottbus
Postfach 10 13 44
D-03013 Cottbus, Germany

Tel. +49-355-7813-114 or -186
Fax +49-355-7813-128 or -132
beyrich@Umwelt.TU-Cottbus.de

Sven-Erik Gryning
Meteorology and Wind Energy
Department
Risø National Laboratory
DK-4000 Roskilde, Denmark

Tel. +45-4677-5005
Fax +45-4677-5970
sven-erik.gryning@risoe.dk

Sylvain M. Joffre
Finnish Meteorological Institute
P.B. 503
FIN-00101 Helsinki, Finland

Tel. +358-9-1929-2250
Fax +358-9-1929-4603
sylvain.joffre@fmi.fi

Alix Rasmussen
Danish Meteorological Institute
Lyngbyvej 100
DK-2100 Copenhagen, Denmark

Tel. +45-39-15 74 31
Fax +45-39-15 74 60
ali@dmi.min.dk

Petra Seibert (chair)
Institute of Meteorology and Physics
Agricultural University Vienna (BOKU)
Türkenschanzstr. 18
A-1180 Wien, Austria

Tel. +43-1-470 58 20-20
Fax +43-1-470 58 20-60
seibert@mail.boku.ac.at

Philippe Tercier
Swiss Meteorological Institute (SMA)
Les Invuardes
CH-1530 Payerne, Switzerland

Tel. +41-26-662 62-45
Fax +41-26-662 62-12
pht@sap.sma.ch